BONDING IN TRANSITION METAL COMPOUNDS

Thesis by

Albert Patrick Mortola

In Partial Fulfillment of the Requirements

For the Degree of

Doctor of Philosophy

California Institute of Technology

Pasadena, California

1972

(Submitted May 16, 1972)

DEDICATION

To my father, whose encouragement and inspiration has enabled me to complete this work, to my mother (RIP) whose drive and brilliance surrounded me in my formative years, and to my sister whose humor and good will always made my life a little bit better, as well as to Glen Loughner, recently fallen but not forgotten comrade,

this thesis is dedicated.

ACKNOWLEDGMENT

It is for this student to say,
As he approaches that final day,
That he owes all he has done,
All the work and the fun,
To two profs named Goddard and Gray.

For one known to have a large repetoire of limericks not always singable in mixed company, such an acknowledgment is dull. However, it is only fitting for a thesis to cramp such style. Naturally, there are many others who should be included in this list: Dr. Jules Moskowitz of NYU for his aid and consultation on the permangate calculations as well as for his friendship; Drs. Chuck Hornback and David Hankins for taking the time to help a new student; my research colleagues and friends at Caltech, especially Carl Melius, George "the Heavy" Levin, Bob Ladner, Dave Huestis, Lt. Tim Surratt, Thom Dunning, Bill Hunt, and Jeff Hay, as well as all those who were always willing to imbibe with me, Vinnie Miskowski (to whom I owe more than can be written), Rafe Vega, Mike Maloney, Big Al Wagner and wife Arlene, Frank and Pat Bobrowicz, Dave and Sally McGinty, Ed and Isabel O'Brien, Luis and Hazel Kahn, H. Leslie Hodges, John Winterle, Wilse and Ellen Robinson, Mary Lou de Leon, and all the others who made Southern California tolerable. Finally, I must acknowledge all those on the home front, especially Bernie the Crap, Tommy the Hat, Jack the Kiak, and the Freakin' Hop, whose letters, phone calls, and insults have managed to keep my morale high. As an afterthought, too, the Caltech administration whose intolerable policy of charging tuition next year must be acknowledged for the motivation it gave me to get out now.

I do wish to thank the National Science Foundation for the two years of support through its fellowship program, as well as the California Institute of Technology for the teaching and research assistantships it has seen fit to give me.

ABSTRACT

The values of the Hartree-Fock (HF) and Generalized Valence Bond (GVB) Theories of molecular structure are considered by theoretical investigations of the MnO_4^-, TiO, TiCO, and $TiCO^+$ molecules. Results of these calculations are used in determining the nature of the bonding in these compounds. From the ideas generated, extensions are made to other oxygen and carbonyl transition metal compounds. The conclusion is reached that GVB theory provides more information but is limited to small model compounds. In larger, real compounds, HF theory must be used.

TABLE OF CONTENTS

SECTION	TITLE	PAGE
I	INTRODUCTION	1
II	THE PERMANGANATE ANION	5
III	THE GROUND STATE OF TITANIUM MONOXIDE	55
IV	THE SPECTRUM OF TITANIUM MONOXIDE	97
V	TITANIUM CARBONYL AND TITANIUM CARBONYL ION	117
VI	CONCLUSION	157

I. INTRODUCTION

The discovery in the late nineteenth century of transition metal compounds which were inexplicable in terms of the current valence theory initiated an extensive study into their nature. S. M. Jørgensen and Alfred Werner were mainly responsible for the classification of such compounds, but were unable to produce an accurate description of the bonding involved. With the advent of quantum mechanics, simple theories such as Pauling's Valence Bond Theory,[1] achieved a degree of success by explaining some of the experimental facts. Pauling's theory described the bonding as an overlapping of metal atomic orbitals and ligand orbitals. The metal orbitals were designed as hybrids of hydrogenic orbitals so as to maximize this overlap. This theory was soon replaced by the more sophisticated Crystal Field Theory of Bethe[2] which was able to explain many spectra of these compounds. It defined the bonding as purely ionic, due only to the electrostatic attraction between the negatively charged ligands and the positively charged transition metal. As it became obvious that such a description was inadequate, chemists sought a new approach. Such was available in Molecular Orbital Theory, a theory based on the Hartree-Fock (HF) Theory developed in the 1930's[3] and formulated by Roothaan in 1951.[4] This theory took linear combinations of the metal and ligand atomic orbitals making doubly occupied molecular orbitals. However, because of the complexity of these transition metal compounds, a large degree of approximation was necessary before a calculation could be done. These approximations differed from system to system, resulting in the inability of the theory to produce a consistent description of the bonding. What was needed was a computational capacity that would allow removal of these approximations and full implementation of the Hartree-Fock Theory. In the late 1960's, such a capacity presented itself in the form of large electronic computers. However, by this time, improvements to the Hartree-Fock Theory were being developed. One such theory, apparently capable of describing transition metal complexes, is the Generalized Valence Bond (GVB) Theory of Hunt, Hay, and Goddard.(5) Such a theory employs a linear combination of atomic orbitals to form singly occupied molecular orbitals. These pair together to form a bond. Hence, it is a combination of Valence Bond Theory and Hartree-Fock Theory. Ironically, it seemed that even before the Hartree-Fock Theory could be fully tested, it was doomed to be replaced by the Generalized Valence Bond Theory.

It is the purpose of this thesis to present calculations and interpretations using both the Hartree-Fock and Generalized Valence Bond Theories. The molecules chosen for study were the permanganate anion (MnO_4^-), titanium monoxide (TiO), and tetranium carbonyl (TiCO) and its monopositive ion ($TiCO^+$). A Hartree-Fock calculation was performed on MnO_4^-, the description and results of which make up Chapter 2. Generalized Valence Bond Theory as well as Hartree-Fock Theory are used in the calculation of TiO. The study of the ground state composes Chapter 3, while the calculation of the excited states and the prediction of the spectrum is contained in Chapter 4.

The Generalized Valence Bond and Hartree-Fock description of TiCO and $TiCO^+$ are presented in Chapter 5. In Chapters 2, 3, and 5 the emphasis is on the description of bonding, whereas in Chapter 4, the separation and ordering of the molecular states is the principal consideration. The aim of this study is the understanding of the bonding in these compounds and the evaluation of the contributions of these theories toward this understanding. It is these contributions that serve as justification for the application of these theories to other transition metal compounds.

References

1. L. Pauling, The Nature of the Chemical Bond, Cornell University Press, Ithaca, N.Y., 1940.

2. H. Bethe, Ann. Physik, [5], **3**, 133 (1929).

3. V. Fock, Z. Physik, **61**, 126 (1930); D. R. Hartree, Proc. Cambridge Phil. Soc., **24**, 89 (1928).

4. C. C. J. Roothaan, Rev. Mod. Phys., **23**, 69 (1951).

5. W. J. Hunt, P. J. Hay, W. A. Goddard, III, J. Chem. Phys., in press.

II. HARTREE-FOCK THEORY - THE PERMANGANATE ANION

A. Introduction

The permanganate ion has been the subject of extensive experimental and theoretical studies for the last 34 years. In 1938 and 1939, Teltow[1] published the visible-UV spectrum of MnO_4 recorded at 20°K. In 1952, the first attempt to explain its structure by means of molecular orbital theory was made by Wolfsberg and Helmholz.[2] Through this theoretical study, they hoped (a) to elucidate the nature of the ground state and (b) to explain Teltow's spectrum thereby characterizing the low lying excited states. Their calculation gave the result that the highest occupied molecular orbitals were of t_2 and t_1 symmetries and that the first virtual orbital was of t_2 symmetry. Hence the two lowest-lying, intense bands in the spectrum were assigned to the transitions $t_1 \rightarrow t_2$ and $t_2 \rightarrow t_2$. However, these results turned out more to be artifacts of the approximations made in adapting the Hartree-Fock theory as formulated by Roothaan[3] than to contain an accurate theoretical description of the ion. This became clear in 1958 when Ballhausen and Liehr[4] pointed out that crystal field theory dictated that a virtual e level should be lower than the virtual t_2 and produced a calculation to show this. They assigned the first two intense bands in the spectrum as $t_1 \rightarrow e$ and $t_1 \rightarrow t_2$. In 1960, Carrington, Schonland, and coworkers[5, 6] introduced evidence taken from electron spin resonance that showed that in manganate ion (MnO_4^{2-}), the unpaired electron is in an e orbital. This favored the

Ballhausen-Liehr assignment. Although an error was later pointed out in their calculation,[7, 8] it affected only the calculated intensities and not the actual assignment. However, the error did put the calculation in a bad light. Fenske and Sweeney[9] weighed both methods of calculation and decided that the original Wolfsberg-Helmholz assignment would correlate better with experimental energies and intensities. However, their method was questioned by Viste and Gray[10] who developed an extended Wolfsberg-Helmholz method resulting in a new assignment: $t_1 \rightarrow e$ and $t_2 \rightarrow e$. The bulk of the discrepancy rested on how to incorporate the experimental data into this semi-empirical method. Such a question seemed unanswerable in a unique way, and since the results depended on this answer, all hope for a meaningful description using such a method seemed gone.

Dahl and Ballhausen[11] realized this in 1968 and presented a semi-quantitative method featuring mathematical approximations but no use of experimental data. The spectral analysis resulted in the assignment of the two principal bands as $t_1 \rightarrow e$ and $t_2 \rightarrow e$, with a third band assigned as $t_1 \rightarrow a_1$. However, there were difficulties that beset this calculation. Ballhausen and Gray pointed to inconsistencies in the approximations in a recent review article.[12] What has been needed for some time is an all-electron Hartree-Fock calculation in which the only approximations made would be those inherent in the theory itself as formulated by Roothaan.[3] Such a calculation is the type reported in this paper. A similar calculation has been reported by Hillier and Sanders[13] using a very small Gaussian basis set. Our calculation makes use of a larger basis set and as such reduces the degree of approximation.

B. Basis Set

The ability of gaussian basis functions to describe accurately the Hartree-Fock orbitals of inorganic complexes has been demonstrated in several recent publications.[14-17] However, since the number of such functions needed to span the fifty-eight electron space of permanganate is quite large, we have employed contracted gaussian type basis functions (CGTF). These functions are a fixed linear combination of gaussian type orbitals (GTO). The exponents of the orbitals as well as the contraction coefficients were derived from atomic self-consistent field calculations of Mn and O atoms as described previously.[18] The philosophy underlying the construction of the basis set is to provide nodeless basis functions in the region of principal electron density, analagous to exponential-type functions, distributed such as to provide a single-zeta representation for the core electrons and a double zeta for the valence electrons. Such a description gives emphasis to the accuracy of the calculation in the valence region where the mechanics of bonding occurs while sacrificing some accuracy in the core region. It has been shown[18] that improvement of the basis set in the core region has no effect on the quality of calculation in the valence region.

The basis functions and the contraction coefficients employed are presented in Table I. The contraction coefficients are constrained to be positive even though lower total energies might be obtained without this constraint. However, the lower energies result due to an improvement of the calculation in the core region at the expense of the valence region. Such an improvement is inconsistent with the basic philosophy of our calculation. The manganese 3d orbital and the oxygen 2p orbital are split into long range and short range components to allow for distortion and polarization of atomic charge density in the complexes. Likewise manganese 4s and 4p functions are added for completeness but as the results show do not play a significant role in the bonding. Their function is merely to add a barely used long range component to the s and p sets of manganese.

C. Results and Discussion of the Ground State Wave Function

A Roothaan Hartree-Fock Self Consistent Field Calculation was carried out on the closed-shell ground state electronic configuration of tetrahedral permanganate. The atomic orbital combinations which serve as various symmetry functions are given in Table 2. It is to be noted that our coordinate system is the ordinary Cartesian system with the axes of all the atoms being in the same directions. Other authors (e.g. ref. 11) have chosen their coordinate systems so that the p_z orbitals of the four oxygen atoms point toward the manganese atom at the center of the tetrahedron.

In such a system, the oxygen p_z orbitals can only enter into the a_1 and t_2 symmetries and serve only as sigma type bonding orbitals.

The oxygen p_x and p_y orbitals are restricted for the e, t_2, and t_1 symmetries as pi bonding and non-bonding type orbitals. While this system is conceptually easier, the calculation of the integrals between basis functions becomes extremely difficult. The conceptual problems can be overcome by simply considering the a_1 and t_2 combinations as the source of sigma bonding, the e and t_2 combination as the sources of pi bonding and the t_1 combination as the nonbonding oxygen lone pair orbitals. The ability of the t_2 orbitals to be both of sigma and pi bonding character creates some confusion in that the distinction between sigma and pi bonding is no longer well defined. Accordingly, the idea of delocalization enters and the question of whether localized orbitals are equivalent becomes important. This is discussed later in the analysis of the orbitals. The manganese-oxygen distance was taken as 1.629Å, the distance determined through X-ray structure analysis by Palenik.[(19)]

The total energy, its components, and the orbital energy levels calculated are tabulated in Table 3. The comparison is with the results of Hillier and Saunders.[(13b)] As can be seen, the ordering of the two highest bound orbitals, the $1t_1$ and $6a_1$, as well as of the lowest two excited orbitals, the $7t_2$ and 2e, is different. This effect could very likely be the result of the difference in basis sets. The $1t_1$ orbital is the non-bonding oxygen lone pair orbital made up entirely of oxygen 2p basis functions. Our calculation having two functions as compared to one for each oxygen 2p orbital is much more flexible and as such should lead to a better description. The same argument holds true for the $6a_1$ orbital which is a bonding orbital between the manganese s functions and the oxygen 2p sigma functions. The excited orbitals 2e and $7t_2$ involve the 3d orbitals of manganese and the oxygen 2p orbitals. Both sets have twice as many basis functions as those used in the comparable calculation. For this reason, we interpret our results as being closer to the actual description.

It is interesting at this time to examine the ground state orbitals determined in the calculation. These are listed in Table 4. The $1a_1$ and $2a_1$ are manganese 1s and 2s orbitals. The $1t_2$ is the manganese 2p orbital, while the $3a_1$ and $2t_2$ are the oxygen 1s orbitals. The $4a_1$ is the manganese 3s orbital, the $3t_2$ the manganese 3p orbital, and the $5a_1$ and $4t_2$ are the oxygen 2s orbitals. It is safe to call these orbitals "core orbitals" even though there is a distinct mixture between manganese and oxygen orbitals taking place in the $5a_1$ and $4t_2$ orbitals. However, this mixing which is to a small degree gets increasingly larger as the orbitals get lower in energy. Hence the designations core orbital and valence orbital do not imply clear-cut distinctions but rather an arbitrariness on the part of the user. While all may agree that the $1a_1$, $2a_1$, $3a_1$, $1t_2$, and $2t_2$ are core orbitals, few would call the $4a_1$, $5a_1$, and $4t_2$ valence orbitals. In this intermediate region, we have chosen to call these core orbitals since we do not feel that the interatomic interaction is strong enough to justify the use of the term valence orbitals. However, this latter term is applicable to the $5t_2$ and subsequent orbitals. The $5t_2$ and $6t_2$ represent sigma and pi bonding orbitals between the manganese 3d orbitals

(d_{xy}, d_{xz}, d_{yz}) and the two combinations of oxygen p t_2 orbitals. The $5t_2$ orbital has more density near the manganese atom while the $6t_2$ is a diffuse bonding orbital. In the localized orbital sense, the $5t_2$ is a sigma bonding orbital since it has a good deal of amplitude in the d orbitals that point toward the oxygen atoms. The $6t_2$ on the other hand is a diffuse orbital with a small amount of pi bonding as well as a small amount of sigma bonding. It has most of its density on the oxygen atoms but cannot be considered a non-bonding orbital. From this one can ascertain that the bonding here is definitely covalent and that it is not correct to describe permanganate as an ionic compound with manganese having a +7 charge and the 4 oxygens each having a charge of -2. The 1e orbital is of distinct pi bonding character with almost an equal sharing of the electrons between the metal and ligands. The $6a_1$ orbital as mentioned above is a sigma bonding orbital and the $1t_1$ is the orbital accounting for the non-bonding oxygen electrons.

Such a description of the ground state contains 24 electrons designated as valence and 32 designated as core. Of the valence electrons 6 (from the $1t_1$ orbitals) are non-bonding, while 18 are involved in the bonding process. The number 18 is the number of electrons comprising a complete shell involving d electrons. This can roughly be broken down into 8 sigma electrons and 10 pi electrons. The sigma electrons account for the principal bond between each oxygen and manganese while the pi electrons are delocalized. One might try to picture a "resonating" structure with a "triple bond" between one of the oxygens and permanganate. Probably the best localized description though would be to assign 2 of these pi electrons to non-bonding duties while allowing the other 8 to form 4 pi bonds between manganese and the four oxygen atoms. This would account for the non-bonding aspects of the $6t_2$ orbital. However, it is not consistent with Hartree-Fock theory to do so. One then assumes delocalization of the 6 non-bonding electrons and of the "extra" 2 pi bonding electrons. The orbitals have been calculated so that these electrons keep out of each other's way. Were one to go beyond Hartree Fock theory and remove the symmetry restrictions, one would probably find 8 non-bonding and 16 bonding electrons. However, until such a calculation is done, this remains speculation.

A quantitative measure of the above qualitative arguments is obtained through population analysis. The results of such an analysis are displayed in Table 5. Once again, they are compared with the results of Hillier and Saunders. The most striking difference is the population of the manganese 4s and 4p orbitals. Our calculation shows a smaller tendency for the electrons to be in these orbitals. Once again this result seems to indicate that their work suffered from basis set deficiencies. The electrons could not find the flexibility in their d function and had to reside in the higher 4s and 4p functions. The description of the ground state changes. Whereas the neutral manganese starts with five 3d electrons and two 4s electrons, our description shows the 4s electrons to be taken by the oxygen atoms and the 3d electrons to be held by manganese and even for their orbitals to take back via sigma and pi bonding part of the lost density. Their description implies loss of d electron density so as to support 4s and 4p density.

Our description is more in line with the usual thoughts on transition metal oxidation--that the 4s electrons ionize first. Both calculations agree that the compound is not completely ionic and that it has a good deal of covalency.

There is no way to check these results experimentally since population and charges are not observables. However, the method of X-ray photoelectron spectroscopy (ESCA) is able to give the binding energies of core electrons and through the theoretical model associated with it, give an approximation to the charge on a given atom. Such experiments have been performed by Ousyannikova and Brusentev[20] and by Best.[21] The former paper predicted a charge of +1.28 on manganese, the prediction being based on an experimental estimate derived from the metal K X-ray spectrum. Both Hillier and Saunders and ourselves are very close to this number. Best on the other hand does not give the charge on manganese but instead measures the binding energies of some of the inner core electrons. His results are compared with ours in Table 6. The method we used is simply Koopman's Theorem which says that the orbital energy calculated is equal to the binding energy of that electron. The argument between theory and experiment is much better for core electrons since in that case less rearrangement of the electrons is probable. In the ionization of a valence electron, one expects a non-negligible rearrangement of the electrons. Hence we need not be discouraged by the poor agreement for the $6t_2$ orbital. It might also be stated that had our basis been large enough to include more functions for the core orbitals, the agreement for the $3t_2$ and $4t_2$ would improve. Best interprets his experiments as showing that the 4p orbital or manganese is not at all involved in the bonding process. This coincides more closely with our population analysis than with that of Hillier and Saunders. Unfortunately, we do not have the data enabling us to match the chemical shifts of the inner core photoionization energies (from ESCA) with the charges on various manganese containing compounds so as to analyze our results with this tool. As more ESCA work is done, these data should become available.

D. Excited States and the Electronic Spectrum

The electronic spectrum of permanganate is given in Table 7. Since its interpretation is the key to the excited states, we calculated it via Virtual Orbital Theory and have tabulated the results in Table 8. As is usual with Virtual Orbital Theory, the calculated values are too high. This error stems from the fact that the orbital energies of the excited states are positive when in reality since the states are bound, they should be negative. We also calculated the position dipole and velocity dipole strengths of each transition. These are presented in Table 9. As can be seen, these also are much higher than those obtained experimentally. This follows since the oscillator strength is proportional to ΔE. In an attempt to remedy this error, we have tried to calculate ΔE from the formula [22]

$$\Delta E_{ij} = \frac{\langle i|\nabla|j\rangle}{\langle i|r|j\rangle}$$

which is rigorous only to first order for $\langle i|\nabla|j\rangle$ and $\langle i|r|j\rangle$. However, the results listed in Table 10 are quite interesting. The spectrum seems closer to the experimental spectrum and the first band agrees with the result of Carrington and coworkers[5,6] from ESR work on manganate (MnO_4^{--}): the extra electron is in the 2e orbital. Furthermore when the excited orbitals are used to calculate the A/D ratio obtained through magnetic circular dichoroism by Schatz, Stevens, et alia[23] excellent agreement is attained (Table 11). Whereas in the earlier paper[23a] assignment of the third allowed band (at 3.99 eV) was ambiguous depending on the choice of parameter for the orbitals, it may now be assigned as a $1t_1 \rightarrow 7t_2$ transition. Further discussion of the experimental work with Dr. Schatz led to the conclusion that the second band with a calculated A/D ratio of -0.23, could easily be masked by the first and third bands. Hence further experiments in an effort to resolve this question are necessary. The experimental work as well as the results calculated leads one to the conclusion that the orbitals obtained in the calculation give a good description of the excited states, whereas the Virtual Orbital Theory method is not good for determining excitation energies. The 2e orbital is a pi orbital having a large part of its density on the metal atom. Hence one could call the $1t_1 \rightarrow 2e$ transition an $n \rightarrow \pi^*$ ligand to metal charge transfer transition. Likewise the $7t_2$ orbital is centered mainly on the metal atom and transitions to it from the $1t_1$ or from the diffuse $6t_2$ are aptly considered ligand to metal charge transfer transitions. As before, since t_2 orbitals can be localized into both sigma and pi two electron orbitals, it is impossible to say that the $7t_2$ is a σ^* or π^* orbital. However, it does have the opposite sense of the $5t_2$ orbital (since it has a negative combination of metal d and oxygen p orbitals as opposed to the positive combination) but also has a substantial amount of metal 4p character. This forbids labelling it σ^* so it remains $7t_2$ and any transition to it from $1t_1$ or $6t_2$ a ligand to metal charge transfer.

E. Summary

In this paper we have used Hartree-Fock Roothaan Molecular Orbital Theory to give a description of the ground state and first two excited states of the permanganate ion. The ground state structure is elucidated as best as can be done within the framework of symmetry restricted orbitals. The results are as expected in that the molecular orbitals are made up of overlaps mostly between manganese 3d and oxygen 2p orbitals. Comparison with experimental results show the description to be accurate. The excited state calculations suffer from defects in the theory rather than in calculational approximation. To account for them accurately one must do each electronic configuration separately and perhaps even allow for configuration interaction. However, since the size prohibits large numbers of configurations, those chosen should be allowed to vary their orbitals during the calculation. A fine example of the interaction of experiment and theory is presented with the discussion of MCD data. It is the author's hope that such discussion continue until the elucidation of the structure of permanganate is at hand.

References

1. J. Teltow, Z. Phys. Chem., B40, 397 (1938); ibid., B43, 198 (1939).
2. M. Wolfsberg and L. Helmholz, J. Chem. Phys., 20, 837 (1952).
3. C. C. J. Roothaan, Rev. Mod. Phys., 23, 69 (1951).
4. C. J. Ballhausen and A. D. Liehr, J. Mol. Spectry., 4, 190 (1960); ibid., 2, 342 (1958).
5. C. Carrington, D. J. E. Ingram, K. A. K. Lott, D. S. Schonland, and M. C. R. Symons, Proc. Roy. Soc., A254, 101 (1960).
6. D. S. Schonland, Proc. Roy. Soc., A254, 111 (1960).
7. A. Carrington and M. C. R. Symons, J. Chem. Soc., 1960, 889.
8. A. Carrington and D. S. Schonland, Mol. Phys., 3, 331 (1960).
9. R. E. Fenske and C. C. Sweeney, Inorg. Chem., 3, 1105 (1964).
10. A. Viste and H. B. Gray, Inorg. Chem., 3, 1113 (1964).
11. J. P. Dahl and C. J. Ballhausen, Advances in Quantum Chemistry, 4, 170 (1968).
12. C. J. Ballhausen and H. B. Gray, "Electronic Structure of Metal Complexes," Chapter 1 in Coordination Chemistry, ed. A. E. Martell, van Nostrand-Reinhold, New York, 1971.
13. I. H. Hillier and V. R. Saunders, a) J. Chem. Soc. D, 1275 (1969); b) Chem. Phys. Lett., 9, 219 (1961); c) Proc. Roy Soc., A320, 161 (1970).
14. H. Basch and A. P. Ginsberg, J. Phys. Chem., 73, 854 (1969).
15. H. Basch, C. W. Hollister, and J. W. Moskowitz, Chem. Phys. Lett., 4, 79 (1969).

16. H. Basch, C. W. Hollister, and J. W. Moskowitz in "Sigma Molecular Orbital Theory," O. Sinanoglu and K. Wiberg, Eds., Yale University Press, New Haven, Conn., (1970), p. 449.

17. J. W. Moskowitz, C. Hollister, C. J. Hornback, and H. Basch, J. Chem. Phys., **53**, 2570 (1970).

18. H. Basch, C. J. Hornback, and J. W. Moskowitz, J. Chem. Phys., **51**, 1311 (1969).

19. G. J. Palenik, Inorg. Chem., **6**, 503 (1967).

20. I. A. Ousyannikova and F. A. Brusentev , J. Struct. Chem., **7**, 457 (1966).

21. P. E. Best, J. Chem. Phys., **44**, 3248 (1966).

22. a) W. Lamb, R. Young, and S. R. LaPaglia, J. Chem. Phys., **49**, 2868 (1968); b) S. R. LaPaglia, J. Mol. Spectry., **24**, 302 (1967).

23. a) P. N. Schatz, A. J. McCaffery, W. Suetaka, G. N. Henning, A. B. Ritchie, and P. J. Stevens, J. Chem. Phys., **45**, 722 (1966); b) P. J. Stevens, R. L. Mowery, and P. N. Schatz, J. Chem. Phys., **55**, 224 (1971).

Table 1. Basis Functions

Atom	Function Type	Approximate Orbital Representation	Exponent	Contraction Coefficient
Mn	S	1S	28270.	.0041970
			4210.	.0307591
			976.5	.1327658
			301.1	.3369145
			115.2	.4274878
			49.64	.2081060
Mn	S	2S	13.31	.4556010
			7.115	.5183264
			2.358	.0585100
Mn	S	3S	1.903	.3408928
			.9421	.6068370
			.3595	.0893281
Mn	S	4S	.09804	.4149608
			.05079	.5311052
			.01831	.0931139
Mn	P	2P	435.3	.0204374
			103.3	.1325751
			33.22	.3886672
			12.37	.4891038
			4.797	.1579899

Table 1 (Continued)

Atom	Function Type	Approximate Orbital Representation	Exponent	Contraction Coefficient
Mn	P	4P	.1569	.4149608
			.08126	.5311052
			.02930	.0931139
Mn	D	3D	27.73	.0465863
			7.612	.2217249
			2.540	.4659702
			.8607	.5095180
Mn	D	3D'	.2829	1.0
O	S	1S	2237.	.0054504
			331.3	.0418480
			75.07	.1843539
			20.93	.4732970
			6.426	.4379310
O	S	2S	.8802	.1005934
			.7737	.5536075
			.2431	.4017961
O	P	2P	35.18	.0195696
			7.904	.1243760
			2.305	.3945936
			.7171	.6273940
	P	2P'	.2137	1.0

Table 2. Molecular Symmetires with Atomic Counterparts*

(The four oxygen atoms are designated by subscripts 1, 2, 3, 4)

Molecular Symmetry	Mn Orbitals	O Orbitals
a_1	1s	$1s_1 + 1s_2 + 1s_3 + 1s_4$
	2s	$2s_1 + 2s_2 + 2s_3 + 2s_4$
	3s	$[(-p_{x_1} + p_{x_2} - p_{x_3} + p_{x_4}) + (-p_{y_1} - p_{y_2} + p_{y_3} + p_{y_4})$ $+ (-p_{z_1} + p_{z_2} + p_{z_3} - p_{z_4})]$
e	$3d_{2z^2-x^2-y^2}$	$[(-p_{x_1} + p_{x_2} - p_{x_3} + p_{x_4}) + (p_{y_1} + p_{y_2} - p_{y_3} - p_{y_4})]$
	$3d_{x^2-y^2}$	$[(-p_{x_1} + p_{x_2} - p_{x_3} + p_{x_4}) + (p_{y_1} - p_{y_2} + p_{y_3} + p_{y_4})$ $+ 2(p_{z_1} - p_{z_2} - p_{z_3} + p_{z_4})]$
t_2	$2p_x$	$1s_1 + 1s_2 - 1s_3 - 1s_4$
	$2p_y$	$1s_1 - 1s_2 + 1s_3 - 1s_4$
	$2p_z$	$1s_1 - 1s_2 - 1s_3 + 1s_4$
	$3p_x$	$2s_1 + 2s_3 - 2s_3 - 2s_4$
	$3p_y$	$2s_1 - 2s_2 + 2s_3 - 2s_4$
	$3p_z$	$2s_1 - 2s_2 - 2s_3 + 2s_4$
	$4p_x$	$[(-p_{x_1} + p_{x_2} + p_{x_3} - p_{x_4}) - (p_{y_1} + p_{y_2} + p_{y_3} + p_{y_4})$
	$4p_y$	$+ (-p_{z_1} + p_{z_2} - p_{z_3} + p_{z_4})]$
	$4p_z$	$[-(p_{x_1} + p_{x_2} + p_{x_3} + p_{x_4}) + (-p_{y_1} + p_{y_2} + p_{y_3} - p_{y_4})$
	$3d_{xy}$	$+ (-p_{z_1} - p_{z_2} + p_{z_3} + p_{z_4})]$

Table 2 (Continued)

Molecular Symmetry	Mn Orbitals	O Orbitals
	$3d_{xz}$	$[(-p_{x_1} - p_{x_2} + p_{x_3} + p_{x_4}) + (-p_{y_1} + p_{y_2} - p_{y_3} + p_{y_4})$ $+ (p_{z_1} + p_{z_2} + p_{z_3} + p_{z_4})]$
	$3d_{yz}$	$[(p_{x_1} - p_{x_2} - p_{x_3} + p_{x_4}) - 2(p_{y_1} + p_{y_2} + p_{y_3} + p_{y_4})$ $+ (p_{z_1} - p_{z_2} + p_{z_3} - p_{z_4})]$
		$[-2(p_{x_1} + p_{x_2} + p_{x_3} + p_{x_4}) + (p_{y_1} - p_{y_2} - p_{y_3} + p_{y_4})$ $+ (p_{z_1} + p_{z_2} - p_{z_3} - p_{z_4})]$
		$[(p_{x_1} + p_{x_2} - p_{x_3} - p_{x_4}) + (p_{y_1} - p_{y_2} + p_{y_3} - p_{y_4})$ $-2\,(p_{z_1} + p_{z_2} + p_{z_3} + p_{z_4})]$
t_1		$[(-p_{x_1} + p_{x_2} + p_{x_3} - p_{x_4}) + (p_{z_1} - p_{z_2} + p_{z_3} - p_{z_4})]$
		$[(p_{y_1} - p_{y_2} - p_{y_3} + p_{y_4}) + (-p_{z_1} - p_{z_2} + p_{z_3} + p_{z_4})]$
		$[(p_{x_1} + p_{x_2} - p_{x_3} - p_{x_4}) + (-p_{y_1} + p_{y_2} - p_{y_3} + p_{y_4})]$

* The oxygen 2p' transforms like the 2p and the manganese 3d' like the 3d O orbitals.

Table 3. Results of Calculation in Atomic Units

	This calc.	Hillier and Saunders (1971)
Total Energy	-1447.193101	
Virial $(\frac{V}{T})$	- 2.001396	
Kinetic Energy	1445.175739	
Electronic Energy	-1783.455141	
Potential Energy	-2892.368840	
Nuclear Repulsion	336.262040	

Orbital	Orbital Energy	
3e	.99999	
$9t_2$	.99090	
$8t_2$	.57084	.4771
$7a_1$	.42065	.4752
2e	.19870	.2266
$7t_2$	+.18525	.2890
$6a_1$	-.27595	-.2436
$1t_1$	-.29393	-.2112
$6t_2$	-.33612	-.2675
1e	-.43198	-.4183
$5t_2$	-.48672	-.4378
$4t_2$	-1.06850	
$5a_1$	-1.08701	
$3t_2$	-2.56460	
$4a_1$	-3.83404	
$3a_1$	-20.42701	

Table 3 (Continued)

$2t_2$	-20.42701
$1t_2$	-25.05650
$2a_1$	-28.99162
$1a_1$	-240.64870

Table 4. Molecular Orbitals

The coefficients are given in the following order for the 57 basis functions:

Mn 1s	O_4 1s	O_3 $2p'_x$	O_3 $2p_y$	O_2 $2p'_z$	Mn $3d'_{z^2}$
Mn 2s	O_4 2s	O_4 $2p_x$	O_3 $2p_y$	O_3 $2p_z$	Mn $3d_{xy}$
Mn 3s	Mn $2p_x$	O_4 $2p'_x$	O_4 $2p_y$	O_3 $2p'_z$	Mn $3d'_{xy}$
Mn 4s	Mn $3p_x$	Mn $2p_y$	O_4 $2p'_y$	O_4 $2p_z$	Mn $3d_{xz}$
O_1 1s	Mn $4p_x$	Mn $3p_y$	Mn $2p_z$	O_4 $2p'_z$	Mn $3d'_{xz}$
O_1 2s	O_1 $2p_x$	Mn $4p_y$	Mn $3p_z$	Mn $3d_{x^2}$	Mn $3d_{yz}$
O_2 1s	O_1 $2p'_x$	O_1 $2p_y$	Mn $4p_z$	Mn $3d'_{x^2}$	Mn $3d'_{yz}$
O_2 2s	O_2 $2p_x$	O_1 $2p'_y$	O_1 $2p_z$	Mn $3d_{y^2}$	
O_3 1s	O_2 $2p'_x$	O_2 $2p_y$	O_1 $2p'_z$	Mn $3d'_{y^2}$	
O_3 2s	O_3 $2p_x$	O_2 $2p'_y$	O_2 $2p_z$	Mn $3d_{z^2}$	

ORBITAL 1

-.9950824	0.0000034	0.0001480	0.0000461	-.0001480	0.0000000
-.0134642	0.0000178	0.0000461	-.0001480	0.0000461	0.0000000
0.0030452	0.0000000	-.0001480	0.0000461	-.0001480	0.0000000
-.0002810	0.0000000	0.0000000	-.0001480	-.0000461	0.0000000
0.0000034	0.0000000	0.0000000	0.0000000	0.0001480	0.0000000
0.0000178	-.0000461	0.0000000	0.0000000	0.0000000	0.0000000
0.0000034	0.0001480	-.0000461	0.0000000	0.0000000	0.0000000
0.0000178	0.0000461	0.0001480	-.0000461	0.0000000	
0.0000034	-.0001480	-.0000461	0.0001480	0.0000000	
0.0000178	-.0000461	0.0001480	0.0000461	0.0000000	

ORBITAL 2

0.4220061	-.0000068	-.0002659	-.0000931	0.0002659	0.0000000
-1.0784284	-.0000380	-.0000931	0.0002659	-.0000931	0.0000000
-.0053123	0.0000000	0.0002659	-.0000931	0.0002659	0.0000000
0.0005096	0.0000000	0.0000000	0.0002659	0.0000931	0.0000000

Table 4 (Continued)

-.0000068	0.0000000	0.0000000	0.0000000	-.0002659	0.0000000
-.0000380	0.0000931	0.0000000	0.0000000	0.0000000	0.0000000
-.0000068	-.0002659	0.0000931	0.0000000	0.0000000	0.0000000
-.0000380	-.0000931	-.0002659	0.0000931	0.0000000	
-.0000068	0.0002659	0.0000931	-.0002659	0.0000000	
-.0000380	0.0000931	-.0002659	-.0000931	0.0000000	

ORBITAL 3

-.0000434	0.4972671	-.0003078	0.0003693	0.0003078	0.0000000
0.0001869	0.0101966	0.0003693	0.0003078	0.0003693	0.0000000
-.0000732	0.0000000	0.0003078	0.0003693	0.0003078	0.0000000
-.0082530	0.0000000	0.0000000	0.0003078	-.0003693	0.0000000
0.4972671	0.0000000	0.0000000	0.0000000	-.0003078	0.0000000
0.0101966	-.0003693	0.0000000	0.0000000	0.0000000	0.0000000
0.4972671	-.0003078	-.0003693	0.0000000	0.0000000	0.0000000
0.0101966	-.0003693	-.0003078	-.0003693	0.0000000	
0.4972671	0.0003078	-.0003693	-.0003078	0.0000000	
0.0101966	-.0003693	-.0003078	0.0003693	0.0000000	

ORBITAL 4

0.1660774	-.0029359	0.0021323	0.0039654	-.0021323	0.0000000
-.7267602	0.0071531	0.0039654	-.0021323	0.0039654	0.0000000
1.2125662	0.0000000	-.0021323	0.0039654	-.0021323	0.0000000
-.0088921	0.0000000	0.0000000	-.0021323	-.0039654	0.0000000
-.0029359	0.0000000	0.0000000	0.0000000	0.0021323	0.0000000
0.0071531	-.0039654	0.0000000	0.0000000	0.0000000	0.0000000
-.0029359	0.0021323	-.0039654	0.0000000	0.0000000	0.0000000
0.0071531	0.0039654	0.0021323	-.0039654	0.0000000	
-.0029359	-.0021323	-.0039654	0.0021323	0.0000000	
0.0071531	-.0039654	0.0021323	0.0039654	0.0000000	

Table 4 (Continued)

ORBITAL 5

0.0233880	0.1498326	0.0161834	-.0246462	-.0161834	0.0000000
-.1083421	-.4907226	-.0246462	-.0161834	-.0246426	0.0000000
0.2377013	0.0000000	-.0161834	-.0246462	-.0161834	0.0000000
-.0565532	0.0000000	0.0000000	-.0161834	0.0246462	0.0000000
0.1498326	0.0000000	0.0000000	0.0000000	0.0161834	0.0000000
-.4907226	0.0246462	0.0000000	0.0000000	0.0000000	0.0000000
0.1498326	0.0161834	0.0246462	0.0000000	0.0000000	0.0000000
-.4907226	-.0246462	0.0161834	0.0246462	0.0000000	
0.1498326	-.0161834	0.0246462	0.0161834	0.0000000	
-.4907226	0.0246462	0.0161834	-.0246462	0.0000000	

ORBITAL 6

0.0327561	-.0312022	0.1236509	-.1867935	-.1236509	0.0000000
-.1547245	0.1157458	-.1867935	-.1236509	-.1867935	0.0000000
0.3763237	0.0000000	-.1236509	-.1867935	-.1236509	0.0000000
-.0502036	0.0000000	0.0000000	-.1236509	0.1867935	0.0000000
-.0312022	0.0000000	0.0000000	0.0000000	0.1236509	0.0000000
0.1157458	0.1867935	0.0000000	0.0000000	0.0000000	0.0000000
-.0312022	0.1236509	0.1867935	0.0000000	0.0000000	0.0000000
0.1157458	-.1867935	0.1236509	0.1867935	0.0000000	
-.0312022	-.1236509	0.1867935	0.1236509	0.0000000	
0.1157458	0.1867935	0.1236509	-.1867935	0.0000000	

ORBITAL 7

-.0187366	0.0906090	0.0946968	-.0268153	-.0946968	0.0000000
0.0911749	-.4682251	-.0268153	-.0946968	-.0268153	0.0000000
-.2619943	0.0000000	-.0946968	-.0268153	-.0946968	0.0000000
1.5362060	0.0000000	0.0000000	-.0946968	0.0268153	0.0000000
0.0906090	0.0000000	0.0000000	0.0000000	0.0946968	0.0000000
-.4682251	0.0268153	0.0000000	0.0000000	0.0000000	0.0000000
0.0906090	0.0946968	0.0268153	0.0000000	0.0000000	0.0000000

Table 4 (Continued)

-.4682251	-.0268153	0.0946968	0.0268153	0.0000000	
0.0906090	-.0946968	0.0268153	0.0946968	0.0000000	
-.4682251	0.0268153	0.0946968	-.0268153	0.0000000	

ORBITAL 8

-.0361930	0.0023741	-.2856264	-.2766827	0.2856264	0.0000000
0.1769183	0.0050074	-.2766827	0.2856264	-.2766827	0.0000000
-.5115796	0.0000000	0.2856264	-.2766827	0.2856264	0.0000000
-.2230705	0.0000000	0.0000000	0.2856264	0.2766827	0.0000000
0.0023741	0.0000000	0.0000000	0.0000000	-.2856264	0.0000000
0.0050074	0.2766827	0.0000000	0.0000000	0.0000000	0.0000000
0.0023741	-.2856264	0.2766827	0.0000000	0.0000000	0.0000000
0.0050074	-.2766827	-.2856264	0.2766827	0.0000000	
0.0023741	0.2856264	0.2766827	-.2856264	0.0000000	
0.0050074	0.2766827	-.2856264	-.2766827	0.0000000	

ORBITAL 9

0.0000000	0.0000000	-.0951864	-.2151485	0.0000000	0.0000000
0.0000000	0.0000000	0.2151485	-.0951864	0.0000000	0.0000000
0.0000000	0.0000000	0.0951864	-.2151485	0.0000000	0.0000000
0.0000000	0.0000000	0.0000000	-.0951864	0.0000000	0.0000000
0.0000000	0.0000000	0.0000000	0.0000000	0.0000000	0.0000000
0.0000000	-.2151485	0.0000000	0.0000000	-.2895641	0.0000000
0.0000000	-.0951864	0.2151485	0.0000000	-.1591006	0.0000000
0.0000000	0.2151485	0.0951864	0.0000000	0.2895641	
0.0000000	0.0951864	0.2151485	0.0000000	0.1591006	
0.0000000	-.2151485	0.0951864	0.0000000	0.0000000	

Table 4 (Continued)

ORBITAL 10

0.0000000	0.0000000	-.1146232	-.1408490	0.0000000	0.0000000
0.0000000	0.0000000	0.1408490	-.1146232	0.0000000	0.0000000
0.0000000	0.0000000	0.1146232	-.1408490	0.0000000	0.0000000
0.0000000	0.0000000	0.0000000	-.1146232	0.0000000	0.0000000
0.0000000	0.0000000	0.0000000	0.0000000	0.0000000	0.0000000
0.0000000	-.1408490	0.0000000	0.0000000	0.6768119	0.0000000
0.0000000	-.1146232	0.1408490	0.0000000	0.2748112	0.0000000
0.0000000	0.1408490	0.1146232	0.0000000	-.6768119	
0.0000000	0.1146232	0.1408490	0.0000000	-.2748112	
0.0000000	-.1408490	0.1146232	0.0000000	0.0000000	

ORBITAL 11

0.0000000	0.0000000	-.4169477	0.3121692	0.0000000	0.0000000
0.0000000	0.0000000	-.3121692	-.4169577	0.0000000	0.0000000
0.0000000	0.0000000	0.4169477	0.3121692	0.0000000	0.0000000
0.0000000	0.0000000	0.0000000	-.4169577	0.0000000	0.0000000
0.0000000	0.0000000	0.0000000	0.0000000	0.0000000	0.0000000
0.0000000	0.3121692	0.0000000	0.0000000	0.0180747	0.0000000
0.0000000	-.4169577	-.3121692	0.0000000	0.2446829	0.0000000
0.0000000	-.3121692	0.4169577	0.0000000	-.0180747	
0.0000000	0.4169577	-.3121692	0.0000000	-.2446829	
0.0000000	0.3121692	0.4169577	0.0000000	0.0000000	

ORBITAL 12

0.0000000	0.0000000	0.2356553	0.0576322	0.0000000	0.0000000
0.0000000	0.0000000	-.0576322	0.2356553	0.0000000	0.0000000
0.0000000	0.0000000	-.2356553	0.0576322	0.0000000	0.0000000
0.0000000	0.0000000	0.0000000	0.2356553	0.0000000	0.0000000
0.0000000	0.0000000	0.0000000	0.0000000	0.0000000	0.0000000
0.0000000	0.0576322	0.0000000	0.0000000	0.6180983	0.0000000
0.0000000	0.2356553	-.0576322	0.0000000	-1.2231569	0.0000000

Table 4 (Continued)

0.0000000	-.0576322	-.2356553	0.0000000	-.6189983	
0.0000000	-.2356553	-.0576322	0.0000000	1.2231569	
0.0000000	0.0576322	-.2356553	0.0000000	0.0000000	

ORBITAL 13

0.0000000	0.0000000	-.0549559	0.1242160	-.1099118	0.1837136
0.0000000	0.0000000	0.1242160	0.0549559	-.2484321	0.0000000
0.0000000	0.0000000	0.0549559	0.1242160	-.1099118	0.0000000
0.0000000	0.0000000	0.0000000	0.0549559	0.2484321	0.0000000
0.0000000	0.0000000	0.0000000	0.0000000	0.1099118	0.0000000
0.0000000	-.1242160	0.0000000	0.0000000	-.1671799	0.0000000
0.0000000	-.0549559	-.1242160	0.0000000	-.0918568	0.0000000
0.0000000	0.1242160	-.0549559	0.2484321	-.1671799	
0.0000000	0.0540559	-.1242160	0.1099118	-.0918568	
0.0000000	-.1242160	-.0549559	-.2484321	0.3343598	

ORBITAL 14

0.0000000	0.0000000	-.0661777	0.813192	-.1323554	-.3173247
0.0000000	0.0000000	0.0813192	0.0661777	-.1626384	0.0000000
0.0000000	0.0000000	0.0661777	0.0813192	-.1323554	0.0000000
0.0000000	0.0000000	0.0000000	0.0661777	0.1626384	0.0000000
0.0000000	0.0000000	0.0000000	0.0000000	0.1323554	0.0000000
0.0000000	-.0813192	0.0000000	0.0000000	0.3907576	0.0000000
0.0000000	-.0661777	-.0813192	0.0000000	0.1586623	0.0000000
0.0000000	0.0813192	-.0661777	0.1626384	0.3907576	
0.0000000	0.0661777	-.0813192	0.1313554	0.1586623	
0.0000000	-.0813192	-.0661777	-.1626384	-.7815151	

Table 4 (Continued)

ORBITAL 15

0.0000000	0.0000000	-.2407306	-.1802310	-.4814613	-.2825354
0.0000000	0.0000000	-.1802310	0.2407306	0.3604619	0.0000000
0.0000000	0.0000000	0.2407306	-.1802310	-.4814613	0.0000000
0.0000000	0.0000000	0.0000000	0.2407306	-.3604619	0.0000000
0.0000000	0.0000000	0.0000000	0.0000000	0.4814613	0.0000000
0.0000000	0.1802310	0.0000000	0.0000000	0.0104354	0.0000000
0.0000000	-.2407306	0.1802310	0.0000000	0.1412677	0.0000000
0.0000000	-.1802310	-.2407306	-.3604619	0.0104354	
0.0000000	0.2407306	0.1802310	0.4814613	0.1412677	
0.0000000	0.1802310	-.2407306	0.3604619	-.0208709	

ORBITAL 16

0.0000000	0.0000000	0.1360557	-.0332740	0.2721113	1.4123799
0.0000000	0.0000000	-.0332740	-.1360557	0.0665479	0.0000000
0.0000000	0.0000000	-.1360557	-.0332740	0.2721113	0.0000000
0.0000000	0.0000000	0.0000000	-.1360557	-.0665479	0.0000000
0.0000000	0.0000000	0.0000000	0.0000000	-.2721113	0.0000000
0.0000000	0.0332740	0.0000000	0.0000000	0.3568592	0.0000000
0.0000000	0.1360557	0.0332740	0.0000000	-.7061900	0.0000000
0.0000000	-.0332740	0.1360557	-.0665479	0.3568592	
0.0000000	-.1360557	0.0332740	-.2721113	-.7061900	
0.0000000	0.0332740	0.1360557	0.0665479	-.7137185	

ORBITAL 17

0.0000000	-.0000208	-.0000618	-.0000204	-.0000618	0.0000000
0.0000000	0.0000047	-.0000316	0.0001584	-.0000316	0.0000000
0.0000000	0.0000000	0.0000618	-.0000204	0.0000618	0.0000000
0.0000000	0.0000000	0.9982346	0.0001584	0.0000316	0.0000343
0.0000208	0.0000000	0.0048393	0.0000000	-.0000618	0.0001123
-.0000047	-.0000316	-.0003858	0.0000000	0.0000000	0.0000000

Table 4 (Continued)

0.0000208	0.0000618	-.0000204	0.0000000	0.0000000	0.0000000
-.0000047	0.0000316	0.0001584	-.0000316	0.0000000	
-.0000208	-.0000618	-.0000204	0.0000618	0.0000000	
0.0000047	0.0000316	0.0001584	0.0000316	0.0000000	

ORBITAL 18

0.0000000	0.4970830	-.0012823	0.0008286	-.0012823	0.0000000
0.0000000	0.0117538	0.0003744	-.0004174	0.0003744	0.0000000
0.0000000	0.0000000	0.0012823	0.0008286	0.0012823	0.0000000
0.0000000	0.0000000	-.0001031	-.0004174	-.0003744	-.0005134
-.4970830	0.0000000	0.0003478	0.0000000	-.0012823	0.0042098
-.0117538	0.0003744	0.0096085	0.0000000	0.0000000	0.0000000
-.4970830	0.0012823	0.0008286	0.0000000	0.0000000	0.0000000
-.0117538	-.0003744	-.0004174	0.0003744	0.0000000	
0.4970830	-.0012823	0.0008286	0.0012823	0.0000000	
0.0117538	-.0003744	-.0004174	-.0003744	0.0000000	

ORBITAL 19

0.0000000	0.0078395	0.0002651	-.0051595	0.0002651	0.0000000
0.0000000	-.0221901	-.0101880	0.0058954	-.0101880	0.0000000
0.0000000	0.0000000	-.0002651	-.0051595	-.0002651	0.0000000
0.0000000	0.0000000	-.3947669	0.0058954	0.0101880	-.0039393
-.0078395	0.0000000	1.0694938	0.0000000	0.0002651	0.0061630
0.0221901	-.0101880	-.0155270	0.0000000	0.0000000	0.0000000
-.0078395	-.0002651	-.0051595	0.0000000	0.0000000	0.0000000
0.0221901	0.0101880	0.0058954	-.0101880	0.0000000	
0.0078395	0.0002651	-.0051595	-.0002651	0.0000000	
-.0221901	0.0101880	0.0058954	0.0101880	0.0000000	

Table 4 (Continued)

ORBITAL 20

0.0000000	0.1492633	0.0087930	-.0231993	0.0087930	0.0000000
0.0000000	-.4832581	-.0215788	-.0139364	-.0215788	0.0000000
0.0000000	0.0000000	-.0087930	-.0231993	-.0087930	0.0000000
0.0000000	0.0000000	0.0570872	-.0139364	0.0215788	0.1711090
-.1492633	0.0000000	-.1695634	0.0000000	0.0087930	0.0512194
0.4832581	-.0215788	0.0463006	0.0000000	0.0000000	0.0000000
-.1492633	-.0087930	-.0231993	0.0000000	0.0000000	0.0000000
0.4832581	0.0215788	-.0139364	-.0215788	0.0000000	
0.1492633	0.0087930	-.0231993	-.0087930	0.0000000	
-.4832581	0.0215788	-.0139364	0.0215788	0.0000000	

ORBITAL 21

0.0000000	-.0352025	0.0173696	-.2194699	0.0173696	0.0000000
0.0000000	0.1346356	-.0302699	-.0838586	-.0302699	0.0000000
0.0000000	0.0000000	-.0173696	-.2194699	-.0173696	0.0000000
0.0000000	0.0000000	-.0031413	-.0838586	0.0302699	0.6217388
0.0352025	0.0000000	0.0096437	0.0000000	0.0173696	0.1780571
-.1346356	-.0302699	-.0938222	0.0000000	0.0000000	0.0000000
0.0352025	-.0173696	-.2194699	0.0000000	0.0000000	0.0000000
-.1346356	0.0302699	-.0838586	-.0302699	0.0000000	
0.0352025	0.0173696	-.2194699	-.0273696	0.0000000	
0.1346356	0.0302699	-.0838586	0.0302699	0.0000000	

ORBITAL 22

0.0000000	0.0218351	-.1238968	-.1489660	-.1238968	0.0000000
0.0000000	-.0848024	0.2143641	-.0619414	0.2143641	0.0000000
0.0000000	0.0000000	0.1238968	-.1489660	0.1238968	0.0000000
0.0000000	0.0000000	-.0546383	-.0619414	-.2143641	-.2215206
-.0218351	0.0000000	0.1711891	0.0000000	-.1238968	-.0064200
0.0848024	0.2143641	-.0749717	0.0000000	0.0000000	0.0000000
-.0218351	0.1238968	-.1489660	0.0000000	0.0000000	0.0000000

Table 4 (Continued)

0.0848024	-.2143641	-.0619414	0.2143641	0.0000000	
0.0218351	-.1238968	-.1489660	0.1238968	0.0000000	
-.0848024	-.2143641	-.0619414	-.2143641	0.0000000	

ORBITAL 23

0.0000000	-.0187212	-.0944430	0.2620149	-.0944430	0.0000000
0.0000000	0.0804864	0.0990549	0.2201839	0.0990549	0.0000000
0.0000000	0.0000000	0.0944430	0.2620149	0.0944430	0.0000000
0.0000000	0.0000000	-.0646342	0.2201836	-.0990549	0.5976477
0.0187212	0.0000000	0.2055764	0.0000000	-.0944430	0.1809100
-.0804864	0.0990549	-.1292675	0.0000000	0.0000000	0.0000000
0.0187212	0.0944430	0.2620149	0.0000000	0.0000000	0.0000000
-.0804864	-.0990549	0.2201836	0.0990549	0.0000000	
-.0187212	-.0944430	0.2620149	0.0944430	0.0000000	
0.0804864	-.0990549	0.2201836	-.0990549	0.0000000	

ORBITAL 24

0.0000000	-.0804260	-.1675852	-.1360624	-.1675852	0.0000000
0.0000000	0.4512251	0.0657476	-.0287006	0.0657476	0.0000000
0.0000000	0.0000000	0.1675852	-.1360624	0.1675852	0.0000000
0.0000000	0.0000000	0.0511485	-.0287006	-.0657476	0.1639326
0.0804260	0.0000000	-.1785144	0.0000000	-.1675852	-.0210955
-.4512251	0.0647476	1.5093847	0.0000000	0.0000000	0.0000000
0.0804260	0.1675852	-.1360624	0.0000000	0.0000000	0.0000000
-.4512251	-.0657476	-.0287006	0.0657476	0.0000000	
-.0804260	-.1675852	-.1360624	0.1675852	0.0000000	
0.4512251	-.0657476	-.0287006	-.0647476	0.0000000	

Table 4 (Continued)

ORBITAL 25

0.0000000	0.0421039	0.3612876	0.0325037	0.3612876	0.0000000
0.0000000	-.2849267	0.2648376	-.2257061	0.2648376	0.0000000
0.0000000	0.0000000	-.3612876	0.0325037	-.3612876	0.0000000
0.0000000	0.0000000	0.0495222	-.2257061	-.2648376	0.3437316
-.0421039	0.0000000	-.1769466	0.0000000	0.3612876	-.6238700
0.2849267	0.2648376	-.3641774	0.0000000	0.0000000	0.0000000
-.0421039	-.3612876	0.0325037	0.0000000	0.0000000	0.0000000
0.2849267	-.2648376	-.2257061	0.2648376	0.0000000	
0.0421039	0.3612876	0.0325037	-.3612876	0.0000000	
-.2849268	-.2648376	-.2257061	-.2648376	0.0000000	

ORBITAL 26

0.0000000	0.0031526	0.2156251	-.3182847	0.2156251	0.0000000
0.0000000	0.0105579	0.1389556	0.7572790	0.1389556	0.0000000
0.0000000	0.0000000	-.2156251	-.3182847	-.2156241	0.0000000
0.0000000	0.0000000	-.0295409	0.7572790	-.1389556	-.2594737
-.0031526	0.0000000	0.1057950	0.0000000	0.2156251	0.7834574
-.0105579	0.1389556	-.8988449	0.0000000	0.0000000	0.0000000
-.0031526	-.2156251	-.3182847	0.0000000	0.0000000	0.0000000
-.0105579	-.1389556	0.7572790	0.1389556	0.0000000	
0.0031526	0.2156251	-.3182847	-.2156251	0.0000000	
0.0105579	-.1389556	0.7572790	-.1389556	0.0000000	

ORBITAL 27

0.0000000	-.0568482	0.1160019	0.3413081	0.1160019	0.0000000
0.0000000	0.4501657	0.1700297	-.2831119	0.1700297	0.0000000
0.0000000	0.0000000	-.1160019	0.3413081	-.1160019	0.0000000
0.0000000	0.0000000	0.0362951	-.2831119	-.1700297	-.4510091

Table 4 (Continued)

0.0568482	0.0000000	-.1426493	0.0000000	0.1160019	1.1666600
-.4501657	0.1700297	0.7278310	0.0000000	0.0000000	0.0000000
0.0568482	-.1160019	0.3413081	0.0000000	0.0000000	0.0000000
-.4501657	-.1700297	-.2831119	0.1700297	0.0000000	
-.0568482	0.1160019	0.3413081	-.1160019	0.0000000	
0.4501657	-.1700297	-.2831119	-.1700297	0.0000000	

ORBITAL 28

0.0000000	-.0000208	0.0001584	0.0000316	0.0000618	0.0000000
0.0000000	0.0000047	-.0000204	-.0000618	0.0000316	0.0000000
0.0000000	0.9982346	0.0001584	-.0000316	-.0000618	0.0000000
0.0000000	0.0048393	0.0000000	0.0000618	0.0000316	0.0000000
0.0000288	-.0003858	0.0000000	0.0000000	-.0000618	0.0000000
-.0000047	-.0000204	0.0000000	0.0000000	0.0000000	0.0000343
-.0000208	0.0001584	-.0000316	0.0000000	0.0000000	0.0001123
0.0000047	-.0000204	0.0000618	-.0000316	0.0000000	
0.0000208	0.0001584	0.0000316	0.0000618	0.0000000	
-.0000047	-.0000204	-.0000618	-.0000316	0.0000000	

ORBITAL 29

0.0000000	0.4970830	-.0004174	-.0003744	0.0012823	0.0000000
0.0000000	0.0117538	0.0008286	-.0012823	-.0003744	0.0000000
0.0000000	-.0001031	-.0004174	0.0003744	-.0012823	0.0000000
0.0000000	0.0003478	0.0000000	0.0012823	-.0003744	0.0000000
-.4970830	0.0096085	0.0000000	0.0000000	-.0012823	0.0000000
-.0115738	0.0008286	0.0000000	0.0000000	0.0000000	-.0051340
0.4970830	-.0004174	0.0003744	0.0000000	0.0000000	0.0042098
0.0117538	0.0009286	0.0012823	0.0003744	0.0000000	
-.4970830	-.0004174	-.0003744	0.0012823	0.0000000	
-.0117538	0.0008286	-.0012823	0.0003744	0.0000000	

Table 4 (Continued)

ORBITAL 30

0.0000000	0.0078394	0.0058954	0.0101880	-.0002651	0.0000000
0.0000000	-.0221901	-.0051595	0.0002651	0.0101880	0.0000000
0.0000000	-.3947669	0.0058954	-.0101880	0.0025661	0.0000000
0.0000000	1.0694938	0.0000000	-.0002651	0.0101880	0.0000000
-.0078395	-.0155270	0.0000000	0.0000000	0.0002651	0.0000000
0.0221901	-.0051595	0.0000000	0.0000000	0.0000000	-.0039393
0.0078395	0.0058954	-.0101880	0.0000000	0.0000000	0.0061630
-.0221901	-.0051595	-.0002651	-.0101880	0.0000000	
-.0078395	0.0058954	-.0101880	0.0002651	0.0000000	
0.0221901	-.0051595	0.0002651	-.0101880	0.0000000	

ORBITAL 31

0.0000000	0.1492633	-.0139364	0.0215788	-.0087930	0.0000000
0.0000000	-.4832581	-.0231993	0.0087930	0.0215788	0.0000000
0.0000000	0.0570872	-.0139364	-.0215788	0.0087930	0.0000000
0.0000000	-.1695634	0.0000000	-.0087930	0.0215788	0.0000000
-.1492633	0.0463006	0.0000000	0.0000000	0.0087930	0.0000000
0.4832581	-.0231993	0.0000000	0.0000000	0.0000000	0.1711090
0.1492633	-.0139364	-.0215788	0.0000000	0.0000000	0.0512194
-.4832581	-.0231993	-.0087930	-.0215788	0.0000000	
-.1492633	-.0139364	0.0215788	-.0087930	0.0000000	
0.4832581	-.0231993	0.0087930	-.0215788	0.0000000	

ORBITAL 32

0.0000000	0.0352025	0.0838586	-.0302699	0.0173696	0.0000000
0.0000000	-.1346356	0.2194699	-.0173696	-.0302699	0.0000000
0.0000000	0.0031413	0.0838586	0.0302699	-.0173797	0.0000000
0.0000000	-.0096437	0.0000000	0.0173696	-.0302699	0.0000000
-.0352025	0.0938222	0.0000000	0.0000000	-.0273696	0.0000000
0.1346356	0.2194699	0.0000000	0.0000000	0.0000000	-.6217388

Table 4 (Continued)

0.0352025	0.0838586	0.0302699	0.0000000	0.0000000	-.1780571
-.1346356	0.2194699	0.0173696	0.0302699	0.0000000	
-.0352025	0.0838586	-.0302699	0.0173696	0.0000000	
0.1346356	0.2194699	-.0173696	0.0302699	0.0000000	

ORBITAL 33

0.0000000	-.0218351	0.0619414	0.2143641	-.1338968	0.0000000
0.0000000	0.0848024	0.1489660	0.1238968	0.2143641	0.0000000
0.0000000	0.0546366	0.0619414	-.2143641	0.1238968	0.0000000
0.0000000	-.1711891	0.0000000	-.1238968	0.2143641	0.0000000
0.0218351	0.0749717	0.0000000	0.0000000	0.1238968	0.0000000
-.0848024	0.1489660	0.0000000	0.0000000	0.0000000	0.2215206
-.0218351	0.0619414	-.2143641	0.0000000	0.0000000	0.0064200
0.0848024	0.1489660	-.1238968	-.2143641	0.0000000	
0.0218351	0.0619414	0.2143641	-.1238968	0.0000000	
-.0848024	0.1489660	0.1238968	-.2143641	0.0000000	

ORBITAL 34

0.0000000	-.0187212	0.2201836	-.0990549	0.0944430	0.0000000
0.0000000	0.0804864	0.2620149	-.0944430	-.0990549	0.0000000
0.0000000	-.0646342	0.2201836	0.0990549	-.0944430	0.0000000
0.0000000	0.2055764	0.0000000	0.0944430	-.0990549	0.0000000
0.0187212	-.1292675	0.0000000	0.0000000	-.0944430	0.0000000
-.0804864	0.2620149	0.0000000	0.0000000	0.0000000	0.5976477
0.0187212	0.2201836	0.0990549	0.0000000	0.0000000	0.1809100
0.0804864	0.2620149	0.0944430	0.0990549	0.0000000	
0.0187212	0.2201836	-.0990549	0.0944430	0.0000000	
-.0804864	0.2620149	-.0944430	0.0990549	0.0000000	

Table 4 (Continued)

ORBITAL 35

0.0000000	-.0804260	-.0287006	-.0657476	0.1675852	0.0000000
0.0000000	0.4512251	-.1360624	-.1675852	-.0657476	0.0000000
0.0000000	0.0511485	-.0287006	0.0657476	-.1675852	0.0000000
0.0000000	-.1785144	0.0000000	0.1675852	-.0657476	0.0000000
0.0804260	1.5093847	0.0000000	0.0000000	-.1675852	0.0000000
-.4512251	-.1360624	0.0000000	0.0000000	0.0000000	0.1639326
0.0804260	-.0287006	0.0657476	0.0000000	0.0000000	-.0210955
0.4512251	-.1360624	0.1675852	0.0657476	0.0000000	
0.0804260	-.0287006	-.0657476	0.1675852	0.0000000	
-.4512251	-.1360624	-.1675852	0.0647476	0.0000000	

ORBITAL 36

0.0000000	0.0421039	-.2257061	-.2648376	-.3612876	0.0000000
0.0000000	-.2849267	0.0325037	0.3612876	-.2648376	0.0000000
0.0000000	0.0495222	-.2257061	0.2648376	0.3612876	0.0000000
0.0000000	-.1769466	0.0000000	-.3612876	-.2648376	0.0000000
-.0421039	-.3641774	0.0000000	0.0000000	0.3612876	0.0000000
0.2849267	0.0325037	0.0000000	0.0000000	0.0000000	0.3437316
0.0421039	-.2257061	0.2648376	0.0000000	0.0000000	-.6238700
-.2849267	0.0325037	-.3612876	0.2648376	0.0000000	
-.0411039	-.2257061	-.2648376	-.3612876	0.0000000	
0.2849267	0.0320537	0.3612876	0.2648376	0.0000000	

ORBITAL 37

0.0000000	0.0031526	0.7572790	-.1389556	-.2156251	0.0000000
0.0000000	0.0105579	-.3182847	0.2156251	-.1389556	0.0000000
0.0000000	-.0295409	0.7572790	0.1389556	0.2156251	0.0000000
0.0000000	0.1057950	0.0000000	-.2156251	-.1389556	0.0000000
-.0031526	-.8988449	0.0000000	0.0000000	0.2156251	0.0000000
-.0105579	-.3182847	0.0000000	0.0000000	0.0000000	-.2594737

Table 4 (Continued)

0.0031526	0.7572790	0.1389556	0.0000000	0.0000000	0.7834574
0.0105579	-.3182847	-.2156251	0.1389556	0.0000000	
-.0031526	0.7572790	-.1389556	-.2156251	0.0000000	
-.0105579	-.3182847	0.2156251	0.1389556	0.0000000	
ORBITAL 38					
0.0000000	-.0568482	-.2831119	-.1700297	-.1160019	0.0000000
0.0000000	0.4501657	0.3413081	0.1160019	-.1700297	0.0000000
0.0000000	0.0362951	-.2831119	0.1700297	0.1160019	0.0000000
0.0000000	-.1426493	0.0000000	-.1160019	-.1700297	0.0000000
0.0568482	0.7278310	0.0000000	0.0000000	0.1160019	0.0000000
-.4501657	0.3413081	0.0000000	0.0000000	0.0000000	-.4510091
-.0568482	-.2831119	0.1700297	0.0000000	0.0000000	1.1666600
0.4501657	0.3413081	-.1160019	0.1700297	0.0000000	
0.0568482	-.2831119	-.1700297	-.1160019	0.0000000	
-.4501657	0.3413081	0.1160019	0.1700297	0.0000000	
ORBITAL 39					
0.0000000	0.0000208	-.0000168	-.0000316	0.0001584	0.0000000
0.0000000	-.0000047	0.0000316	0.0000618	-.0000204	0.0000343
0.0000000	0.0000000	-.0000618	0.0000316	0.0001584	0.0001123
0.0000000	0.0000000	0.0000000	-.0000618	-.0000240	0.0000000
0.0000208	0.0000000	0.0000000	0.9982346	0.0001584	0.0000000
-.0000047	-.0003160	0.0000000	0.0048393	0.0000000	0.0000000
-.0000208	0.0000618	-.0000316	-.0003858	0.0000000	0.0000000
0.0000047	-.0000316	0.0000618	-.0000204	0.0000000	
-.0000208	0.0000618	0.0000316	0.0001584	0.0000000	
0.0000047	0.0000316	-.0000618	-.0000204	0.0000000	

Table 4 (Continued)

ORBITAL 40

0.0000000	-.4970830	-.0012823	0.0003744	-.0004174	0.0000000
0.0000000	-.0117538	-.0003744	0.0012823	0.0008286	-.0005134
0.0000000	0.0000000	-.0012283	-.0003744	-.0004174	0.0042098
0.0000000	0.0000000	0.0000000	-.0012823	0.0008286	0.0000000
-.4970830	0.0000000	0.0000000	-.0001031	-.0004174	0.0000000
-.0117538	0.0003744	0.0000000	0.0003478	0.0000000	0.0000000
0.4970830	0.0012823	0.0003744	0.0096085	0.0000000	0.0000000
0.0117538	0.0003744	0.0012823	0.0008286	0.0000000	
0.4970830	0.0012223	-.0003744	-.0004174	0.0000000	
0.0117538	-.0003744	-.0012823	0.0008286	0.0000000	

ORBITAL 41

0.0000000	-.0078395	0.0002651	-.0101880	0.0058954	0.0000000
0.0000000	0.0221901	0.0101880	-.0002651	-.0051595	-.0039393
0.0000000	0.0000000	0.0002651	0.0101880	0.0058954	0.0061630
0.0000000	0.0000000	0.0000000	0.0002651	-.0051595	0.0000000
-.0078395	0.0000000	0.0000000	-.3947669	0.0058954	0.0000000
0.0221901	-.0101880	0.0000000	1.0694938	0.0000000	0.0000000
0.0078395	-.0002651	-.0101880	-.0155270	0.0000000	0.0000000
-.0221901	-.0101880	-.0026511	-.0051595	0.0000000	
0.0078395	-.0002651	0.0101880	0.0058954	0.0000000	
-.0221901	0.0101880	0.0002651	-.0051595	0.0000000	

ORBITAL 42

0.0000000	-.1492633	0.0087930	-.0215788	-.0139364	0.0000000
0.0000000	0.4832581	0.0215788	-.0087930	-.0231993	0.1711090
0.0000000	0.0000000	0.0087930	0.0215788	-.0139364	0.0512194
0.0000000	0.0000000	0.0000000	0.0087930	-.0231993	0.0000000
-.1492633	0.0000000	0.0000000	0.0570872	-.0139364	0.0000000
0.4832581	-.0215788	0.0000000	-.1695634	0.0000000	0.0000000

Table 4 (Continued)

0.1492633	-.0087930	-.0215788	0.0463006	0.0000000	0.0000000
-.4832581	-.p215788	-.0087930	-.0231993	0.0000000	
0.1492633	-.0087930	0.0215788	-.0139364	0.0000000	
-.4832581	0.0215788	0.0087930	-.0231993	0.0000000	

ORBITAL 43

0.0000000	0.0352025	0.0173696	-.0302699	-.0838586	0.0000000
0.0000000	-.1346356	0.0302699	-.0173797	-.2194699	0.6217388
0.0000000	0.0000000	0.0173696	0.0302699	-.0838586	0.1780571
0.0000000	0.0000000	0.0000000	0.0173696	-.2194699	0.0000000
0.0352052	0.0000000	0.0000000	-.0031413	-.0838586	0.0000000
-.1346356	-.0302699	0.0000000	0.0096437	0.0000000	0.0000000
-.0352025	-.0173696	-.0302699	-.0938222	0.0000000	0.0000000
0.1346356	-.0302699	-.0173696	-.2194699	0.0000000	
-.0352025	-.0173696	0.0302699	-.0838586	0.0000000	
0.1346356	0.0302699	0.0173696	-.2194699	0.0000000	

ORBITAL 44

0.0000000	-.0218351	-.1238968	0.2143641	-.0619414	0.0000000
0.0000000	0.0848024	-.2143641	0.1238968	-.1489660	-.2215206
0.0000000	0.0000000	-.1238968	-.2143641	-.0619414	-.0064200
0.0000000	0.0000000	0.0000000	-.1238968	-.1489660	0.0000000
-.0218351	0.0000000	0.0000000	-.0546393	-.0169414	0.0000000
0.0848024	0.2143641	0.0000000	0.1711891	0.0000000	0.0000000
0.0218351	0.1238968	0.2143641	-.0749717	0.0000000	0.0000000
-.0848024	0.2143641	0.1238968	-.1489660	0.0000000	
0.0218351	0.1238968	-.2143641	-.0619414	0.0000000	
-.0848024	-.2143641	-.1238968	-.1489660	0.0000000	

Table 4 (Continued)

ORBITAL 45

0.0000000	0.0187212	-.0944430	0.0990549	0.2201836	0.0000000
0.0000000	-.0804864	-.0990549	0.0944430	0.2620149	0.5796477
0.0000000	0.0000000	-.0944430	-.0900549	0.2201836	0.1809100
0.0000000	0.0000000	0.0000000	-.0944430	0.2620149	0.0000000
0.0187212	0.0000000	0.0000000	-.0646342	0.2201836	0.0000000
-.0804864	0.0990549	0.0000000	0.2055764	0.0000000	0 0.0000000
-.0187212	0.0944430	0.0990549	-.1292675	0.0000000	0.0000000
0.0804864	0.0990549	0.0944430	0.2620149	0.0000000	
0.0187212	0.0944430	-.0990549	0.2201836	0.0000000	
0.0804864	-.0990549	-.0944430	0.2620149	0.0000000	

ORBITAL 46

0.0000000	0.0804260	-.1675852	0.0657476	-.0287006	0.0000000
0.0000000	-.4512251	-.0657476	0.1675852	-.1360624	0.1639326
0.0000000	0.0000000	-.1675852	-.0657476	-.0287006	0.0210955
0.0000000	0.0000000	0.0000000	-.1675852	-.1360624	0.0000000
0.0804260	0.0000000	0.0000000	0.5110485	-.0287006	0.0000000
-.4512251	0.0657476	0.0000000	-.1785144	0.0000000	0.0000000
-.0804260	0.1675852	0.0657476	1.5093847	0.0000000	0.0000000
0.4512251	0.0657476	0.1675842	-.1360624	0.0000000	
-.0804260	0.1675852	-.0657476	-.0287006	0.0000000	
0.4512251	-.0657476	-.1675852	-.1360624	0.0000000	

ORBITAL 47

0.0000000	-.0421039	0.3612876	0.2648376	-.2257061	0.0000000
0.0000000	0.2849267	-.2648376	-.3612876	0.0325037	0.3437316
0.0000000	0.0000000	0.3612876	-.2648376	-.2257061	-.6238700
0.0000000	0.0000000	0.0000000	0.3612876	0.0325037	0.0000000
-.0421039	0.0000000	0.0000000	0.0495222	-.2257061	0.0000000
0.2849267	0.2648376	0.0000000	-.1769666	0.0000000	0.0000000

Table 4 (Continued)

0.0421039	-.3612876	0.2648376	-.3641774	0.0000000	0.0000000
-.2849267	0.2648376	-.3612876	0.0325037	0.0000000	
0.0421039	-.3612876	-.2648376	-.2257061	0.0000000	
-.2849267	-.2648376	0.3612876	0.0325037	0.0000000	

ORBITAL 48

0.0000000	-.0031526	0.2156251	0.1389556	0.7572790	0.0000000
0.0000000	-.0105570	-.1389556	-.2156251	-.3182847	-.2594737
0.0000000	0.0000000	0.2156251	-.1389556	0.7572790	0.7834574
0.0000000	0.0000000	0.0000000	0.2156251	-.3182847	0.0000000
-.0031526	0.0000000	0.0000000	-.0295409	0.7572790	0.0000000
-.0105579	0.1389556	0.0000000	0.1057950	0.0000000	0.0000000
0.0031526	-.2156251	0.1389556	-.8988449	0.0000000	0.0000000
0.0105579	0.1389556	-.2156251	-.3182847	0.0000000	
0.0031526	-.2156251	-.1389556	0.7572790	0.0000000	
0.0105579	-.1389556	0.2156251	-.3182847	0.0000000	

ORBITAL 49

0.0000000	0.0568482	0.1160019	0.1700297	-.2831119	0.0000000
0.0000000	-.4501657	-.1700197	-.1160019	0.3413081	-.4510091
0.0000000	0.0000000	0.1160019	-.1700297	-.2831119	1.1666660
0.0000000	0.0000000	0.0000000	0.1160019	0.3413081	0.0000000
0.0568482	0.0000000	0.0000000	0.0362951	-.2831119	0.0000000
-.4501657	0.1700297	0.0000000	-.1426493	0.0000000	0.0000000
-.0568482	-.1160019	0.1700297	0.7278310	0.0000000	0.0000000
0.4501657	0.1700297	-.1160019	0.3413081	0.0000000	
-.0568482	-.1160019	-.1700297	-.2831119	0.0000000	
0.4501657	-.1700297	0.1160019	0.3413081	0.0000000	

Table 4 (Continued)

ORBITAL 50

0.0000000	0.0000000	-.1473422	0.0000000	0.1473422	0.0000000
0.0000000	0.0000000	0.2677770	0.0000000	-.2677770	0.0000000
0.0000000	0.0000000	0.1473422	0.0000000	-.1473422	0.0000000
0.0000000	0.0000000	0.0000000	0.0000000	0.2677770	0.0000000
0.0000000	0.0000000	0.0000000	0.0000000	0.1473422	0.0000000
0.0000000	0.2677770	0.0000000	0.0000000	0.0000000	0.0000000
0.0000000	0.1473422	0.0000000	0.0000000	0.0000000	0.0000000
0.0000000	-.2677770	0.0000000	-.2677770	0.0000000	
0.0000000	-1473422	0.0000000	-.1473422	0.0000000	
0.0000000	-.2677770	0.0000000	0.2677770	0.0000000	

ORBITAL 51

0.0000000	0.0000000	-.4621680	0.0000000	0.4621680	0.0000000
0.0000000	0.0000000	-.3243192	0.0000000	0.3243192	0.0000000
0.0000000	0.0000000	0.4621680	0.0000000	-.4621680	0.0000000
0.0000000	0.0000000	0.0000000	0.0000000	-.3243192	0.0000000
0.0000000	0.0000000	0.0000000	0.0000000	0.4621680	0.0000000
0.0000000	-.3243192	0.0000000	0.0000000	0.0000000	0.0000000
0.0000000	0.4621680	0.0000000	0.0000000	0.0000000	0.0000000
0.0000000	0.3443192	0.0000000	0.3443102	0.0000000	
0.0000000	-.4621680	0.0000000	-.4621680	0.0000000	
0.0000000	0.3443192	0.0000000	-.3443192	0.0000000	

ORBITAL 52

0.0000000	0.0000000	0.0000000	0.2677770	0.1473422	0.0000000
0.0000000	0.0000000	0.0000000	0.1473422	-.2677770	0.0000000
0.0000000	0.0000000	0.0000000	-.2677770	-.1473422	0.0000000
0.0000000	0.0000000	0.0000000	0.0000000	-.1473422	0.0000000
0.0000000	0.0000000	0.0000000	0.0000000	0.0000000	0.0000000
0.0000000	0.0000000	-.2677770	0.0000000	0.0000000	0.0000000
0.0000000	0.0000000	-.1473422	0.2677770	0.0000000	
0.0000000	0.0000000	0.2677770	0.1473422	0.0000000	

Table 4 (Continued)

0.0000000	0.0000000	0.1473422	0.2677770	0.0000000	

ORBITAL 53

0.0000000	0.0000000	0.0000000	-.3243192	0.4621680	0.0000000
0.0000000	0.0000000	0.0000000	0.4621680	0.3243192	0.0000000
0.0000000	0.0000000	0.0000000	0.3243192	-.4621680	0.0000000
0.0000000	0.0000000	0.0000000	-.4621680	0.3243192	0.0000000
0.0000000	0.0000000	0.0000000	0.0000000	-.4621680	0.0000000
0.0000000	0.0000000	0.0000000	0.0000000	0.0000000	0.0000000
0.0000000	0.0000000	0.3243192	0.0000000	0.0000000	0.0000000
0.0000000	0.0000000	-.4621680	-.3243192	0.0000000	
0.0000000	0.0000000	-.3243192	0.4621680	0.0000000	
0.0000000	0.0000000	0.4621680	-.3243192	0.0000000	

ORBITAL 54

0.0000000	0.0000000	0.1473422	0.2677770	0.0000000	0.0000000
0.0000000	0.0000000	0.2677770	0.1473422	0.0000000	0.0000000
0.0000000	0.0000000	0.1473422	-.2677700	0.0000000	0.0000000
0.0000000	0.0000000	0.0000000	-.1473422	0.0000000	0.0000000
0.0000000	0.0000000	0.0000000	0.0000000	0.0000000	0.0000000
0.0000000	-.2677770	0.0000000	0.0000000	0.0000000	0.0000000
0.0000000	-.1473422	0.2677770	0.0000000	0.0000000	0.0000000
0.0000000	-.2677770	0.1473422	0.0000000	0.0000000	
0.0000000	-.1473422	-.2677770	0.0000000	0.0000000	
0.0000000	0.2677770	-.1473422	0.0000000	0.0000000	

Table 4 (Continued)

ORBITAL 55

0.0000000	0.0000000	0.4621680	-.3243192	0.0000000	0.0000000
0.0000000	0.0000000	-.3423192	0.4621680	0.0000000	0.0000000
0.0000000	0.0000000	0.4621680	0.3243192	0.0000000	0.0000000
0.0000000	0.0000000	0.0000000	-.4621680	0.0000000	0.0000000
0.0000000	0.0000000	0.0000000	0.0000000	0.0000000	0.0000000
0.0000000	0.3243192	0.0000000	0.0000000	0.0000000	0.0000000
0.0000000	-.4621680	-.3243192	0.0000000	0.0000000	0.0000000
0.0000000	0.3243192	0.4621680	0.0000000	0.0000000	
0.0000000	-.4621680	0.3243192	0.0000000	0.0000000	
0.0000000	-.3243192	-.4621680	0.0000000	0.0000000	

Table 5. Population Analysis

Orbital	This Calc.	Hillier and Saunders[8]
Mn		
1s	1.99996	2.0000
2s	1.99977	2.0001
3s	2.01355	2.0000
4s	.08109	.2764
2p	5.99982	5.9987
3p	6.01719	5.9709
4p	.44193	1.2904
3d(e)	1.13781	.8833
$3d(t_2)$	3.99366	3.2892
$3d(e + t_2)$	5.13147	4.1725
O		
1s	1.99743	1.9987
2s	1.93200	1.9292
2p	4.64937	4.6448
Charges		
Mn	+1.31520	+1.29
O	- .57880	- .5725

Table 6. Binding Energies

Orbital	Observed (eV)	Calculated (eV)
$3t_2$	66.1	69.8
$4t_2$	33.1	29.1
$6t_2$	17.1	9.1

Table 7. Experimental Spectrum of MnO_4^-

State	Energy (eV)	Oscillator Strength (12)
$^1T_1$	1.8	
$^1T_2$	2.27	.032
$^1T_2$	3.0 - 3.7	.021
$^1T_2$	3.99	.035
$^1T_2$	5.45	.04 - .07
$^1T_2$	6.6	

Table 8. Spectrum Calculated From Virtual Orbital Theory

State	Assignment	Energy (eV)	Hillier & Saunders Energy (eV)
$^1T_1$	$1t_1 \rightarrow 7t_2$	4.679	
$^1T_1$	$1t_1 \rightarrow 2e$	5.1763	3.09
$^1T_1$	$6t_2 \rightarrow 2e$	5.6490	
$^1T_2$	$1t_1 \rightarrow 7t_2$	5.6738	3.42
$^1T_2$	$6t_2 \rightarrow 2e$	6.7557	4.24
$^1T_2$	$1t_1 \rightarrow 2e$	6.8536	3.81
$^1T_2$	$6t_2 \rightarrow 7t_2$	7.0052	

Table 9. Dipole Strengths

(These were calculated 3 ways[21]:

A - using $\frac{2}{3}(\Delta E)_j G \, |\langle i|r|j\rangle|^2$

B - using $\frac{2}{3}\frac{G}{\Delta E_{ij}} \, |\langle i|\nabla|j\rangle|^2$

C - using $\frac{2}{3} G \, |\langle i|r|j\rangle| \, |\langle i|\nabla|j\rangle|$)

State	Transition	A	B	C	Hillier & Saunders(A)
$^1T_2$	$1t_1 \rightarrow 7t_2$	.10119	.08345	.07957	.0019
$^1T_2$	$6t_2 \rightarrow 2e$	.19885	.09680	.13874	.0084
$^1T_2$	$1t_1 \rightarrow 2e$	.42580	.12759	.23308	.0085
$^1T_2$	$6t_2 \rightarrow 7t_2$	.33692	.19866	.25871	--
$^1T_2$	$6t_2 \rightarrow 7a_1$	.08918	.03423	.05525	--
$^1T_2$	$6a_1 \rightarrow 7t_2$	--	--	.66758	--

Table 10. Spectrum from $\Delta E_{ij} = \frac{\langle i|\nabla|j\rangle}{\langle i|r|j\rangle}$

State	Transition	Energy (eV)
$^1T_2$	$1t_1 \rightarrow 2e$	3.7517
$^1T_2$	$1t_1 \rightarrow 7t_2$	4.4613
$^1T_2$	$6a_1 \rightarrow 7t_2$	4.4980
$^1T_2$	$6t_2 \rightarrow 2e$	4.7134
$^1T_2$	$6t_2 \rightarrow 7t_2$	5.3792
$^1T_2$	$6t_2 \rightarrow 7a_1$	8.9383

Table 11. Magnetic Circular Dichroism A/D

Transition	Measured	Calculated
$1t_1 \rightarrow 2e$	-.24	-.25
$6t_2 \rightarrow 2e$	--	-.230
$1t_1 \rightarrow 7t_2$	.432	+.399
$6t_2 \rightarrow 7t_2$	--	-.379

III. THE GROUND STATE OF TITANIUM MONOXIDE

Introduction

There is an extensive theoretical literature on transition metal compounds going back to the first theories of Werner about their structure in 1893. After the advent of quantum mechanics Bethe,[1] Mulliken,[2] Van Vleck,[3] and Pauling[4] all made significant contributions. More recently, a number of workers such as Wolfsberg and Helmholtz[5] and Ballhausen and Gray,[6] have made important advances toward the understanding of the electronic structure of these compounds, both in their ground and excited states. This progress has been based mainly on very simple theoretical models of the complex using semiempirical parameters to match the experiment. Only recently have *ab initio* methods been used for transition metal compounds and even then only for the simple compounds such as NiF_4,[7] MnO_4^-,[8] TiO and ScF.[9,10]

Here we apply *ab initio* methods to TiO. However, in addition to the Hartree-Fock (HF) wavefunctions, we also examine the generalized valence bond (GVB) and multi-configuration self-consistent field (MCSCF) wavefunctions. These latter methods go beyond HF and lead to a consistent treatment of different electronic states. In addition, the GVB wavefunctions often lead to simple useful interpretations of the bonding and properties of the molecule. Using the information about the bonding gathered from these wavefunctions of TiO we are able to make predictions about the bonding in TiF, TiO_2, TiF_2 and in the oxides and fluorides of the other transition metals.

Description of the Calculation

The methods used herein are described in detail elsewhere,[11,12] but we will review some aspects of the wavefunctions for use in the discussion. The principal concept is that where one had doubly occupied orbitals in the Hartree-Fock (HF) wavefunction

$$\psi_{HF} = \mathcal{A}[\varphi_1\alpha\varphi_1\beta\varphi_2\alpha\varphi_2\beta\cdots\varphi_n\alpha\varphi_n\beta],$$

one now replaces these with singlet-coupled pairs or orbitals giving:

$$\psi_{GVB} = \mathcal{A}[(\varphi_{1a}\varphi_{1b}+\varphi_{1b}\varphi_{1a})(\varphi_{2a}\varphi_{2b}+\varphi_{2b}\varphi_{2a})\cdots (\varphi_{na}\varphi_{nb}+\varphi_{nb}\varphi_{na})\,\alpha\beta\alpha\beta\cdots\alpha\beta] \tag{1}$$

Hence there is now a pair of orbitals $(\varphi_{ia}, \varphi_{ib})$ each containing one electron, where previously there had been one orbital containing two electrons. As in the HF method, the orbitals are solved for variationally so as to obtain the optimum orbitals. The GVB wavefunction (a) is less restricted than the HF wavefunction and hence leads to a lower energy, E. However, the more important attributes are that the GVB wavefunction leads to a consistent treatment of various states (e.g., singlet and triplet) of a molecule; (b) allows proper dissociation of molecule into ground states of atoms, and (c) often leads to simple useful interpretation of bonding.

As was originally shown by Hurley, Lennard-Jones and Pople,[13] each pair in (1) can be represented in terms of two natural orbitals (NO's):

$$[\varphi_{1_a}(1)\varphi_{1_b}(2)+\varphi_{1_b}(2)\varphi_{1_a}(1)] = C_{1_i}\varphi_{1_i}(1)\varphi_{1_i}(2)+C_{2_i}\varphi_{2_i}(1)\varphi_{2_i}(2). \qquad (2)$$

This simplifies the method of solution for the optimal orbitals of (1) allowing them to be determined from general MCSCF calculations. Having the optimum orbitals, they can be transformed back to the GVB orbitals via (2). In the calculation reported herein we used the general MCSCF program written by J. Hinze, making use of the general integral program (for linear polyatomic molecules) written by X. Liu.

The basis set for expansion of the HF and GVB orbitals consisted of a minimum basis set of Slater orbitals as given by Clementi and Raimondi.[14] The internuclear distance was the experimental equilibrium value for the ground state, 3.06 a.u.[15]

Results

A. Energies. In the HF description the $^1\Sigma^+$ and $^{3,1}\Delta$ states of TiO are described as:

$$^1\Sigma^+\text{:}\ \ (\text{core})(8\sigma)^2(9\sigma)^2(3\pi)^4 \tag{3}$$

$$^{3,1}\Delta\text{:}\ \ (\text{core})(8\sigma)^2(9\sigma)^1(3\pi)^4(1\delta)^1 \tag{4}$$

where "(core)" includes the orbitals corresponding to the argon core of Ti and the 1s and 2s electrons of oxygen. The orbitals for these core electrons were calculated self-consistently but do not significantly enter into the bonding process and hence are designated "core orbitals." The HF calculations lead to a $^3\Delta$-$^1\Delta$ separation of .147 eV and a $^3\Delta$-$^1\Sigma^+$ separation of .063 eV. However, as is well known, the HF description of an open shell state such as $^{3,1}\Delta$ leads to a smaller correlation energy error than that of a closed shell state such as $^1\Sigma^+$. Hence the HF calculations do not prove that the $^3\Delta$ is the ground state.

In the GVB calculation, we allow all the valence pairs to be split keeping the core orbitals doubly occupied but solving for all orbitals self-consistently. The energies obtained for the atomic and molecular calculations are given in Tables 2 and 3. As is seen, the $^1\Sigma^+$ state is the lowest state having dropped 2.14 eV in energy while the $^3\Delta$ and $^1\Delta$ dropped 1.27 eV in going from the HF to the GVB description. The resulting energy differences are now

$^3\Delta - {}^1\Sigma^+$ .808 eV (6516 cm^{-1})

$^3\Delta - {}^1\Delta$ .143 eV (1153 cm^{-1})

$^1\Sigma^+ - {}^1\Delta$ .951 eV (7670 cm^{-1})

Experiments have estimated the $^3\Delta - {}^1\Delta$ separation at about 581 cm^{-1} give or take a few hundred cm^{-1} [16,17] and have made only a guess of about 2300 cm^{-1} for the $^3\Delta - {}^1\Sigma^+$ separation.[17] We find that the singlet spectra[18] can be reinterpreted in terms of a $^1\Sigma^+$ ground state with a $^1\Sigma^+ - {}^1\Delta$ separation of 6567 cm^{-1}. Besides being in agreement with the GVB results, this interpretation is consistent with experimental evidence indicating that the ground states of ZrO and HfO [17] as well as the isoelectronic SCF[19] are $^1\Sigma^+$.

The binding energies of the states as calculated are given in Table 4. The $^1\Sigma^+$ binding energy is 2.718 eV, quite low compared with the experimentally determined value of 6.82 eV.[20] However, a minimum basis set is well known to yield relatively poor bond dissociation energies. For example, this type of basis function, for the GVB description of CO yields a binding energy of 6.43 eV whereas the experimental value is 11.08 eV.[21]

B. Wavefunction. The ground states of Ti and O are ^3F and ^3P respectively, corresponding to the configurations Ti (core) $(3d)^2$ $(4s)^2$ and O $(1s)^2(2s)^2(2p)^4$. Such configurations can be described by the following tableaux in which orbitals in the same row are coupled into singlet pairs [as in (2)] and the unpaired orbitals are coupled into a high spin state,

py	py
px	
pz	

$O(^3P)$

4sa	4sb
$3d_{z^2}$	
$3d_{xy}$	

$Ti(^3F)$

(3)

Here we show the tableaux only for one of the wavefunctions of $O(^3P)$ and $Ti(^3F)$. With a MBS the GVB oxygen orbitals are just as in HF, however, as shown in Fig. 1 the GVB description of Ti is slightly different. Namely, the Ti 4s orbitals split [see (2)] so that each orbital builds in p character but in opposite ways so as to hybridize in opposite directions. This allows the electrons in the 4s orbitals to get farther apart while staying close to the nucleus and hence leads to a decrease in the energy.

To form a bond requires combining the atomic states so that an orbital from each atom is coupled into a singlet pair with high overlap between the orbitals in a pair and low overlap between the orbitals in different pairs. For example below we show the diagram for the case in which the Ti $3d_\sigma$ and O p_σ orbitals are coupled into a sigma bond while the O $p_{\pi x}$ and Ti $d_{\pi xz}$ orbitals are coupled into a π bond,

O $p_{\pi y}$	O $p_{\pi y}$
O p_σ	Ti d_σ
Ti 4s	Ti 4s
O $p_{\pi x}$	Ti d_{xz}

The self-consistent orbitals are shown in Fig. 2. The orbitals of the σ bond are shown in Fig. 2ab. Fig. 2b started out as the Op_{σ} orbital and even in the molecule is not changed much. Fig. 2a started out as the Ti $3d_{z^2}$ orbital. It still has the character of this orbital but has been sucked somewhat onto the O.

Fig. 2fg shows what started out as the Ti 4spair. The main changes in these orbitals upon bond formation is some rotation back away from the bond.

In TiO we obtain two equivalent sets of π orbitals. In Fig. 2cd we show the GVB pairs while in Fig. 2e we show the first natural orbital, which corresponds to the doubly occupied orbital in the HF wavefunction. We can consider Fig. 2c to arise from Ti $3d_{xz}$, Fig. 2d from O p_x and Fig. 2e from $O(p_y)^2$. Here we see that the Ti orbital is sucked somewhat onto the O. Because of orthogonality to the Ti 3p core orbitals the O π orbitals get some antibonding character in the Ti.

One could consider this state of TiO to have a triple bond, although the π bonds may not be all too strong. The Ti 4s orbitals do not participate in the bond and hence we can expect to obtain low-lying excited states of TiO by exciting these 4s electrons to suitable empty orbitals. The only suitable empty orbitals involving 3d character are the $3d_{\sigma}$ orbitals since the π orbitals are involved in π bonds. This leads to the $^3\Delta$ and $^1\Delta$ states considered in (4). As expected, these states are low-lying. If the character of the bonding orbitals is not changed, these Δ states would correspond to sd^3 states of Ti rather than s^2d^2 as for the $^1\Sigma$ state.

In Fig. 3 we compare the σ bonding orbitals for the three states of TiO and the atoms. It becomes immediately obvious that the orbitals for the three states of TiO are very much alike. They are all combinations of the Ti $3d_{z^2}$ orbital and the O p_z orbital. Of the two bonding orbitals, one has greater amplitude on the titanium while the other on the oxygen. Both orbitals show amplitude in the internuclear bonding region. However, both orbitals also get more diffuse in the nonbonding region. GVB-ϕ_A which very strongly resembles the Ti $3d_{z^2}$ orbital, has become very diffuse on the non-bonding side of the Ti while a bit tighter in the bonding region. One can see minute differences in this orbital for the three states: it being most diffuse in the $^1\Sigma^+$ state, less in the $^3\Delta$ state, and least in the $^1\Delta$ state. Conversely on the oxygen non-bonding side of this orbital, the $^1\Delta$ is the most diffuse followed by the $^3\Delta$ and $^1\Sigma^+$ orbitals. Hence in the bond region, the orbital is tighter in the energetically favored state. This means the electrons are closer to the nuclei since they tend to be nearer to the line between the nuclei. This would imply an energetically more favorable state. The greater diffuseness on the titanium in the $^1\Sigma^+$ state is due, as we shall see in Figure 4, to the fact that the non-bonding electrons are not occupying that region of space as they are in the $^3\Delta$ and $^1\Delta$ states. Hence electronic repulsion is less and the orbital spreads out. GVB-ϕ_B shows the distinct character of the O $2p_z$ orbital. The three orbitals are just about identical which is expected since the states differ by changes in non-bonding electrons on the titanium side of the molecule. The bonding region shows the orbital to be strongly bonding. The $^1\Sigma^+$ orbital has a more diffuse negative "doughnut" than does either Δ state, this being due to the availability of that part of space since a δ electron is not there as in the Δ states. One can also see in the $^1\Sigma^+$ state orbital a shift of the node towards the titanium. This, of course, favors bonding interactions and such an occurrence is expected in the energetically favored state. The HF orbitals are an average of the GVB orbitals and as such do not allow the fine analysis available with localized one-electron orbitals.

In Figure 4, the 9σ orbitals of the three states are plotted. It is obvious that these are the non-bonding orbitals on titanium since their amplitude is almost entirely on the far (non-oxygen) side of the titanium. The HF and GVB orbitals of the $^3\Delta$ and $^1\Delta$ states are essentially the same since they all contain only one electron. In each case the orbital is distorted away from the bond region.

In the $^1\Sigma^+$ state, the orbitals change drastically. The HF orbital now has anti-bonding character in the internuclear region. This is due to its requirement to stay orthogonal to the other doubly occupied orbitals as well as to the fact that is is now doubly occupied itself. The GVB orbitals, however, are quite different. The most striking difference is that they tend to inhabit different regions of space, hence deviating from sigma <u>orbital</u> symmetry (molecular $^1\Sigma^+$ symmetry is preserved) and reducing their mutual repulsion. This is due to the fact that the orbitals were allowed to mix in Ti $4p_\pi$

character just as the corresponding orbital in Ti mixes in Ti 4p character. A similar result occurs in the $^2\pi$ state of BH [21] and $^1\Sigma^+$ ground state of CO.[22] In the molecule, the lobes are bent away from the bonding region so as to minimize repulsion with pi-bonding electrons. However, in contrast to the HF doubly-occupied orbitals, the GVB orbitals have some slight bonding character in the inter-nuclear region. It is these two effects, the lessening of repulsion and the bonding character of the orbitals, that cause the GVB description to give a more energetically favorable $^1\Sigma^+$ state than the HF description. Since the $^3\Delta$ and $^1\Delta$ states did not show any significant change in these non-bonding orbitals, the $^1\Sigma^+$ state becomes the predicted ground state.

The pi orbitals are plotted in Figure 5. One must remember that the oxygen contributes three electrons towards the four one-electron orbitals while the titanium only contributes one. The orbitals as calculated are constrained to be the same in the x and y directions. Hence one is not surprised to find the greater density of each orbital on the oxygen. The GVB-φ_A orbital is almost entirely an O $2p_\pi$ orbital. A bit of $3d_{xz}$ and $3p_x$ is mixed in so as to shift the node into the bonding region but also to enhance the amplitude of the O $2p_\pi$ orbital in this region. In the $^1\Sigma^+$ state, the enhancement is stronger as the orbital shifts more toward the titanium. Ti $4p_x$

character is now evident as well as stronger $3d_{xz}$ character. The orbitals of the $^3\Delta$ and $^1\Delta$ states do not show this enhancement and are best described in almost entirely O $2p_\pi$ orbitals. The GVB-ϕ_B orbital on the other hand shows distinct Ti $3d_{xz}$-O $2p_\pi$ overlap. This is the pi orbital that is the source of pi bonding. Once again we see a difference in its size between the $^1\Sigma^+$ and the Δ states. In these latter states, the orbital is more diffuse thereby indicating that it is not as energetically favorable. This may be due to the presence of the non-bonding electrons which in the Δ states inhabit an orbital on the far side of the titanium as well as a δ orbital centered on it. The δ orbital is more tightly bound than the other orbital so to minimize repulsion, these orbitals have to stay diffuse. For the $^1\Sigma^+$ state, the non-bonding electrons are both in diffuse orbitals, so the pi orbital can become less diffuse and energetically more favorable.

The fact that the GVB orbitals are held equivalent in the xz and yz plane causes these orbitals to be not quite what we expected. That there is not strong bonding in both planes is obvious. If such were so, it would imply that a reasonable degree of "back-bonding", i.e., the tendency of the oxygen $2p_y$ pair to move into the internuclear region by forming an orbital with the empty $3d_{yz}$ orbital would exist. This does not happen to a significant degree though one might argue for it to a small degree in the $^1\Sigma^+$ state. Instead the pi orbitals present themselves as two bonding and two non-bonding, indicating that a proper description would show the π_y orbitals as O $2p_y$ orbitals (with a small increase in amplitude in the internuclear region--more pronounced in the $^1\Sigma^+$ state) and the π_x orbitals as bonding orbitals formed from the O $2_{\pi x}$ and the Ti $3d_{xz}$. Needless to say, the HF description provides only an average of these orbitals and tells us very little about the actual bonding process.

These plots of the valence orbitals lead us to a refined view of the bonding process in these three states of TiO. The $^1\Sigma^+$ state remains basically as

O $p_{\pi y}$	O $p_{\pi y}$
O p_σ	Ti d_σ
Ti 4s	Ti 4s
O $p_{\pi x}$	Ti $d_{\pi xz}$

i.e., the O p_y electrons and Ti4s electrons stay coupled while the O p_z and Ti d_{z^2} couple to form a sigma bond and the O p_x and Ti d_{z^2} couple to form a pi bond. The $^3\Delta$ state is now described as

O $p_{\pi y}$	O $p_{\pi y}$
O p_σ	Ti d_σ
O $p_{\pi x}$	Ti d_{xz}
Ti 4s	
Ti $d_{\delta xy}$	

i.e., the O p_y orbitals stay coupled and the O p_x and Ti d_{xz} form a pi bond but now the sigma bond is formed by the Ti d_{z^2} orbital and the

O p_z orbital and not by the Ti4s orbital and the O p_z orbital. Hence the molecule separates in this stage into O with the usual $(2p)^4$ configuration and Ti with a configuration of $[AR](4s)^1(3d)^3$! The same thing happens with the $^1\Delta$ state which is now represented as

O $p_{\pi y}$	O $p_{\pi y}$
O p_σ	Ti d_σ
O $p_{\pi x}$	Ti d_{xz}
Ti 4s	Ti $d_{\delta xy}$

The states of the Ti atom corresponding to these situations are ^5F and ^3F which are listed by Moore[23] as 6557 cm^{-1} and 11532 cm^{-1} above the ground state ^3F (s^2d^2). The experimental (18) energy difference between the $^1\Sigma^+$ state and $^3\Delta$ state is 5413 cm^{-1} indicating that the binding energy of TiO $^3\Delta$ with regard to Ti ^5F plus O ^3P is the same as that of TiO $^1\Sigma$ with regard to Ti ^3F plus O ^3P. This is reasonable since the bonding interactions involve the d_σ and d_π orbitals which are the same in both cases. For the $^1\Delta$ state, however, there is no such simple correspondence. Probably the TiO $^1\Delta$ state involves a combination of Ti atomic characters (eg., Ti ^3F s^2d^2, Ti ^3F sd^3, etc.). The experimental TiO $^1\Delta$ - $^1\Sigma$ separation (18) is 6567 cm^{-1}. Thus the $^3\Delta$ - $^1\Sigma$ and $^1\Delta$ - $^1\Sigma$ excitation energies can be considered as basically the energy required to change a 4s electron to a 3d electron. Once this is done and the coupling of the 4s electrons destroyed, the bonds form in the usual manner, i.e., one sigma bond between Ti d_{z^2} and O p_z and one pi bond between Ti d_{xz} and O p_x.

Discussion

It is appropriate to apply the interpretation found for TiO to other systems to see how far and how general the concepts generated are. Let us first consider the monoxides of the first transition row. The first of these is ScO which has an $(4s)^2(3d)^1$ ground state (^2D). To form a double bond such as in TiO requires the Ti $3d_{z^2}$ orbitals to form a sigma bond with the O $2p_z$ and the Ti $3d_{xz}$ orbital to form a pi bond with the O $2p_x$. If Sc is $(4s)^2(3d)^1$ this cannot happen since there is only one d electron. Hence it must be promoted to $(4s)^1(3d)^2$ to form the bond. This gives us (omitting now the O $2p_y$-O $2p_y$ coupling from the scheme)

Sc $3d_{z^2}$	O $2p_z$
Sc $3d_{x^2}$	O $2p_x$
4s	

a $^2\Sigma^+$ state rather than the $^2\Pi$ state

Sc $3d_{z^2}$	O $2p_z$
Sc 4s	Sc 4s
O $2p_x$	

The $^2\Sigma^+$ state benefits from two bonds and this overcomes the energy required to go from the $(4s)^2(3d)^1$ to the $(4s)^1(3d)^2$ configuration which Moore[24] gives as 11, 520 cm^{-1}. The $^2\Sigma^+$ state has been experimentally determined by E. S. R. to be the ground state.[26] The $^2\Pi$ state is reported at 16.441 cm^{-1}.[25] If one were to promote the 4s electron to a 3d orbital to give a $(3d)^3$ configuration, this last electron would go in a δ orbital and give a $^2\Delta$ state. From Moore one would expect this excitation to be about 22,200 cm^{-1}. However, such a transition is not dipole allowed, and no such transition is reported.

For VO the case is different. One can start from the ground state $(4s)^2(3d)^3$ configuration for V, form the sigma and pi bonds with two of the 3d orbitals and arrive at a $^2\Delta$ state:

V $3d_{z^2}$	O 2p
V $3d_{xz}$	O $2p_x$
V 4s	V 4s
V $3d_\sigma$	

One could promote one of the 4s electrons to 3d orbital to arrive at the high spin $^4\Sigma^-$ state:

V $3d_{z^2}$	O $2p_\sigma$
V $3d_{xz}$	O $2p_x$
V 4s	
V $3d_\delta$	
V $3d_\delta$	

According to Moore[27] the energy required in going from $(4s)^2(3d)^3$ to $(4s)^1(3d)^4$ is 2113 cm^{-1}. On this basis we would have expected the $^4\Sigma^-$ state to be about 2000 cm^{-1} = 0.25 eV higher than the $^2\Delta$ state.

However, this type of reasoning is not good enough for such small differences. Experimentally, via E.S.R., the $^4\Sigma^-$ state has been shown to be the ground state.[28] As we proceed to the right in the transition elements the nuclear charge increases bringing the 3d orbitals more and more into the core (in the limit of $Z = \infty$ the 3s, 3p, and 3d orbitals have the same size). Thus relative to the 4s orbitals the 3d orbitals get progressively tighter and their energies get relatively lower.

For V the 4s and 3d levels are close enough so that the $4s^2$ and $4s^1$ states ($^2\Delta$ and $^4\Sigma^-$) are very close. For Cr we can expect the $4s^1$ case to be favored. In Cr, the ground state is $^7S\ (3d)^5(4s)^1$. Hence one would expect a ground state such as $^3\Delta$

CR $3d_\sigma$	O $2p_\sigma$
CR $3d_{xz}$	O $2p_x$
CR $3d_\delta$	CR $3d_\delta$
CR $3d_\delta$	
CR 4s	

or $^5\Pi$

CR $3d_\sigma$	O $2p_\sigma$
CR $3d_{xz}$	O $2p_x$
CR $3d_\delta$	
CR $3d_\delta$	
CR $3d_{yz}$	
CR 4s	

or $^3\Sigma^-$

CR $3d_\sigma$	O $2p_\sigma$
CR $3d_{xz}$	O $2p_x$
CR 4s	CR 4s
CR $3d_\delta$	
CR $3d_\delta$	

The high spin state creates a problem since the occupied $3d_{yz}$ orbital is repulsed by the electrons in the O $2p_y$ orbitals (GVB description; 1 doubly occupied orbital in the HF description). This rules out any "back bonding" as well as weakens the existing pi bond. The $^3\Delta$ state involves coupling between the δ orbitals whereas the $^3\Sigma^-$ state involves it between the 4s orbitals. Moore[29] gives the energy of going from the $(3d)^5(4s)^1$ configuration (^7S) to $(3d)^4(4s)^2$ (^5D) as 7751 cm^{-1}. To recouple the $(3d)^5(4s)$ configuration to a ^5G state necessitates an energy of 20,517 cm^{-1}. Hence it seems likely that the ground state is the $^5\Pi$ state with $^3\Sigma^-$ as the first excited state. This would mean that the Cr-O bond is weaker than in the molecules considered so far. Experiments bare this out since as determined by mass spectrographic methods[30] the dissociation energy of TiO is 163 kcal/mole while that of Cr is 103 kcal/mole. The reduction is significant, being approximately 21,000 cm^{-1} enough to allow recoupling of the ground state of Cr. Since no experiment has determined the ground state, one obtains no help in the prediction. Since VO has a $^4\Sigma^-$ ground state, one can rule out coupling between 4s orbitals and hence the $^3\Sigma^-$ ground state. It appears to be sensible to choose the $^5\Pi$ state since this comes directly from the ground state. It seems doubtful that the repulsion between the new d_π electron and the O 2_π electrons is sufficient to cause a jump of 21,000 cm^{-1} to get to the state which relieves this repulsion. This prediction corresponds to that of Ninomiya[31] but waits for calculation or experiment to be verified. One band has been observed at 16520 cm^{-1} [32] but is unassigned. It could be due to a promotion of the 4s electron into a $3d_\pi$ or $4p_\pi$ orbital. In the atom, a 4s to 4p transition requires 23,300 cm^{-1} but it is conceivable that this could be reduced in the molecule.

The ground state of Mn is 6s $(3d)^5(4s)^2$ with an excited state ^6D $(3d)^6(4s)^1$ 17,052 cm^{-1} higher.[33] One is tempted to take the $^5\Pi$ configuration of CrO and couple another 4s electron to give a $^4\Pi$

Mn $3d_\sigma$	O $2p_\sigma$
Mn $3d_{xz}$	O $2p_x$
Mn 4s	Mn 4s
Mn $3d_\delta$	
Mn $3d_\delta$	
Mn $3d_{yz}$	

or to couple on a $3d_\delta$ to give a $^4\phi$ or a $^4\Pi$

Mn $3d_\sigma$	O $2p_\sigma$
Mn $3d_{xz}$	O $2p_x$
Mn $3d_\sigma$	Mn $3d_\sigma$
Mn $3d_\delta$	
Mn 4s	
Mn $3d_{yz}$	

From the stability of the ground state, we would predict the first $^4\Pi$ even though it would be more in the pattern to have the δ orbitals be more stable. However, when we rationalized VO, the difference in energy was 2000 cm^{-1} which is much less than 17000 cm^{-1}. The ground state of this system is not known. One band is observed at 17,000 cm^{-1},[32] which may be due to a $4s \rightarrow 3d_{\pi}$ transition. The corresponding atomic $4s \rightarrow 3d$ transition is 17052 cm^{-1} but since the bond is weakened, it may require more energy. Analysis of this bond remains to be done.

In Fe, the ground state configuration is $(3d)^6(4s)^2(^5D)$ and the $(3d)^7(4s)^1(^5F)$ state 7000 cm^{-1} higher.[33] Hence we now have six non-bonding electrons to place. The δ orbitals should be paired since one pair of 3d orbitals are singly coupled. The remaining electrons most probably form another pair, that of the 4s electrons. This gives a $^3\phi$ or $^3\Pi$ state.

Fe $3d_{z^2}$	O $2p_{\sigma}$
Fe $3d_{xz}$	O $2p_x$
Fe $3d_{\delta}$	Fe $3d_{\delta}$
Fe 4s	Fe 4s
Fe $3d_{\delta}$	
Fe $3d_{yz}$	

To pair the $3d_{yz}$ orbital with the third $3d_{\delta}$ orbital, thereby making a $^1\Pi$ state is not practical since the ^3P state of Fe is 18378 cm^{-1} higher than the ^5D ground state. To start from the $(3d)^7(4s)^1$ configuration would mean a $^3\Delta$ state starting from a ^5F

Fe $3d_{z^2}$	O $2p_\sigma$
Fe $3d_{xz}$	O $2p_x$
Fe $3d_\delta$	Fe $3d_\delta$
Fe $3d_{yz}$	Fe $3d_{yz}$
Fe 4s	
Fe $3d_\delta$	

This is bad since there are now two electrons in the $d_{\pi y}$ orbital and they would suffer repulsion from the oxygen $d_{\pi y}$ electrons. If one were to couple all four δ electrons one would get a $^3\Pi$ state

Fe $3d_{z^2}$	O $2p_\sigma$
Fe $3d_{xz}$	O $2p_x$
Fe $3d_\delta$	Fe $3d_\delta$
Fe $3d_\delta$	Fe $3d_\delta$
Fe 4s	
Fe $3d_{yz}$	

However, such a state would arise from a mixture of ^5F and ^5P and as such would be from 7000 to 17000 cm^{-1} too high. Hence we predict the ground state to be $^3\Phi$ with $^3\Pi$ (the first) very close by. The FeO spectrum while not analyzed fully shows there to be a state about 5000 cm^{-1} above the ground state. Since no transition from this state to the ground state has been observed, it is likely that this is the second $^3\Pi$ state, not the one associated with the $^3\Phi$ ground state. A transition from the $^3\Phi$ to the $^3\Delta$ excited state would require a transition of a 4s electron to a $3d_{yz}$ orbital (a $\sigma \rightarrow \pi$ transition), a 4p orbital or most likely a mixture of the two. Since the $4s \rightarrow 4p$ transition requires 26000 cm^{-1} and the $4s \rightarrow 3d_{yz}$ 7000 cm^{-1}, some mixture would place the state at about 17000 cm^{-1} -- 20000 cm^{-1}, a region containing three states. The transition from the second $^3\Pi$ state to the $^3\Delta$ state is allowed and would be about 12000 cm^{-1} -- 15000 cm^{-1}. A transition is observed at this energy. Hence we feel confident in assigning the ground state as $^3\Phi$.

Cobalt has a ^4F ground state with configuration $(3d)^7(4s)^2$. A low-lying ^4F excited state with configuration $(3d)^8(4s)^1$ is found 3500 cm^{-1} above the ground state.[34] There are now seven non-bonding electrons to consider after the sigma and pi bonds are made. The obvious choices are $^2\Sigma^+$ and $^2\Pi$.

Co $3d_{z^2}$	O $2p_\sigma$
Co $3d_{xz}$	O $2p_x$
Co $3d_\delta$	Co $3d_\delta$
Co $3d_\delta$	Co $3d_\delta$
Co $3d_{yz}$	Co $3d_{yz}$
Co 4s	

Co $3d_{z^2}$	O $2p_\sigma$
Co $3d_{xz}$	O $2p_x$
Co $3d_\delta$	Co $3d_\delta$
Co $3d_\delta$	Co $3d_\delta$
Co 4s	Co 4s
Co $3d_{yz}$	

In the $^2\Sigma^+$ state, there are two $3d_{\pi y}$ electrons which would feel repulsion from the $O_{\pi y}$ electrons. In the $^2\Pi$ state, the 4s electrons are coupled and such a configuration might not be as energetically favorable as two 3d electrons. Hence the choice remains around how much stability is gained or lost in going from a 4s electron to a $3d_\pi$ electron.

From the small energy needed for the atomic excitation, it seems plausible that the $^2\Sigma^+$ state is favored. It is expected that the $^2\Pi$ state is close by and that the first band in the spectrum be a $^2\Sigma^+ \rightarrow {}^2\Pi$ band. No bands have been isolated in the spectrum which shows activity in the 11000 to 16000 cm^{-1} range. This is too high for the $^2\Sigma^+ \rightarrow {}^2\Pi$ transition and too low for a 4s → 4p transition.

In NiO, the prediction of the ground state should be straightforward. The Ni ground state is ^3F [$(3d)^8 (4s)^2$] with a low-lying ^3D excited state of configuration [$(3d)^9 (4s)^1$].[35] Hence the expected ground state is $^1\Sigma^+$:

Ni $3d_{z^2}$	O $2p_z$
Ni $3d_{xz}$	O $2p_x$
Ni $3d_\delta$	Ni $3d_\delta$
Ni $3d_\delta$	Ni $3d_\delta$
Ni $3d_{yz}$	Ni $3d_{yz}$
Ni 4s	Ni 4s

The spectrum shows two bands, one at 12,700 cm^{-1} and the other at 16447 cm^{-1}, which are assumed to be transitions to the ground state as well as a third band at 21262 cm^{-1} between two excited states. If one were to average the excitation energy for the Ni 4s → 4p $^3F \rightarrow {}^3D$ (33000 cm^{-1}) with that for 4s → 3d (200 cm^{-1}), one arrives at about 17000 cm^{-1}. Thus if the transition is $9\sigma \rightarrow 4\pi$ which would give a $^1\Pi$ state and if the 4π is a mixture of Ni $3d_\pi$ and Ni $4p_\pi$, one would expect an energy such as around 17000 cm^{-1}. If the transition is $\delta \rightarrow \pi$, or $^1\Sigma^+ \rightarrow {}^1\Pi$, $^1\Phi$, one might also expect an energy in this range. The third band might be due to a triplet-triplet transition between a $^3\Pi$ state ($\sigma \rightarrow \pi$) and perhaps another $^3\Pi$ state ($\delta \rightarrow \pi$). Analysis and calculations are needed to support this conjecture.

For CuO, an interesting problem presents itself. The ground state of Cu is $(3d)^{10}(4s)^1$, a ^2S. The ^2D $(3d)^9(4s)^2$ excited state is 11,203 cm^{-1},[36] higher. If one wishes to form the sigma bond with the $3d_{z^2}$ orbital, one must undergo a sizeable transition. However, this transition is about the same as that required in ScO. Hence it does not seem unreasonable if the $3d_{z^2}$ is doing the bonding. However, it may be that in these higher transition metals that the 3d orbitals are almost core like and that the bond now forms with the 4s orbitals. The bond length of CuO is 1.728 Å[30] while FeO, CrO and TiO are about the 1.62 Å. Bond lengths in NiO and CoO are not reported. Since the d orbitals contract as the nuclear charge increases, it seems likely that in this case, the bonding occurs with the Cu 4s orbital and the O $2p_z$ orbital. This is the state reported experimentally.[37]

One would expect CuF_2 to be linear if the bonding occurred through the 4s orbitals since GVB theory shows them to separate. A HF calculation by Basch, Hollister and Moskowitz[46] showed this to be the case. This molecule would separate to the $(3d)^9(4s)^2$ state but the compensation of the extra bond outweighs the energy that has to be expended to get it there.

To the oxides of the second and third transition row metals, one can apply the same criteria used for the first row. YO and LAO are expected to have $^2\Sigma^+$ ground states. Such has been found experimentally.[38,39] ZrO and HfO have $^1\Sigma^+$ ground state.[19] NbO and TaO have $^2\Delta$ ground states.[40-42] WO is reported to have a $^3\Sigma^-$ ground state[43] but this is not certain. This is not unreasonable since W has a ground state configuration of $(5d)^4(6s)^2$ whereas Cr was $(3d)^5(4s)^1$. Hence one expects $^3\Sigma^-$:

W $5d_{z^2}$	O $2p_z$
W $5d_{xz}$	O $2p_x$
W 4s	W 4s
W $5d_\delta$	
W $5d_\delta$	

RuO has been observed at tentatively assigned $^3\Sigma^+$ ground state[43] but a $^3\Delta$ ground state is more probable--especially since some splittings in the spectra are associated with rotational isotope effects. Such a state was described for FeO assuming one started with the $(3d)^7(4s)^1$ configuration. The ground state of Ru has the configuration $(4d)^7(4s)^1$. Spectra of the other transition metals have not been reported.

One could also characterize the fluorides of the transition metals, assuming the formation of one sigma bond since the ground state of F atom is ^2P

F p_x	F p_x
F p_y	F p_y
F p_z	

The structure of ScF is predicted to be a $^1\Sigma^+$ (being isoelectronic with TiO)

Sc $3d_{z^2}$	F $2p_\sigma$
F $2p_x$	F $2p_x$
F $2p_y$	F $2p_y$
Sc 4s	Sc 4s

Experimentally this has been verified for ScF,[44] YF, and LaF.[45] One can go through and analyze the fluorides as has been done with the oxides, but such is tedious and can probably best be left as an exercise for the interested reader.

As has become obvious during this discussion, the stability of the compound depends on the placement of the non-bonding electrons. As more of these are added, the stability decreases until as in CoO and NiO, the compounds barely exist and few experimental results are available. The bonding is the same in each compound; a sigma bond between the $3d_{z^2}$ and the O $2p_z$ (or F $2p_z$) and a pi bond between the $3d_{xz}$ and the O $2p_x$. (This may not be the bonding in CuO). It is intriguing that the sigma bond involves the $3d_{z^2}$ orbital and not the 4s orbital. Perhaps it is because the $3d_{z^2}$ orbital is more stable--being closer to the nucleus or because the orbitals are in some way "right for each other" i.e., conducive to efficient spin coupling. Such ideas lead to speculation about the compounds formed when one or more oxygens are added. TiO_2 for example could not be linear but would probably have an O-Ti-O angle of between 90° and 150°. This is due to the desire of the second oxygen to form a sigma bond with a d_{z^2}-like orbital. Using the $3d_{z^2}$ orbital in both bonds would lead to large repulsive interactions. IR frequencies have been observed which indicate this.[19] All the stable oxides (MnO_4^-, $CrO_4^=$, etc.) have electrons available to form a double bond with each O.[8] This is the take home lesson from the calculation--that free oxygen bond transition metals with both a single bond and a double bond, both emanating from d orbitals.

Summary

The GVB calculations on TiO lead to an interpretation of the bonding as involving both a sigma bond made up of Ti $3d_{z^2}$, O $2p_z$ electron pair and a pi bond formed from the Ti $3d_{xz}$ and O $2p_x$ orbitals. Such bonding forces the Ti 4s electrons to remain spin-paired thereby making the ground state $^1\Sigma^+$. Application of this interpretation to the other transition metal oxides allows predictions to be made of the ground and low-lying excited states of these molecules.

References

1. H. Bethe, Ann. Physik., [5], 3, 133 (1929).
2. R. S. Mulliken, Phys. Rev., 40, 55 (1932).
3. J. H. Van Vleck, J. Chem. Phys., 3, 803 (1935); ibid., 807.
4. L. Pauling, The Nature of the Chemical Bond, Cornell University Press, Ithaca, New York, 1940; Third ed. 1960.
5. M. Wolfsberg and L. Helmholtz, J. Chem. Phys., 20, 837 (1952).
6. C. J. Ballhauser and H. B. Gray, Molecular Orbital Theory, W. A. Benjamin, Inc., New York, New York, 1964.
7. H. Basch, C. W. Hollister, and J. W. Moskowitz, Sigma Molecular Theory, Sinanoglu and Wiberg, eds., Yale Univ. Press, 1970.
8. A. P. Mortola, J. W. Moskowitz and H. Basch--to be published.
9. K. D. Carlson and C. Moser, J. Chem. Phys., 46, 35 (1967); J. Phys. Chem., 67, 2644 (1963).
10. K. D. Carlson and R. K. Nesbit, J. Chem. Phys., 41, 1051 (1964).
11. W. J. Hunt, P. J. Hay and W. A. Goddard III to be published, Contribution No. 4360, 4364 from California Institute of Technology.
12. P. J. Hay, W. J. Hunt, and W. A. Goddard III to be published, Contribution No. 4407 from California Institute of Technology.
13. A. C. Hurley, J. E. Lennard-Jones and J. A. Pople, Proc. Roy. Soc. (London), A220, 446 (1963).

14. E. Clementi and D. L. Raimondi, J. Chem. Phys., **38**, 2686 (1963).

15. G. Herzberg, Spectra of Diatomic Molecules, D. Van Nostrand Company, Inc., Princeton, New Jersey, 1950, p. 576.

16. J. G. Phillips, Astrophys. J., **115**, 567 (1952).

17. W. Weltner and D. McLeod, J. Phys. Chem., **69**, 3488 (1965).

18. A. P. Mortola and W. A. Goddard III, to be published.

19. D. McLeod and W. Weltner, J. Phys. Chem., 70, 3293 (1966).

20. U. Uhler, dissertation, University of Stockholm, Sweden, 1954.

21. R. J. Blint and W. A. Goddard III, J. Chem. Phys., **56**, 0000 (1972).

22. A. P. Mortola and W. A. Goddard III, to be published.

23. C. E. Moore, Atomic Energy Levels, Circular of the National Bureau of Standards, 467, Vol. 1, U.S. Government Printing Office, Washington, D.C., 1949, p. 274.

24. ibid., p. 260.

25. W. Weltner, D. McLeod and P. H. Kasai, J. Chem. Phys., **46**, 3172 (1967).

26. P. Kasai and W. Weltner, J. Chem. Phys., **43**, 2553 (1965).

27. Ref. 23, p. 292.

28. P. H. Kasai, J. Chem. Phys., **49**, 4979 (1968).

29. Ref. 23, Vol. II, p. 3.

30. Tables of Constants and Numerical Data, S. Bourcher, edit., Pergamon Press, Ltd., Oxford, England 1970.

31. M. Ninomiya, J. Phys. Soc. Japan, 10, 829 (1955).

32. G. Herzberg, Spectra of Diatomic Molecules, D. Van Nostrand Company, Inc., Princeton, New Jersey 1950.

33. Ref. 29, p. 27.

34. Ref. 29, p. 79.

35. Ref. 29, p. 98.

36. Ref. 29, p. 112.

37. J. S. Shirk and A. M. Bass, J. Chem. Phys., 52, 1894 (1970).

38. P. Kasai and W. Weltner, J. Chem. Phys., 43, 2553 (1965).

39. W. Weltner, D. McLeod and P. H. Kasai, J. Chem. Phys., 46 3172 (1967).

40. C. J. Cheetham and R. F. Barrow, Trans. Far. Soc., 63, 1835 (1967).

41. W. Weltner and D. McLeod, J. Chem. Phys., 42, 882 (1965).

42. U. Uhler, Arkiv. Fysik, 8, 265 (1954).

43. V. Raziunas, G. Macur, and S. Katz, J. Chem. Phys., 43, 1010 (1965).

44. D. McLeod and W. Weltner, J. Phys. Chem., 70, 3293 (1966).

45. R. F. Barrow, M. W. Bastin, D. L. G. Moore and C. J. Pott, Nature, 215, 1072 (1967).

Table I. Basis Functions

Atom	Type	Exponent
Ti	1s	21.44
Ti	2s	7.69
Ti	$2p_\sigma$	9.03
Ti	3s	3.68
Ti	$3p_\sigma$	3.37
Ti	$3d_\sigma$	2.71
Ti	4s	1.20
Ti	$4p_\sigma$	1.12
Ti	$2p_\pi$	9.03
Ti	$3p_\pi$	3.37
Ti	$3d_\pi$	2.23
Ti	$4p_\pi$	1.12
Ti	$3d_\delta$	2.71
O	1s	7.66
O	2s	2.25
O	$2p_\sigma$	2.23
O	$2p_\pi$	2.71

Table 2. Atomic Energies

Atom	State	Conf.	Type	Energy (a.u.)
Ti	^3F	$(4s)^2(3d)^2$	HF	-846.8402097
			GVB[a]	-846.8632540
O	^3P	$(2p)^4$	HF	- 74.5403620[b]

[a] One pair correlated: 4s with 4p.

[b] From reference 10.

Table 3. TiO Results

State	Conf.	Type	Energy (a.u.)	ΔE
$^3\Delta$	$(9\sigma)^1(1\delta)^1$	HF	-921.4207966	
		GVB	-921.4738185	.0468
		8σ mixed $\overline{\omega}$ 10σ*		
		3π mixed $\overline{\omega}$ 4π		
$^1\Delta$	$(9\sigma)^1(1\delta)^1$	HF	-921.4216817	
		GVB		
		8σ mixed $\overline{\omega}$ 10σ*	-921.4685545	.0469
		3π mixed $\overline{\omega}$ 4π		
$^1\Sigma^+$	$(9\sigma)^2$	HF	-921.4247725	
		GVB	-921.5035053	.0787
		8σ mixed $\overline{\omega}$ 10σ		
		3π mixed $\overline{\omega}$ 4π		
		9σ mixed $\overline{\omega}$ 5π		

* Another configuration [$(8\sigma)^1(10\sigma)^1$] has been allowed to mix in these results but contributes very little.

Table 4. Binding Energies

State	Type	Binding Energy (a.u.)	eV
$^3\Delta$	HF	.046419	1.263
$^1\Delta$	HF	.041004	1.116
$^1\Sigma^+$	HF	.044095	1.120
$^3\Delta$	GVB	.0702025	1.910
$^1\Delta$	GVB	.0648385	1.764
$^1\Sigma^+$	GVB	.099889	2.718

Figure Captions

Figure 1. Titanium Orbitals

(a, b) 4s orbitals with 4p character mixed in.

(c) $3d_{z^2}$ orbital

(d) $3d_\delta$ orbital

Figure 2. Orbitals of TiO $^1\Sigma^+$ state

(a, b) Sigma bonding orbitals

(c, d) Pi bonding orbitals

(e) Doubly occupied Pi orbital

(f, g) Non-bonding orbitals

Figure 3. Sigma Bonding Orbitals

(a) Ti $3d_{z^2}$ orbital

(b) O $2p_z$ orbital

(c, d) GVB sigma bonding orbitals of $^1\Sigma^+$ state.

(e) HF sigma bonding orbitals of $^1\Sigma^+$ state

(f, g) GVB sigma bonding orbitals of $^1\Delta$ state

(h) HF sigma bonding orbitals of $^1\Delta$ state

(i, j) GVB sigma bonding orbitals of $^3\Delta$ state

(k) HF sigma bonding orbitals of $^3\Delta$ state

Figure 4. Non-Bonding Orbitals

(a, b) GVB orbitals of Ti 4s electrons

(c, d) GVB non-bonding orbitals of $^1\Sigma^+$ state

(e) HF doubly occupied non-bonding orbital of $^1\Sigma^+$ state

(f) GVB singly occupied non-bonding orbital of $^1\Delta$ state

(g) HF singly occupied non-bonding orbital of $^1\Delta$ state

(h) GVB singly occupied non-bonding orbital of $^3\Delta$ state

(i) HF singly occupied non-bonding orbital of $^3\Delta$ state

Figure 5. Pi Bonding Orbitals

(a) O p_x orbital

(b) Ti $3d_{xz}$ orbital

(c, d) GVB pi bonding orbitals of $^1\Sigma^+$ state

(e) HF pi bonding orbitals of $^1\Sigma^+$ state

(f, g) GVB pi bonding orbitals of $^1\Delta$ state

(h) HF pi bonding orbitals of $^1\Delta$ state

(i, j) GVB pi bonding orbitals of $^3\Delta$ state

(k) HF pi bonding orbitals of $^3\Delta$ state

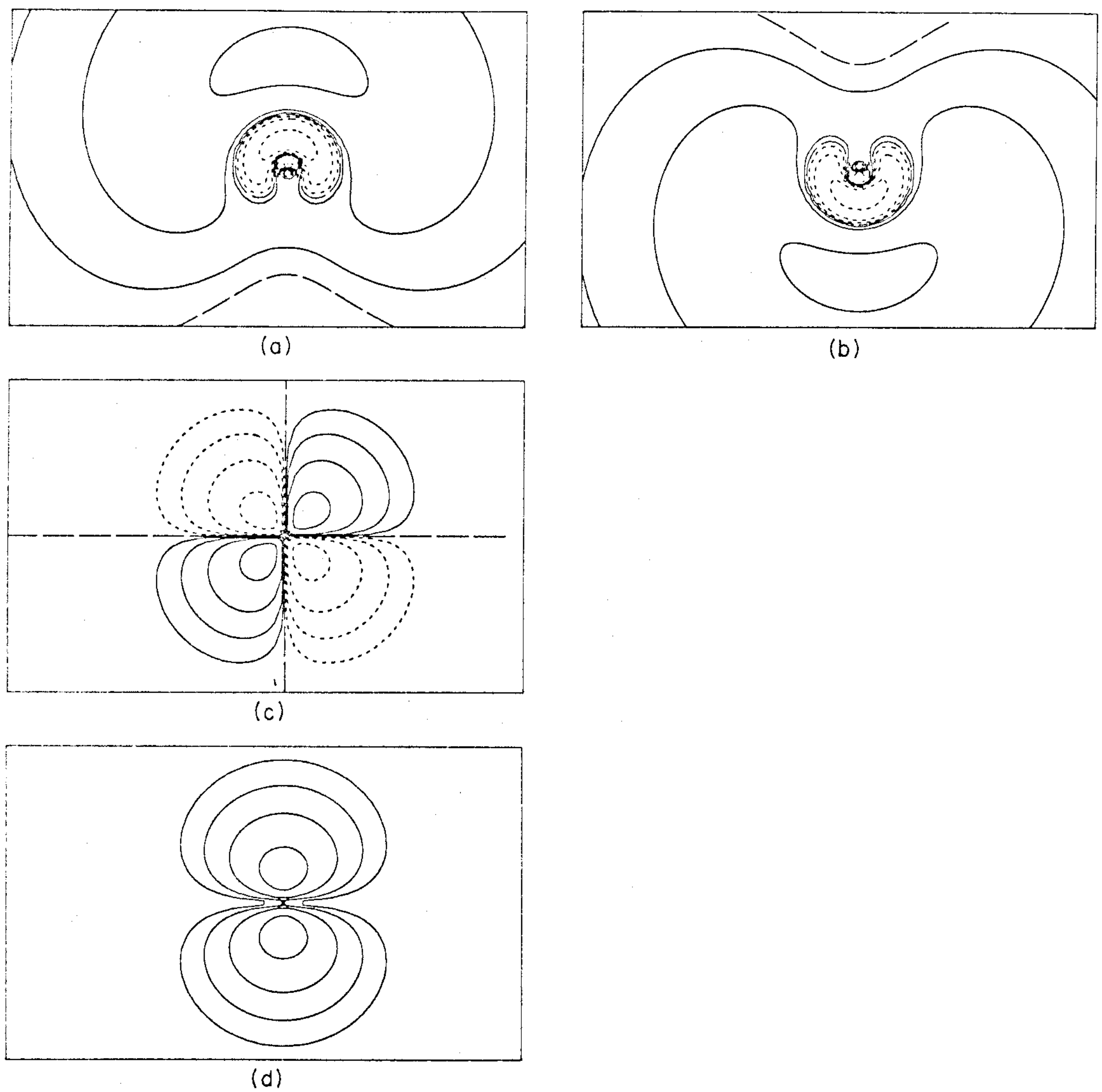

FIGURE 1

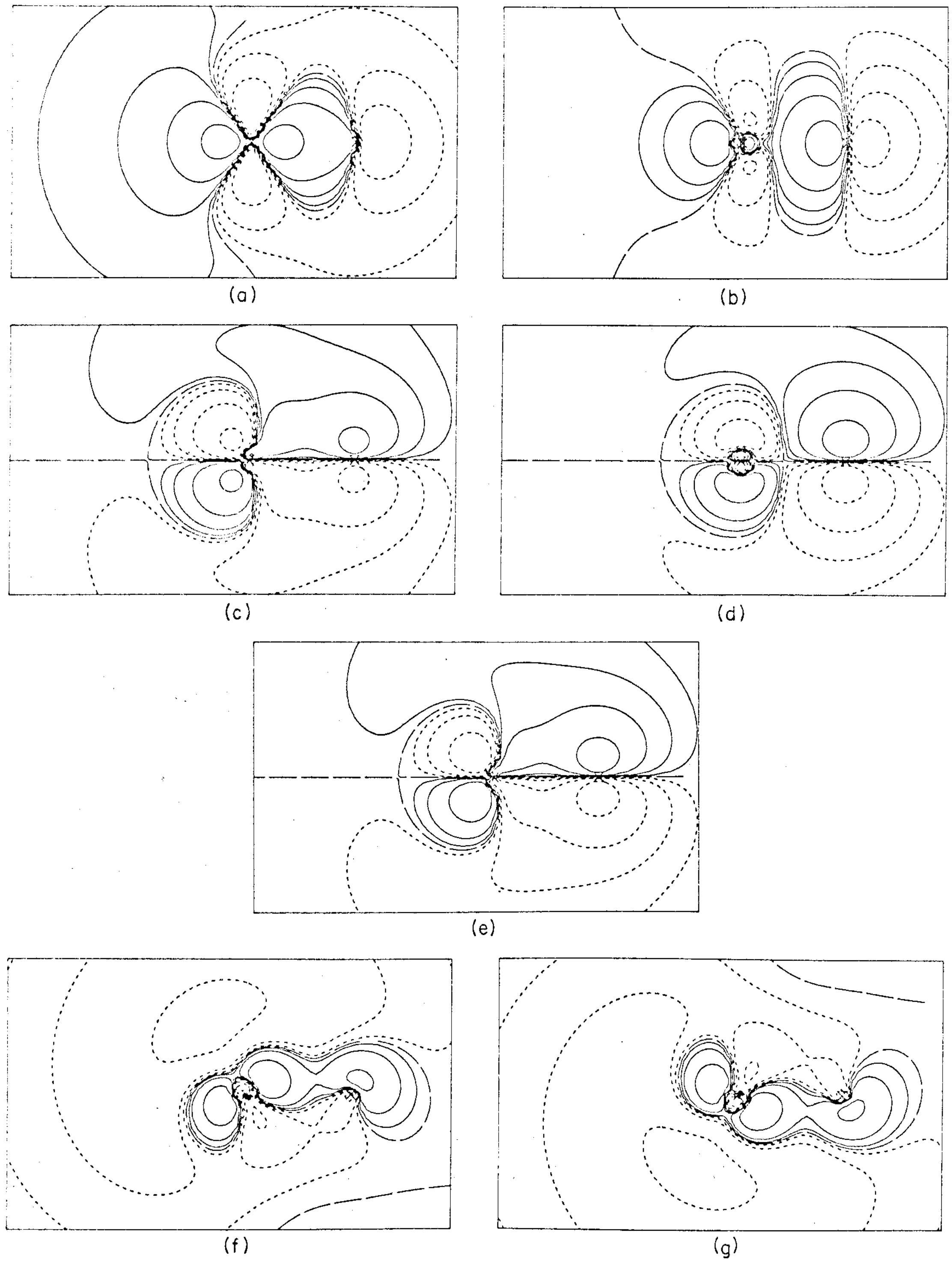

FIGURE 2

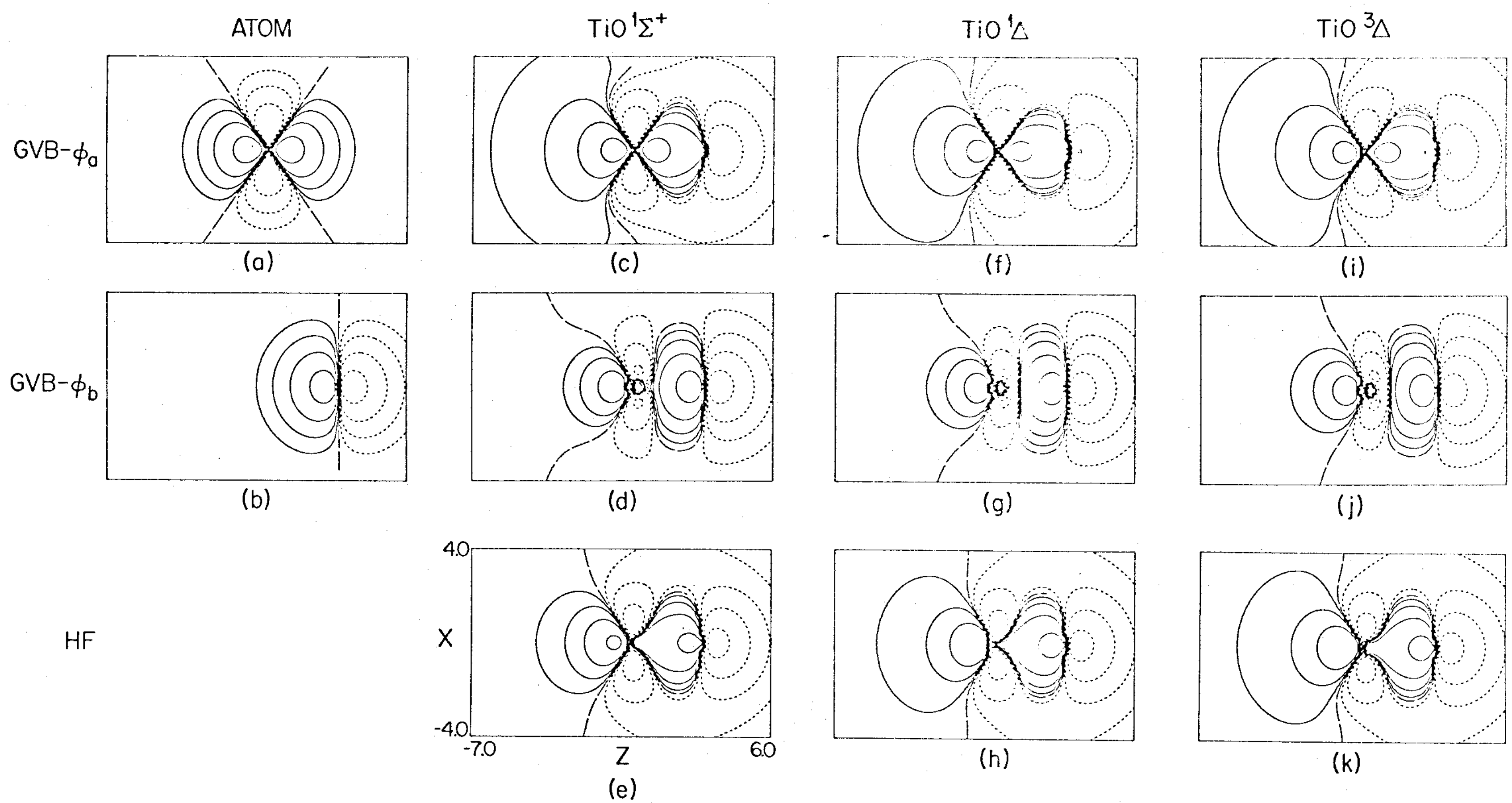

ATOM
TiO $^1\Sigma^+$
TiO $^1\Delta$
TiO $^3\Delta$
GVB-ϕ_a
GVB-ϕ_b
HF
(a)
(b)
(c)
(d)
(e)
(f)
(g)
(h)
(i)
(j)
(k)
4.0
-4.0
X
-7.0
Z
6.0

FIGURE 3

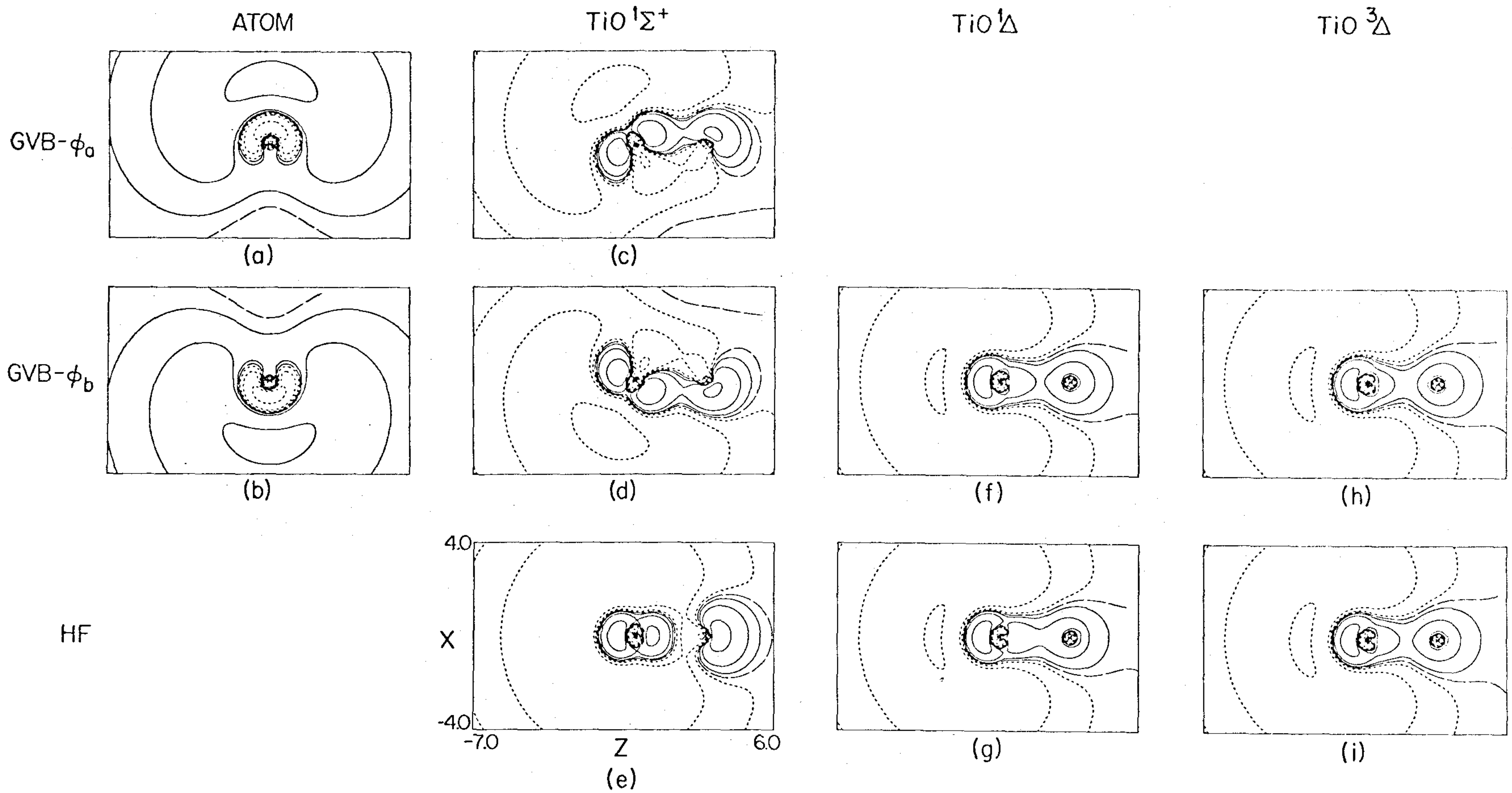
ATOM
TiO $^1\Sigma^+$
TiO $^1\Delta$
TiO $^3\Delta$
GVB-ϕ_a
GVB-ϕ_b
HF
(a)
(b)
(c)
(d)
(e)
(f)
(g)
(h)
(i)
4.0
-4.0
X
-7.0
6.0
Z

FIGURE 4

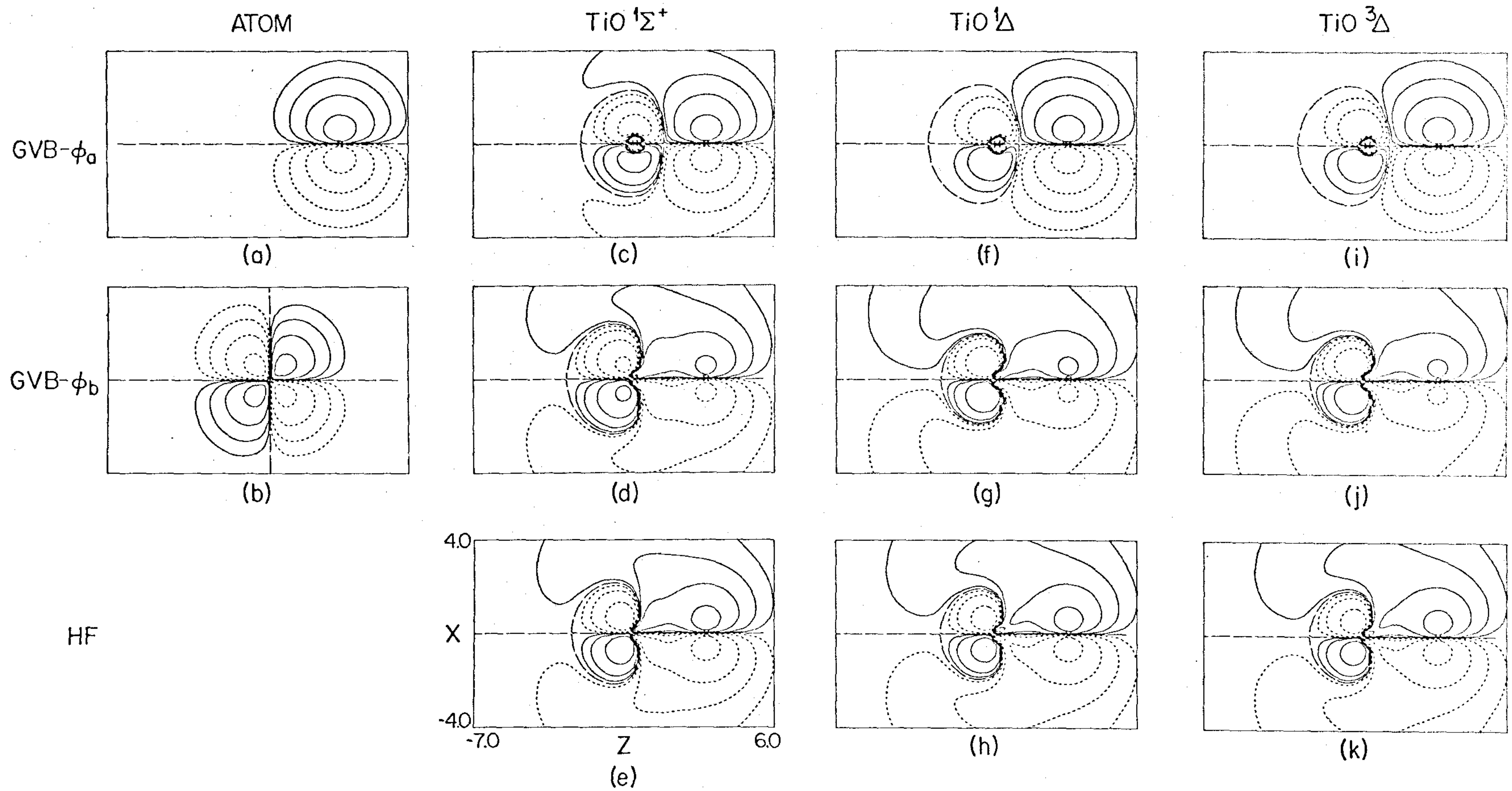
ATOM
TiO $^1\Sigma^+$
TiO $^1\Delta$
TiO $^3\Delta$
GVB-ϕ_a
GVB-ϕ_b
HF
(a)
(b)
(c)
(d)
(e)
(f)
(g)
(h)
(i)
(j)
(k)
4.0
X
-4.0
-7.0
Z
6.0

FIGURE 5

IV. THE SPECTRUM OF TITANIUM MONOXIDE

I. INTRODUCTION

Investigations of the spectrum of TiO have been carried on for over 40 years, the original interest in the molecule being that it is observed strongly in the spectrum of class M and S stars. During this time many revisions of the spectral assignments have been made, all based on the analysis of the complex spectrum. No detailed theoretical investigation has been made, such a project being beyond the scope of theory until recently. As a result, assignments were based on various assumptions concerning the nature of the electronic states. We have carried out ab initio calculations of these states and from these results suggest reassignments of the spectrum and predict locations of several lines not yet observed.

II. COMPUTATIONAL METHOD

We use a form of the multiconfiguration self-consistent field (MCSCF) method, developed by Wahl and Das, Roothaan and Hinze, Clementi and Veillard, Hunt, Hay and Goddard, and others.[1] In this method the wavefunction is described by an expansion in terms of a linear combination of determinental wavefunctions (as in the configuration interaction method), however, the orbitals in the determinants are solved for self-consistently [as in the Hartree-Fock (HF) method]. Since the orbitals are optimal a short expansion can be used and the wavefunctions can often be interpreted in terms of simple concepts. The specific way in which the wavefunction is constructed and interpreted is based on the generalized valence bond (GVB) method, however, the details of this will not be important herein. As compared to Hartree-Fock, the GVB method involves correlating each of the doubly occupied orbitals involved in a bond or describing a valence-like non-bonding pair of electrons. As a result the wavefunctions properly describe the process of dissociating a molecule, and generally lead to good values for excitation energies.

The calculations reported in this paper were performed on an IBM 370 computer using a program written by J. Hinze and X. Liu A minimum basis set of Slater orbitals was used (using experiments from Clementi and Raimondi) as in our former calculations[2] and the internuclear distance set at 1.62 Å, the reported experimental internuclear distance for the $^3\Delta$ state.[3]

III. RESULTS

The energies calculated via the HF and GVB methods are given in Table I.

The experimental spectrum has been classified into six band systems, three assigned as singlets and three as triplets. The singlet bands are known as the β, δ, and φ systems and do not seem to be as well characterized as the triplet systems. The β system was first observed by Lowater in 1929[4] and has been studied by Phillips[5] and Linton and Nichols.[6] At the present time, it is classified as $^1\Phi - {}^1\Delta$. Lowater had classified this band as $^1\Pi$ - $^1\Sigma$ transition and Phillips admits that this is indeed a possibility, but rules it out since the spectra is interpreted to indicate that this transition must have a state in common with the δ band. This δ band has been studied by Phillips in 1950[5] and assigned as a $^1\Pi$ - $^1\Delta$ transition. The φ band has been characterized as a $^1\Pi$ - $^1\Sigma$ transition by Pettersson and Lindgren.[7, 8]

The triplet bands are known as the α, γ, and γ' systems. The α system is assigned as a $^3\Delta$ - $^3\Delta$ transition by Phillips.[9] The γ system was assigned as a $^3\Pi$ - $^3\Delta$ transition by Phillips[10] in 1951 but changed to a $^3\Phi$ - $^3\Delta$ transition in 1969.[9] The reason for this was to explain the γ' system observed by Coheur[11] as a $^3\Pi$ - $^3\Delta$ transition. The energies of the 0-0 vibrational band of these six systems are given in Table 2. It must be pointed out that all these spectra were obtained via emission techniques. The only recorded absorption spectra are those of Weltner and McLeod[12] taken at 4°K and 20°K in neon and argon matrices respectively. These spectra seem to agree closely with the emission spectra of the free gas.

The previous interpretations concluded that the $^3\Delta$ state is the ground state and that $^1\Sigma$ has above $^1\Delta$. However, we find that $^1\Sigma$ lies below both $^3\Delta$ and $^1\Delta$ and is the ground state. Two allowed transitions have this state as the common lower state: the $^1\Pi_B \rightarrow {}^1\Sigma^+$ and the $^1\Pi_a \rightarrow {}^1\Sigma^+$ emissions. The energy calculated for the $^1\Sigma^+$ transition is 20651 cm^{-1}. This is fairly close to the energy of 17, 841 cm^{-1} recorded for the (0-0) line of the β band. This band had previously been assigned as a $^1\Phi - {}^1\Delta$ band with a suggestion that it might also be a $^1\Pi - {}^1\Sigma^+$ band. The reason for that assignment was that it should have a state in common with the δ band. This can easily be arranged if one assigns the δ band as the $^1\Pi_B - {}^1\Delta$ transition. Such a transition has a calculated energy of 12981 cm^{-1}, not far from the experimental energy of 11, 273 cm^{-1}. This leaves the φ band with experimental energy of 9054 cm^{-1} to correspond to the $^1\Pi_A - {}^1\Sigma^+$ transition with calculated energy of 11, 958 cm^{-1}. These discrepancies between the experimental and theoretical values are reasonable. The calculations used the same bond length for all states and should lead to a ΔE larger than the experimental 0-0 value.

If we decide to hold the $^1\Pi_B$ state fixed and raise the $^1\Sigma^+$ state so that the energy of the $^1\Pi_B - {}^1\Sigma^+$ state equals that observed as the (0-0) energy of the β band, one raises the state by 20651 - 17841 cm^{-1} = 2810 cm^{-1}. One then finds for the energy difference between the $^1\Pi_A$ and $^1\Sigma^+$ states 11958 cm^{-1} - 2810 cm^{-1} = 9148 cm^{-1}. This requires a lowering of the $^1\Pi_A$ state by only 94 cm^{-1} to have the energy difference equal that of the φ band. One then can make the ${}^1\Pi_B$ - ${}^1\Delta$ energy difference equal that recorded for the δ band by raising the energy of the ${}^1\Delta$ state by 1708 cm^{-1}. Hence one can arrive at the diagram shown in Figure 1 for the states of the singlet spectrum. The states are assigned so that the transitions occur only between those states which are dipole allowed. Hence a transition between the ${}^1\Phi$ state and the ${}^1\Sigma$ state is forbidden. The β transition (${}^1\Pi_B$ - ${}^1\Sigma^+$) can be described in terms of one-electron orbitals as a $4\pi \rightarrow 9\sigma$ transition. This $\pi^* \rightarrow n$ transition could be looked upon as a transition from a 4p Ti orbital to a 4s-like orbital. The corresponding atomic transition [Ti ${}^3D$ of $(3d)^2(4s)^1(4p)^1 \rightarrow {}^3F$ of $(3d)^2(4s)^2$] is 9900 cm^{-1}.[13] The δ transition (${}^1\Pi_B \rightarrow {}^1\Delta$) can be described as $4\pi \rightarrow 1\delta$ transition. This is similar to the $4p \rightarrow 3d$ transition in Ti, which has a transition energy of 8500 cm^{-1} [${}^3D$ of $(3d)^2(4s)^1(4p)^1 \rightarrow {}^3F$ of $(3d)^3(4s)^1$]. This time the molecular transition has increased in energy, perhaps due to some stabilization of the δ orbital. The φ band is due to a $1\delta \rightarrow 3\pi$ transition which is a non-bonding to bonding transition. Such a transition has no atomic counterpart since both orbitals come from Ti 3d orbitals.

The energy level diagram as constructed shows that the transitions ${}^1\Pi_A$ - ${}^1\Delta$ and ${}^1\Phi$- ${}^1\Delta$ are also allowed and predicted to occur at 2487 and 1987 cm^{-1}. No IR work has been reported on TiO and hence these states have not yet been verified. The transition between the ${}^1\Delta$ and ${}^1\Sigma^+$ state is not dipole allowed, and hence should not have been observed. Transitions from the higher ${}^1\Delta$, ${}^1\Sigma^+$, and ${}^1\Sigma^-$ states to the ${}^1\Pi_B$ as well as to the ${}^1\Pi_A$ and ${}^1\Phi$ states ($9\sigma \rightarrow 3\pi$ in the first case,

$4\pi - 1\delta$ in the second cases) are dipole allowed and must be watched for both in the 4000-8000 cm^{-1} range and in the 13000 cm^{-1} to 17000 cm^{-1} range in emission spectra. However, such transitions would be fairly weak and are probably hidden by the well characterized ones.

The interpretation of the triplet spectrum is much more difficult. If one starts with the lowest state being $^3\Delta_A$, one sees that the $^3\Phi$ - $^3\Delta_A$, $^3\Pi_A$ - $^3\Delta_A$, $^3\Pi_B$ - $^3\Delta_A$ transitions all have energy too small to correspond to the observed spectral bands. The $^3\Phi$, $^3\Pi$ - $^3\Delta_A$ transitions involve 3π - 9σ transitions--a type of bonding orbital, non-bonding orbital transitions. One would expect such transitions to require little energy. The $^3\Pi_B$ - $^3\Delta_A$ is a (4π) - (1δ) transition which can be related to an atomic 4p - 3d transition. Such a transition between the ^5F $[(3d)^3(4s)^1]$ and the ^5G $[(3d)^2(4s)^1(4p)^1]$ levels of titanium requires 9300 cm^{-1} of energy. Allowing for mixing of orbitals other than the 4p in the 4π orbital, the energy of 7562 cm^{-1} is not unreasonable. The $^3\Delta_c$ - $^3\Delta_A$ transition with calculated energy of 25,397 cm^{-1} most probably corresponds to the observed α transition of 19347 cm^{-1}. Such a transition is a $4\pi - 3\pi$ transition. If one considers that the atomic transition of 4p-3d involving the ^5F $[(3d)^3(4s)^1]$ and the ^5D $[(3d)^2(4s)^1(4p)^1]$ states has an energy of 12000 cm^{-1}, the α transition seems to require more energy since it is a π^* - π transition. However, no other allowed state falls in a region close to 19,300 cm^{-1} above the $^3\Delta_A$. To fit this α band requires a change in state position of 6050 cm^{-1}. Such a change is rather drastic. It may be that the strong orthogonality condition imposed during the calculation has not allowed for a proper description of states involving an occupied 4π orbital. If we recall that the $^1\Delta$ state was raised by 1708 cm^{-1} in the interpretation of the singlet spectrum, we can assume the $^3\Delta$ state should be raised by approximately the same amount, say 1700 cm^{-1}. Hence we lower the $^3\Delta_C$ by 4350 cm^{-1}. Now if one looks at the γ band with V_{00} of 14096 cm^{-1}, one sees that the possibility of an emission to the $^3\Pi_B$ state from the $^3\Delta_C$ might be its source. Such an emission would have an energy of 13,485 cm^{-1}. A lowering of the $^3\Pi_B$ state by 611 cm^{-1} would allow for a fit to the observed γ band. The most recent assignment of this band (a) labels it a $^3\Phi$ - $^3\Delta$ transition whereas previously it had been conclusively assigned as a $^3\Pi$ - $^3\Delta$ transition[10] in which the higher state was the $^3\Delta$. The reason for the change in assignment was that the γ' band was assigned as the $^3\Pi$ - $^3\Delta$ transition where the ground state was $^3\Delta$. Since no calculation had been done, the $^3\Pi$ state was assumed to be of $(3\pi)^3(9\sigma)^2(1\delta)^1$ configuration. Since this configuration can also give rise to a $^3\Phi$, the γ band was thought to be the transition from that state to the ground state ($^3\Delta$). Since there are two $^3\Pi$ states lying reasonably close together, assigning the γ bands as $^3\Delta_C$- $^3\Pi_B$ is not inconsistent with assigning the γ' band as a $^3\Delta$ - $^3\Pi$ transition. Hence we return to the old assignment. The γ' band can then be assigned as the $^3\Delta_C$ - $^3\Pi_A$ transition and as such would have an uncorrected energy of 16,590 cm^{-1}. An upward correction of 450 cm^{-1} is all that is necessary to give theoretical and experimental agreement. The γ transition is a $1\delta \rightarrow 3\pi$ transition with no atomic counterpart since it involves what would be 3d electrons in the atom. The γ'

transition is a $4\pi \rightarrow 9\sigma$ transition which is a $\pi^* \rightarrow n$ transition. It is similar to an atomic $4p \rightarrow 4s$ transition such as from the $^3D\ [(3d)^2 (4s)(4p)]$ to the ^3P or ^3F (both being $(3d)^2(4s)^2$] which have energies of 11,600 cm^{-1} and 19,900 cm^{-1} respectively. The molecular energy is what would be expected if the atomic states were mixed. The transition in the singlet system corresponding to this orbital change was the $^1\Pi_B \rightarrow {}^1\Sigma^+$ transition at 17840 cm^{-1}. These energies are close as expected for such an assignment.

The triplet spectrum as corrected appears in Figure 2. Naturally there are other transitions that are allowed. Both the $^3\Pi_B \rightarrow {}^3\Delta_A$ and $^3\Pi_A$, $^3\Phi \rightarrow {}^3\Delta_A$ transitions. This latter set could account for the emission band seen by Weltner and McLeod at 3590 cm^{-1} - 3730 cm^{-1} in neon and argon matrices.[12] Other allowed bands are the $^3\Delta_c \rightarrow {}^3\Phi$, which should lie at almost the same energy as the γ' band; the $^3\Gamma \rightarrow {}^3\Phi$ which also should lie very close in energy to the γ' band (the $^3\Gamma$ state not having been calculated); the $^3\Sigma^-$, $^3\Delta_B$, $^3\Sigma^+ \rightarrow {}^3\Pi_B$ bands which should lie from about 5000 - 8000 cm^{-1}; the $^3\Sigma^-$, $^3\Delta_B$, $^3\Sigma^+ \rightarrow {}^3\Pi_A$, $^3\Phi$ bands which should lie in the 8000-1000 cm^{-1} range; and the $^3\Sigma^+ \rightarrow {}^3\Pi_B$ band around 17000 cm^{-1}. Such bands are probably not very intense through bands such as the $^3\Delta_c \rightarrow {}^3\Phi$ band would be as intense as the γ' band and may be responsible for the very complex spectrum in that region.

A correlation of the electronic states, orbitals, and energies associated with the assigned transitions for the triplet and singlet systems is given in Table 3. One would expect the energies to be in about the same range though perturbed by the environment. This expectation is upheld in most cases. The $1\delta \rightarrow 3\pi$ is a classical d-d transition from non-bonding to bonding orbital and depends strongly on the electronic states. The $4\pi \rightarrow 1\delta$ orbital transition shows remarkable energetic similarity between the unobserved electronic transitions but a large difference in the energies of the observed transitions in the singlet and triplet systems. This difference is to be expected since the splitting between the $^1\Pi_B$ state and the $^3\Pi_b$ state is 6400 cm^{-1} whereas between the $^1\Delta_A$ and $^3\Delta_A$ only about 1000 cm^{-1}. A splitting of 5600 cm^{-1} occurs in the Ti atom between the ^5G and ^3G states of the configuration $(3d)^2(4s)^1(4p)^1$ indicating that the molecular splitting is anticipated. This transition can be characterized as pi antibonding to non-bonding transition ($\pi^* \rightarrow n$). The $4\pi \rightarrow p_\sigma$ transitions can also be classified as $\pi^* \rightarrow n$ or as Ti $4p \rightarrow 4s$ transitions. The similarity in their energy indicates similarity of environment. The $4\pi \rightarrow 3\pi$ transitions are classical $\pi^* \rightarrow \pi$ transitions and as such usually occur at high energy. Since the $^1\Sigma^+$ state is not observed, its location cannot be made specifically. However, it is of high enough energy to allow the correlation.

IV. DISCUSSION

The GVB method appears to do an adequate job in describing the spectrum of the singlet states. Of the three assigned bands, it justifies two of the assignments while reassigning the third to what had been a suggested assignment. It must be remembered that when the bands were being assigned, the $^3\Delta_A$ state was thought to be the ground state of the system. Hence any interpretation would favor this assumption. Now that is seems quite feasible that the $^1\Sigma^+$ state is the ground state, the spectrum must be looked at in the light of this assumption. When going back and reviewing the papers making the spectral assignments, we found no inconsistency with our interpretation. It remains to be seen what difficulties are created or destroyed by our interpretation.

The triplet spectrum is described adequately, once the initial fitting of the α band is made. The γ band is returned to its previous designation and the complexity of the region surrounding the γ' band is shown to be due to the probability of a $^3\Delta_C \rightarrow {}^3\Phi$ band in the same region. As far as emission spectra go, the assignments fit the spectrum.

When one considers the absorption spectrum of TiO as reported by Weltner and McLeod, grave problems with our interpretation arise. The bands observed seem to correlate very well with the observed triplet emission spectrum. One would expect to see the singlet spectrum if the $^1\Sigma^+$ is the ground state.

One could explain this by saying that possibly only 2 bands were seen, the forbidden $^1\Sigma^- \leftarrow {}^1\Sigma^+$ $4\pi \leftarrow 3\pi$ band at high energy (~20,000 cm^{-1}) and the $^1\Pi_B \leftarrow {}^1\Sigma^+$ $4\pi \leftarrow 9\sigma$ band around 16,000--17,000 cm^{-1}. This interpretation seems far-fetched but feasible since perturbation caused by matrices are known. Another possibility is that the molecule was trapped in an excited state at 2000°C and frozen to 4°K almost immediately. However at this temperature kT is about 1600 cm^{-1} which is large enough to cause thermal population of the $^3\Delta$ state if the $^1\Delta$ state is populated in any way. The fact that emission spectra were not observed indicates some strange occurrences. Thus it seems likely that this spectrum and our assignments are not in conflict.

V. SUMMARY

From the analysis of the spectrum provided by GVB calculations the states involved in the emission spectrum of TiO are determined. The singlet spectrum is fit better than the triplet spectrum and it is implied that the $^3\Delta_c$ state is not described adequately by the theory. Of the six previous spectral assignments, only two are changed and these back to assignments which had previously been suggested. From such results, it seems reasonable that GVB theory can be used in the future as a theoretical tool for examining spectra.

VI. ACKNOWLEDGEMENT

Professor J. Hinze and Dr. Liu of the University of Chicago are thanked for the use of their MCSCF (multi-configuration self-consistent field) programs.

REFERENCES

1a. W. J. Hunt, P. J. Hay, and W. A. Goddard III, J. Chem. Phys. and references therein, in press.

1b. P. J. Hay, W. J. Hunt, and W. A. Goddard III, Chem. Phys. Lett., in press.

2. A. P. Mortola and W. A. Goddard III, to be published.

3. G. Herzberg, Spectra of Diatomic Molecules, D. Van Nostrand Company, Inc., Princeton, New Jersey, 1950, p. 576.

4. F. Lowater, Proc. Phys. Soc., **41**, 557 (1929).

5. J. G. Phillips, Astrophys. J., **111**, 314 (1950).

6. C. Linton and R. W. Nichols, J. Phys. B., 490 (1969).

7. A. V. Pettersson, Arkiv. Fys., **16**, 185 (1959).

8. A. V. Pettersson and B. Lindgren, Arkiv. Fys., **22**, 491 (1962).

9. J. G. Phillips, Astrophys. J., **157**, 449 (1969).

10. J. G. Phillips, Astrophys. J., **114**, 152 (1951).

11. F. P. Coheur, Bull. Soc. Roy. Sci. Leige., **12**, 98 (1943).

12. W. Weltner and D. McLeod, J. Phys. Chem., **69**, 3488 (1965).

13. C. E. Moore, Atomic Energy Levels, Circular of the National Bureau of Standards 467, Vol. I, U.S. Government Printing Office, Washington, D.C., 1949, p. 274.

TABLE 1

Calculated Energies for TiO. R = 3.07 a_0 = 1.62 Å

Configuration	State	Total Energy (Hartrees)	
		HF	GVB
$(8\sigma)^2(3\pi)^4(9\sigma)^2$	$^1\Sigma^+$	-921.4247725	-921.5035053
$(8\sigma)^2(3\pi)^4(9\sigma)^1(1\delta)^1$	$^1\Delta$	-921.4216817	-921.4685545
$(8\sigma)^2(3\pi)^3(9\sigma)^2(1\delta)^1$	$^1\Phi$	-921.4186483	-921.4517443
$(8\sigma)^2(3\pi)^3(9\sigma)^2(1\delta)^1$	$^1\Pi_a$	-921.4157161	-921.4490129
$(8\sigma)^2(3\pi)^4(9\sigma)^1(4\pi)^1$	$^1\Pi_b$	-921.3723530	-921.4093997
$(8\sigma)^2(3\pi)^3(9\sigma)^2(4\pi)^1$	$^1\Delta$	-921.3744418	-921.40369
$(8\sigma)^2(3\pi)^3(9\sigma)^2(4\pi)^1$	$^1\Sigma^-$	-921.3638626	
$(8\sigma)^2(3\pi)^3(9\sigma)^2(4\pi)^1$	$^1\Sigma^+$	-921.3567768	
$(8\sigma)^2(3\pi)^3(9\sigma)^1(4\pi)^1(1\delta)^1$	$^1\Delta$	-921.3426	
$(8\sigma)^2(3\pi)^4(9\sigma)^1(1\delta)^1$	$^3\Delta_A$	-921.4270966	-921.4738185
$(8\sigma)^2(3\pi)^3(9\sigma)^2(1\delta)^1$	$^3\Phi$	-921.4205608	-921.4535278
$(8\sigma)^2(3\pi)^3(9\sigma)^2(1\delta)^1$	$^3\Pi_A$	-921.4205608	-921.4535272
$(8\sigma)^2(3\pi)^4(9\sigma)^1(4\pi)^1$	$^3\Pi_B$	-921.3980408	-921.4393830
$(8\sigma)^2(3\pi)^3(9\sigma)^2(4\pi)^1$	$^3\Sigma^+$	-921.3928729	
	$^3\Delta_B$	-921.3832974	-921.4126441
	$^3\Sigma^-$	-921.3753456	
$(8\sigma)^2(3\pi)^3(9\sigma)^1(4\pi)^1(1\delta)^1$	$^3\Delta_C$	-921.3423863	-921.3580977
$(8\sigma)^1(3\pi)^4(9\sigma)^1(4\pi)^1(1\delta)^1$	$^3\Phi$	-921.3377539	-921.3438261
$(8\sigma)^2(3\pi)^4(9\sigma)^1(10\sigma)^1$	$^3\Sigma^+$	-921.3248885	-921.3618
$(8\sigma)^2(3\pi)^3(9\sigma)^2(10\sigma)^1$	$^3\Pi$	-921.2998634	

Table 1 (cont'd)

Configuration	State	Total Energy (Harteees)	
		HF	GVB
$(8\sigma)^2(3\pi)^3(9\sigma)^1(1\delta)^1(10\sigma)^1$	$^3\Phi$	-921.2974786	
$(8\sigma)^2(3\pi)^3(9\sigma)^1(1\delta)^1(10\sigma)^1$	$^3\Pi$	-921.2966197	
$(8\sigma)^2(3\pi)^4(4\pi)^1(1\delta)^1$	$^3\Phi$	-921.2897689	
	$^3\Pi$	-921.2842702	
$(8\sigma)^2(3\pi)^3(9\sigma)^1(1\delta)^2$	$^3\Phi$	-921.2367720	
$(8\sigma)^2(3\pi)^4(1\delta)^1(10\sigma)^1$	$^3\Delta$	-921.1981481	
$(8\sigma)^2(3\pi)^4(1\delta)^2$	$^3\Sigma^-$	-921.1811957	-921.2847392
$(8\sigma)^2(3\pi)^4(4\pi)^1(10\sigma)^1$	$^3\Pi$	-921.1642533	
$(8\sigma)^2(3\pi)^2(9\sigma)^2(4\pi)^1(1\delta)^1$	$^3\Pi$	-921.1292593	
$(8\sigma)^2(3\pi)^3(9\sigma)^1(4\pi)^1(1\delta)^1$	$^5\Gamma$	-921.3802259	
$(8\sigma)^1(3\pi)^4(9\sigma)^1(4\pi)^1(1\delta)^1$	$^5\Phi$	-921.3538706	
$(8\sigma)^2(3\pi)^3(9\sigma)^1(4\pi)^1(10\sigma)^1$	$^5\Delta$	-921.2874766	
$(8\sigma)^2(3\pi)^2(9\sigma)^2(1\delta)^2$	$^5\Sigma^-$	-921.1857250	

TABLE 2

Observed Spectral Energies

Band	Expt'l Energy (cm^{-1}) (0-0)	Assignment	
		Experimental	Theoretical
φ	9,054	$^1\Sigma^+ - {}^1\Pi$	$^1\Sigma^+ - {}^1\Pi_A$
δ	11,273	$^1\Pi - {}^1\Delta$	$^1\Delta_A - {}^1\Pi_B$
β	17,841	$^1\Phi - {}^1\Delta$	$^1\Sigma^+ - {}^1\Pi_B$
γ	14,096	$^3\Phi - {}^3\Delta$	$^3\Pi_B - {}^3\Delta_C$
γ'	16,150	$^3\Pi - {}^3\Delta$	$^3\Pi_A - {}^3\Delta_C$
α	19,347	$^3\Delta - {}^3\Delta$	$^3\Delta_A - {}^3\Delta_C$

TABLE 3

Orbital Trans	Triplet System			Singlet System		
	States	Starting Configuration	Energy (cm^{-1})	States	Starting Configuration	Energy (cm^{-1})
$1\delta \to 3\pi$	${}^3\Delta_C \to {}^3\Pi_B$	$(3\pi)^3(9\sigma)^1(4\pi)^1(1\delta)^1$	14096	${}^1\Pi_A \to {}^1\Sigma^+$	$(3\pi)^3(9\sigma)^2(1\delta)^1$	9,054
$4\pi \to 1\delta$	${}^3\Pi_B \to {}^3\Delta_A$	$(3\pi)^4(9\sigma)^1(4\pi)^1$	5251*	${}^1\Pi_B \to {}^1\Delta_A$	$(3\pi)^4(9\sigma)^1(4\pi)^1$	11,273
	${}^3\Sigma^-$, ${}^3\Delta_B$, ${}^3\Sigma^+$ $\to {}^3\Pi_A$, ${}^3P$	$(3\pi)^3(9\sigma)^2(4\pi)^1$	7000 - 10,000*	${}^1\Delta_B \to {}^1\Pi_A$, ${}^1\Phi$	$(3\pi)^3(9\sigma)^2(4\pi)^1$	13,000* 12,000*
$4\pi \to 9\sigma$	${}^3\Delta_C \to {}^3\Pi_A$	$(3\pi)^3(9\sigma)^1(4\pi)^1(1\delta)^1$	16150	${}^1\Pi_B \to {}^1\Sigma^+$	$(3\pi)^4(9\sigma)^1(4\pi)^1$	17,840
$4\pi \to 3\pi$	${}^3\Delta_C \to {}^3\Delta_A$	$(3\pi)^3(9\sigma)^1(4\pi)^1(1\delta)^1$	19347	${}^1\Sigma^- \to {}^1\Sigma^+$	$(3\pi)^3(9\sigma)^2(4\pi)^1$	24,500*

* Unobserved.

Figure 1. The Singlet Spectrum of TiO

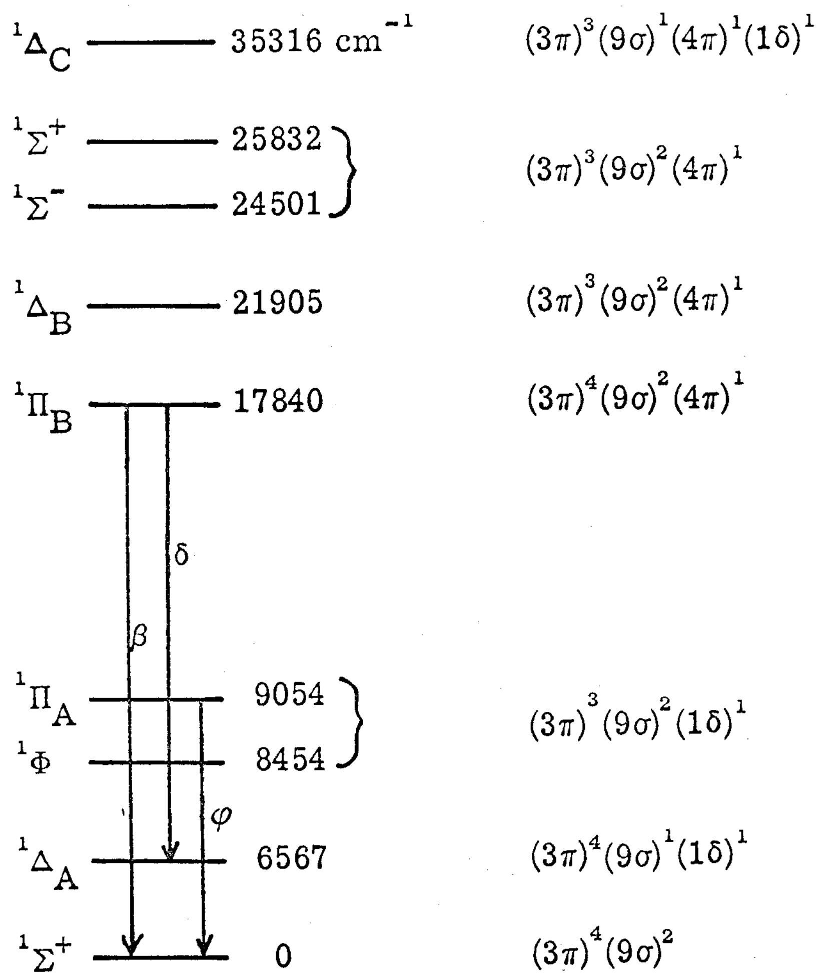

FIGURE 2. The Triplet Spectrum of TiO

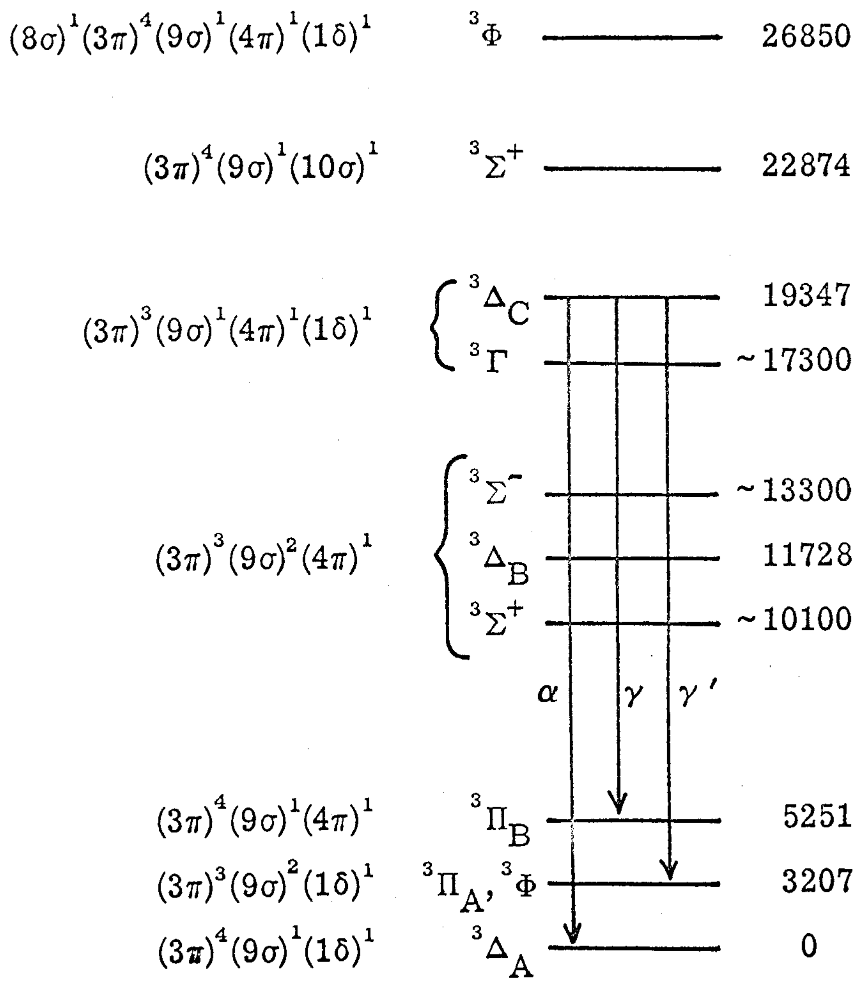

V. TITANIUM CARBONYL AND TITANIUM CARBONYL ION

Introduction

Transition metal carbonyls have been of immense interest to chemists ever since the discovery of nickel tetracarbonyl in 1890 by Mond, Langer, and Quincke.[1] Since that time a great deal of progress has been made both in synthesizing new compounds and in understanding the nature of the bonding between the carbon and the metal atom. One of the principle successes of molecular orbital theory for inorganic molecules was its application by Beach and Gray[2] to the metal hexacarbonyls resulting in a lucid interpretation of their spectra. The method used in their calculation was the "extended Wolfsberg-Helmholtz method" as outlined by Basch, Viste and Gray in 1966.[3] In recent years, theoretical and calculational methods have been developed to the point that it is now possible to carry out *ab initio* calculations on transition metal carbonyls. Such methods have demonstrated that doubly occupied molecular orbitals or Hartree-Fock wavefunctions do not generally lead to consistent descriptions of the ground and excited states of molecules. In many cases, it is necessary to include some configuration interaction to obtain the proper consistency. One particularly useful method of including such correlation effects while retaining easy interpretability, is the generalized valence bond (GVB) method,[4,5] in which the wavefunction is taken to have the form of a valence bond (VB) wavefunction but the orbitals are solved for self-consistently rather than taken as (hybridized) atomic orbitals as in the VB method.

In this paper we consider the very simple carbonyls $TiCO^+$ and TiCO and report results from both HF and GVB calculations. The bonding in the various states of these compounds is interpreted in terms of the GVB orbitals and this interpretation is in turn applied to other carbonyls such as $Fe(CO)_5$ and $Ni(CO)_4$.

Methods of Calculation

The GVB method has been described in detail elsewhere[4] so it will suffice to give only a brief outline of it here. The principal facet of this approach is the replacing of doubly occupied orbitals φ_i in the Hartree Fock (HF) wavefunction.

$$\psi_{HF} = \mathcal{A}[\varphi_1\alpha\varphi_1\beta\varphi_2\alpha\varphi_2\beta\cdots\varphi_n\alpha\varphi_n\beta] \tag{1}$$

by singlet-coupled pairs of singly occupied orbitals:

$$\begin{aligned}\psi_{GVB} = \mathcal{A}[&(\varphi_{1a}\varphi_{1b}+\varphi_{1b}\varphi_{1a})\alpha\beta(\varphi_{2a}\varphi_{2b}+\varphi_{2b}\varphi_{2a})\alpha\beta\cdots \\ &\cdots(\varphi_{na}\varphi_{nb}+\varphi_{nb}\varphi_{na})\alpha\beta].\end{aligned} \tag{2}$$

If the orbitals were taken to be atomic orbitals, this would lead to the Valence Bond wavefunction of Pauling and Slater.[6] However, the orbitals are solved for variationally (as in the HF method).

Since each electron is allowed to be in a different orbital, one obtains a proper description of bond dissociations, avoiding one of the major difficulties in the HF method. Since each orbital is solved for variationally, one obtains quantitatively good results near the equilibrium geometry R_e leading to better energies than either the HF or VB wavefunctions. An additional bonus is that the resulting orbitals in the molecule lead to simple interpretations of the bonding in terms of such common concepts as hybridizations, ionic versus covalent character, bond-bond interactions, etc.

The method of solving for the variationally optimum GVB orbitals in (2) is to expand each pair function in terms of two natural orbitals

$$[\varphi_{1_a}(1)\varphi_{1_b}(2)+\varphi_{1_b}(2)\varphi_{1_a}(1)] = C_{1_i}\varphi_{1_i}(1)\varphi_{1_i}(2)-C_{2_i}\varphi_{2_i}(1)\varphi_{2_i} \qquad (2)$$

where C_{1_i} and C_{2_i} are related to the overlap of φ_{1_a} and φ_{1_b}. If the orbitals of different pairs are taken as orthogonal (strong orthogonality), then the resulting variational equations for ϕ_{1_i} and ϕ_{2_i} involve just Coulomb and exchange operators comparable to those in the HF equations, leading to rapid computational procedures.

In terms of the natural orbitals the GVB wavefunction has the form of a multi-configuration wavefunction in which the first configuration corresponds to the Hartree-Fock configuration with each subsequent configuration having a doubly occupied pair of orbitals replaced by a new doubly occupied pair. Thus from a Multiconfiguration SCF (MCSCF) wavefunction of this form we can obtain the GVB orbitals by reversing(2). For these calculations we used the general MCSCF program written by Hinze[7] with the configurations chosen to match a GVB wavefunction.

The basis set consisted of a minimum basis set of Slater orbitals from the calculation by Clementi and Raimondi[8] except for the addition of a set of Ti 4p, and the change of the carbon 2p exponents from 1.5679 to 1.75 as indicated by optimized exponents obtained by Pitzer,[9] Stevens,[10] and Pople.[11] The CO bond length was taken to be 2.17 a_0 (1.15 Å) and the Ti-C distance 3.70 a_0

(1.96 Å). This latter distance was extrapolated from the known metal-carbon distances of 1.84 Å in $Fe(CO)_5$ and 1.92 Å in $Cr(CO)_6$.[12]

Results

A. Energies. The orbital energies of the various orbitals of the $^3\Phi$ state of TiCO are presented in Table 2 as well as are the orbital energies of the corresponding orbitals of Ti and CO. As can be seen, the inner orbitals of TiCO just correspond to the orbitals of the argon core of titanium and the helium cores of carbon and oxygen. These orbitals do not change significantly upon bond formation and will be omitted from our discussion. The 8σ orbital corresponds to the O sigma non-bonding orbital of CO and will also not be discussed. The 9σ orbital corresponds to CO non-bonding pair that is donated to the Ti to form a donor-acceptor sigma bond between Ti and CO. The 10σ and 3π orbitals correspond to the sigma and pi bonding pairs of CO. The 1δ, 11σ, and 4π orbitals correspond primarily to Ti valence orbitals and have varying occupations in the low-lying states of TiCO and $TiCO^+$. The 1δ is a $3d_\delta$ orbital while the 11σ generally has the characteristics of a 4s orbital and the 4π has varying amounts of $3d_\pi$ and $4p_\pi$ mixed with the CO π^* orbital.

As shown in Table 3, the lowest states of TiCO correspond to the configuration

$$(11\sigma)^2(4\pi)^1(1\delta)^1 \tag{1}$$

which leads to $^3\Phi$, $^1\Phi$, $^3\Pi$, and $^1\Pi$ states with $^3\Phi$ the lowest. Such a configuration corresponds to the $(3d)^2(4s)^2$ configuration of Ti atom and its four possible states -- ^3F, ^3P, ^1G and ^1D. In the atom the ^3F state is lower than the ^3P by 1.05 eV[13] whereas in the molecule the $^3\Phi$ is .11 eV lower. The $^3\Phi$ - $^1\Phi$ separation is .27 eV in the molecule whereas the ^3F state is stabilized by the ^3F state from the $(3d)^3(4s)^1$ configuration which when taken with the fact that no similar $^3\Phi$ state can arise from that configuration in the molecule accounts for the differences in separation energy. The next state of the molecule is the $^5\Delta$ state arising from the configuration

$$(11\sigma)^1(4\pi)^2(1\delta)^1. \tag{2}$$

Other states calculated from this configuration are the $^3\Gamma$ and $^3\Delta_A$ states. This configuration arises from the Ti $(3d)^3(4s)^1$ configuration. The ^5F state of this atomic configuration lies .80 eV above the ground state whereas the $^5\Delta$ lies .27 eV above the TiCO $^3\Phi$ state. Again there is more stabilization in the atom. The next TiCO state is the $^3\Sigma_A^-$ coming from the

$$(11\sigma)^2(4\pi)^2 \tag{3}$$

configuration. It falls .54 eV above the $^3\Phi$ state. The $^3\Sigma_B^-$ state from the

$$(11\sigma)^2(1\delta)^2 \tag{4}$$

configuration falls 2.72 eV above the $^3\Phi$ state. These states both come from mixtures of the ^3F and ^3P states of the atomic $(3d)^2(4s)^2$ configuration. Electron repulsion is the cause for their large separation. Upon going to the GVB wavefunction, one expects the states with the 11σ orbital doubly occupied to drop about .01 h (.27 eV) more than the other states due to the correlation energy obtained when such a pair is split. Thus one would expect the $^3\Phi$ to be about .02 h (.54 eV) lower than the $^5\Delta$ and $^3\Sigma^-$ states which should be very close in energy. Some typical GVB splitting energies for the CO bonding pairs (10σ mixed with 12σ) and (3π mixed with 4π or 5π) are included in Table 3. Since convergence difficulties were experienced with many of the states of TiCO, the GVB results are unavailable.

In the $TiCO^+$ ion, the HF calculations (see Table 4) indicate that $^4\Sigma^-$ state of configuration

$$(11\sigma)^1(4\pi)^2$$

is of lower energy than the $^2\Delta$ state

$$(11\sigma)^2(1\delta)^1$$

the $^2\Pi$ state

$$(11\sigma)^2(4\pi)^1$$

or the $^4\Phi$ state

$$(11\sigma)^1(4\pi)^1(1\delta)^1.$$

That the $^4\Sigma^-$ is of lower energy than the $^2\Delta$ and $^2\Pi$ states is not surprising since the $(3d)^2(4s)^1$ ground state of Ti^+ is 3 eV lower than the $(3d)^1(4s)^2$ state. However, that the $^4\Sigma^-$ state should be lower than the $^4\Phi$ state is surprising. Both states arise from the ^4F $(3d)^2(4s)^1$ state of Ti, but their order in $TiCO^+$ is reversed from their order in TiCO and the energy difference is larger (1.14 eV as opposed to .54 eV). The significance of this will be discussed in the next section. When the GVB wavefunction is calculated, one expects the $^2\Pi$ and $^2\Delta$ states to drop more than the $^4\Sigma^-$ state. Such is the case, but the $^4\Sigma^-$ state is still slightly lower.

The HF and GVB energies for the lower states of Ti^+ and Ti are given in Table 5 while the results for CO are given in Table 6. Although a minimum basis set such as used here is often adequate for predicting excitation energies [14] (to non-Rydberg excited states), it generally does not lead to good dissociation energies. For example for CO, the calculated dissociation energy is 5.0 eV for the HF wavefunction and 6.0 eV for the GVB wavefunctions as compared to an experimental value of 11.09 eV. Similarly, we find the minimum basis set GVB description of Ti CO^+ leads to a dissociation energy of -.49 eV for the $^4\Sigma^-$ state [dissociating into Ti^+ (^4F) and CO ($^1\Sigma^+$)] and + .52 eV for the $^2\Pi$ state [with $Ti^+(^2D)$ and $CO(^1\Sigma^+)$]. For the $^3\Phi$ state of Ti CO, the dissociation energy is -.87 eV. Such calculations do not mean the molecules are unbound, but that they are not strongly bound. It would seem though, that the ion is more strongly bound than the neutral molecule.

B. Orbitals. In the GVB description, two natural orbitals (NO) of the MCSCF wavefunction are associated as in equation (2) to lead to the GVB orbitals. The names of the natural orbitals used in the GVB pairs are given in Table 7. Occupying the first NO of each pair leads to a wavefunction nearly identical with the HF wavefunction.

However, the first NO's themselves do not generally correspond to HF orbitals since the process of splitting each pair requires a unitary transformation (rotation) of the HF orbitals among themselves to obtain the set of NO's.

In Figure 1, we compare the GVB, CO σ bonding pair ($\varphi_{CO\sigma a}$, $\varphi_{CO\sigma b}$) obtained for $CO(^1\Sigma^+)$ and for the $^4\Sigma^-$ and $^2\Pi$ states of $TiCO^+$ and for the $^5\Delta$ state of TiCO. The HF CO bonding orbital is also shown for the $^4\Sigma^-$ and $^2\Pi$ states of $TiCO^+$ and for the $^5\Delta$ and $^3\Phi$ states of TiCO. It must be remembered that each GVB orbital contains only one electron whereas an HF orbital contains two. As can be seen, the orbitals are similar in each case. Each retains a large amplitude between the C and the O, but each also mixes with the Ti $3d_{z^2}$ orbital (also shown) to give a bit of Ti-C bonding character in that internuclear region. In $TiCO^+$ the ($\varphi_{Ti\ C\sigma_A}$, $\varphi_{Ti\ C\sigma_B}$) pair shifts somewhat toward the Ti leading to a sigma bond.

The CO bond appears to be weakened somewhat (but not much) by this shift towards the Ti since it is now slightly more diffuse. However, it may feel less repulsion in that region due to the shift of the CO non-bonding pair and may actually be a stronger bond. Such is hard to tell from just these orbitals. It does appear, however, that whatever happens in $TiCO^+$ happens in TiCO judging from the similarity of the GVB orbitals of the $^5\Delta$ state and the HF orbitals of the $^5\Delta$ state and the HF orbitals of the $^5\Delta$ and $^3\Phi$ states of TiCO and their $TiCO^+$ counterparts.

In Fig. 2 we compare the nonbonding σ pair of CO with the Ti C bonding pair in the $^2\Pi$ and $^4\Sigma^-$ states of $TiCO^+$. These orbitals correspond closely however. We see that in $TiCO^+$ they build in a significant amount of Ti $3d_{z^2}$ character. In CO these orbitals are split angularly so that electrons in these orbitals would tend to be on opposite sides of the molecular axis. They have some antibonding character, indicated by the nodal surfaces near the O. This is due to bad interactions with the CO bonding pairs. As a result of moving away from the CO bonding pairs, it loses some of its antibonding character near the oxygen. This happens because the former density on the oxygen has now shifted into the CO bonding region in an effort to get closer to the titanium. This should allow the sigma and pi bonds of the CO to be strengthened somewhat. The fact that this density from oxygen is shifted more in the $^4\Sigma^-$ case than in the $^2\Pi$ case implies qualitatively a stronger Ti-C sigma bond. This bond can be viewed as a donor-acceptor bond such as that between BH_3 and NH_3. The CO(donor) provides a pair of non-bonding electrons which shift to occupy an available orbital of the acceptor (Ti^+).

This leaves us with the Ti-4s like sigma orbitals shown in Fig. 3 both for the Ti atom and for the $^4\Sigma^-$ and $^2\Pi$ states of $TiCO^+$ and $^3\Phi$ and $^5\Delta$ states of TiCO. (Some of these orbitals are shown to smaller scale in Fig. 7.) In the atom, the GVB wavefunction allows mixing of the 4p giving two separate regions of occupied space. The same thing happens in the $^2\Pi$ state of $TiCO^+$. The orbitals show slight bonding character both in the Ti-C and the C-O bonding region.

The HF orbital of this state was anti-bonding in the C-O region. Hence splitting by removing this anti-bonding character as well as lowering electronic repulsion allowing different regions of space to be occupied has improved the calculated energy of this state. The electrons in these orbitals are clearly non-bonding. The $^4\Sigma^-$ state of $TiCO^+$ has a similar HF orbital, but since it only has one electron, it remains about the same. The HF orbitals of the $^3\Phi$ and $^5\Delta$ states of TiCO are doubly occupied and one can assume that they would split in a similar manner as the $^2\Pi$ orbitals did. What is important is that these orbitals are non-bonding orbitals and as such do not show any Ti 3d character but only 4s and 4p character. The sigma bonding that has occurred, occurred through a $3d_{z^2}$ orbital and not through a 4s orbital. A similar result was observed in TiO.[14]

The pi orbitals are displayed in Figs. 4 and 5. Figure 4 shows the π bonding orbitals of CO and their counterparts in the $^4\Sigma^-$ and $^2\Pi$ states of $TiCO^+$. The $\phi_{CO\pi a}$ pi orbital of CO is a bit more concentrated on the carbon than on the oxygen while the $\phi_{CO\pi b}$ orbital is essentially a Op_π orbital. These orbitals have similar character in Ti CO^+. Here $\phi_{CO\pi a}$ possesses a nodal plane (antibonding character) between the Ti and C, probably due to interactions with the Ti $3p_\pi$ core orbitals. On the other hand $\phi_{CO\pi b}$ has smaller amplitude in the Ti core region and does not obtain a new nodal plane (it seems to have a slight increase in amplitude in the titanium-carbon bonding region).

In Fig. 5 we show the $3d_\pi$ orbital of Ti along with the corresponding pi orbital (the 4π) of $TiCO^+$. Here we see that there is some indication of bonding character in the 4π orbital. The component of this $3d_\pi$-like orbital on the CO has the form of a CO antibonding pi orbital (possessing a node plane between the carbon and the oxygen). In comparing the $^4\Sigma^-$ and $^2\Pi$ states, the ϕ_{3d_π} orbital of the $^4\Sigma^-$ state appears to have a bit more bonding character, although it must be remembered that the $^4\Sigma^-$ state has two electrons in such orbitals (in perpendicular planes) while the $^2\Pi$ has only one such electron.

In Fig. 6, the HF 4π orbitals of the $^4\Sigma^-$ state of $TiCO^+$ and of the $^3\Sigma_A^-$, $^3\Phi$, and $^5\Delta$ states of TiCO are depicted. (Fig. 8c shows the $^3\Phi$ 4π to smaller scale.) Two things are immediately obvious. The $^4\Sigma^-$ orbital looks exactly like the orbital obtained in the GVB description. The 4π orbitals in the $^3\Phi$ and $^5\Delta$ states are similar to each other but completely different from the $^4\Sigma^-$ orbital while the $^3\Sigma_A^-$ orbital is somewhere between the two. The TiCO $^3\Phi$ and $^5\Delta$ orbitals are very diffuse and as such contain a lot of titanium 4p character. Hence they are more non-bonding than bonding in character. The 4π orbital of the $^3\Sigma_A^-$ state is halfway between non-bonding and bonding having weak bonding character. One cannot help but feel that this may be so because $TiCO^+$ is bound and TiCO is not. These figures do show that the phenomenon known as retrodative pi bonding or pi back bonding does exist in $TiCO^+$ but not in the lowest states of TiCO. It is felt that this may be the reason why $TiCO^+$ is bound and TiCO not bound.

Discussion

From the results of these calculations one can get a feel for the nature of the bonding between a metal and a carbonyl. There appears to be both sigma and pi bonding between the Ti and CO. The sigma bonding is due essentially to the lone pair orbitals of CO which delocalize slightly into the vacant Ti $3d_{z^2}$ orbital. In CO these orbitals have some antibonding character on the O but in $TiCO^+$ this antibonding character is nearly completely removed. This results from the shift of this pair toward the Ti. This interaction can then be described as the classical sigma donating effect--the electrons coming exclusively from the carbonyl ligand. Concomitantly, there is a movement of electron density from the Ti back to the CO through the pi interaction. Such a shift can be expected to help counterbalance the shift in charge from the CO towards the Ti in the sigma interaction. This back shift results in some pi bonding between the Ti and CO and as such has been named retrodative pi bonding or pi backbonding. Thus the CO ligand retains its classification as sigma donor, pi acceptor since the delocalizing of the Ti $3d_{\pi}$ into the vacant CO π^* orbitals is a donor-acceptor effect with the Ti being the donor.

It is important to note that the 4s and 4p orbitals of Ti do not seem to participate in the bonding. The sigma bonding which takes place involves the Ti $3d_{z^2}$ orbital whereas the pi-bonding involves the Ti $3d_{xz}$, $3d_{yz}$ orbitals. In $TiCO^+$, the $^4\Sigma^-$ state is calculated to be .005 h (.14 eV) lower than the $^2\Pi$ state. Such can be explained since the $^4\Sigma^-$ state has the configuration $(11\sigma)^1(4\pi)^2$ giving one non-bonding electron and two pi bonding electrons, whereas the $^2\Pi$ state with the configuration $(11\sigma)^2(4\pi)^1$ has two non-bonding electrons and one pi-bonding electron. However, the energy difference is too small to be due to the difference between a bond and no bond. This implies that there is a stability in the $(11\sigma)^2$ configuration. The fact that the $^2\Pi$ $[(11\sigma)^2(4\pi)^1]$ state is preferred over the ^{4} $[(11\sigma)^1(4\pi)^1(1\delta)^1]$ states supports this assertion. A similar result had been found in the calculations on TiO in which the $^3\Delta\,[(9\sigma)^1(1\delta)^1]$ state was of higher energy than the $^1\Sigma^+\,[(9\sigma)^2]$ state.[14] One can rationalize this in TiO where the $^3\Delta$ state dissociates into a $(4s)^1(3d)^3$ state of Ti which is 0.80 eV higher than the $(4s)^3(3d)^2$ ground state which the $^1\Sigma^+$ dissociates into. However, in Ti^+, the $(4s)^2(3d)^1$ ^1D state is 3 eV higher than the $(4s)^1(3d)^2$ ^4F state. This would imply that the Ti in the $^2\Pi$ state of $TiCO^+$ is not Ti^+ but that the electron donation in the sigma interaction has made it more Ti°. In the $^4\Sigma^-$ state, two electrons are being donated to the Ti by the CO sigma interaction, but two are returning to some degree via the pi interaction. Hence one has a pseudo $(3d)^2(4s)^1$ configuration around the Ti making it Ti^+. In the $^2\Pi$ state, there is effectively only one electron involved in pi back bonding, allowing the Ti to have the effective $(4s)^2(3d)^2$ configuration of Ti°. Hence one could classify the transition from the $^4\Sigma^-$ state to the $^2\Pi$ state as a ligand to metal charge transition. Were one to synthesize $TiCO^+$, one should be able to see such a transition $(^2\Sigma^- \rightarrow {}^2\Pi)$ at very low energy (~ 1000 cm^{-1}).

When one carries these arguments to TiCO, one expects to find the same sort of interaction for Ti: sigma accepting and pi donating. The sigma accepting interaction occurs as is obvious from Fig. 1. However, the pi donating interaction does <u>not</u> occur in the $^3\Phi$ and $^5\Delta$ states and only slightly in the $^3\Sigma_A^-$ (Fig. 6). The 4 pi orbital is not a strong pi back-bonding orbital but instead is a diffuse orbital having a great deal of Ti 4p non-bonding character. Such a result is puzzling since one would not expect the addition of one electron to affect the bonding so drastically. One expects that adding one electron to the $^4\Sigma^-$ state should result in a configuration $(11\sigma)^2(4\pi)^2(^3\Sigma_A^-)$ or $(11\sigma)^1(4\pi)^2(1\delta)^1(^5\Delta)$. Addition to the $^2\Pi$ state would lead to $(11\sigma)^2(4\pi)^2$ $(^3\Sigma_A^-)$ or $(11\sigma)^2(4\pi)^1(1\delta)^1(^3\Phi)$. These are the states that are the lowest but not in the order that one would expect: $^5\Delta$ or $^5\Sigma^-$ followed by $^3\Phi$. The order is changed because the 4π orbital is non-bonding rather than bonding. If one allows one (3d) electron to be the result of sigma donation, the effective configuration of Ti in the $^3\Phi$ state of TiCO is $(4s)^2(3d)^2(4p)^1$ and in the $^5\Delta$ state $(4s)^1(3d)^2(4p)^2$. Both of these configurations correspond to a Ti^- anion which is of dubious stability. The $^3\Sigma_A^-$ state has pi back-bonding character in the 4π orbital, but also has Ti 4p non-bonding character. It can probably be described as having a $Ti^{\frac{1}{2}-}$ rather than a Ti° or Ti^-. The problem is that TiCO cannot handle the extra electron. The repulsion due to it affects the bonding orbitals which now get diffuse to get out of its way. Putting it in the delta orbital forces it to occupy the same area of space as the $3d_\pi$ orbitals. Hence these diffuse by adding in Ti 4p character.

Arranging it to give the $(11\sigma)^2(4\pi)^2$ configuration also forces inter-electronic repulsion between the 11σ and 4π orbitals. The nuclear charge on Ti cannot support this extra electron and the result is that TiCO is weakly bound if it is bound at all.

Consider now what would happen if a second CO is bonded to the Ti. With a linear geometry, we must promote the 4s electrons to get them out of the way of the lobe pairs on the second CO. Hence the four valence electrons of Ti must be either in pi orbitals or delta orbitals. With one valence electron in a pi orbital, it will delocalize onto both carbonyl groups giving rise to pi bonding on both of them. With two electrons in, for example, a π_x orbital, the orbitals would split in GVB fashion leading to one orbital more pi bonding to, say, the left CO and one more to the right one. The π_y electrons would follow suit resulting in two pi electrons donated to each carbonyl and two sigma electrons received from each carbonyl. One expects all the valence electrons to be involved in bonding so that the Ti does not feel a negative charge. Hence this compound should be stable and bound and have the configuration $(15\sigma)^2(5\pi)^4$ (a ${}^1\Sigma_g^+$ state).

One can extend these bonding concepts to other carbonyl systems. In $Cr(CO)_6$, there are six electrons provided by the chromium. One expects each carbonyl to donate two electrons toward the formation of a Cr-CO sigma bond and each of the six valence electrons to enter into a pi back-bond. The pi orbitals in an octahedral system are the d_{xy}, d_{xz}, d_{yz} and if the GVB description is applied, these orbitals split into localized pi orbitals. Only one pi orbital is available per ligand. The GVB description would show the six chromium sigma accepting orbitals to be $d^2 sp^3$ hybrids as valence bond theory would suggest. Thus the CO orbitals would delocalize into such hybrid orbitals and pick up their character. This description of $Cr(CO)_6$ is consistent with the crystal field description of $(t_{2g})^6(e_g)^0$. It is this pi back-bonding which causes the complex to be low spin.

In iron, there are eight valence electrons. Immediately one sees that if one tries to make $Fe(CO)_6$, he runs into trouble. This is so since it requires six electrons to account for the pi back-bonding leaving two electrons left over to interfere with the sigma electrons donated from the carbonyls. Thus there are just too many electrons and this compound doesn't form. If one were to go to five carbonyls one would have ten electrons donated from the carbonyls leaving eight on the iron for pi back-bonding or non-bonding. If one were to assign five electrons to pi back-bonding, three would remain in non-bonding orbitals and the result would be a triplet. If, instead, the eight electrons were all assigned to pi back-bonding orbitals, one would have three ligands which were doubly back-bonded and two that were singly back-bonded. Hence the equatorial and axial ligands are not equivalent. This would explain the difference in reactivity of axial and equatorial ligands. The reaction

$$Fe(CO)_5 + X_2 \rightarrow Fe(CO)_4X_2 + CO$$

where X is a halide is thought to go by axial attack since the product is the <u>cis</u> isomer. This implies that the axial ligands are more weakly bound.

With nickel, ten electrons present themselves. As such, this eliminates the possibility of five carbonyls since ten electrons cannot distribute themselves in a trigonal bipyramid. This is so because the donated sigma electrons occupy empty hybrid orbitals formed from a combination $d\,sp^3$ and d^3sp hybrid orbitals leaving the pi orbitals to form from a combination of four d orbitals and two p and two d orbitals. There is only room for eight pi electrons and any other electrons go into diffuse orbitals which interact with the donated sigma pairs. Hence nickel forms a compound with four carbonyls. The structure for four coordinate species is either square planar or tetrahedral. A square planar geometry allows for four pi back bonds (made by the delocalization of the d_{xz} and d_{yz} orbitals onto the CO π^* orbitals). The tetrahedral structure allows for double pi back-bonds thereby employing eight of the ten electrons. The remaining two are a non-bonding pair. Because of this arrangement $Ni(CO)_4$ is very reactive--not being thermally stable much above room temperature.

Summary

The calculation of several states of $TiCO^+$ and TiCO have indicated some of the characteristic features of a metal carbonyl. As expected, carbonyls bind through a sigma donating, pi accepting interaction. It was found that the pi back-bonding was considerably weaker in TiCO than in $TiCO^+$ and that this leads to instability of that compound with respect to TiCO. Extrapolation to real systems as $Cr(CO)_6$, $Fe(CO)_5$, and $Ni(CO)_4$ was made using the same concepts. In each case, the structure of the complex agreed well with the bonding concepts.

Acknowledgements

Prof. J. Hinze and X. Liu are thanked for the use of their MCSCF programs and Dr. T. H. Dunning is thanked for aid in the use of these programs.

References

1. L. Maud, C. Langer, and F. Quincke, J. Chem. Soc., **57**, 749 (1890).
2. N. A. Beach and H. B. Gray, J. Amer. Chem. Soc., **90**, 5713 (1968).
3. H. Basch, A. Viste, and H. B. Gray, J. Chem. Phys., **44**, 10 (1966).
4. W. J. Hunt, P. J. Hay, W. A. Goddard III, J. Chem. Phys., in press.
5. P. J. Hay, W. J. Hunt, W. A. Goddard III, Chem. Phys. Lett., **13**, 30 (1972).
6. L. Pauling, J. Amer. Chem. Soc., **53**, (1931), 1367; J. C. Slater, Phys. Rev., **37**, (1931), 481; **38** (1931), 1109.
7. J. Hinze, private communication; see also J. Hinze and C. C. J. Roothaan.
8. E. Clementi and D. L. Raimondi, J. Chem. Phys., **38** (1963), 2686.
9. R. M. Pitzer, J. Chem. Phys., **46**, 4871 (1967).
10. E. Switkes, R. M. Stevens, and W. N. Lipscomb, J. Chem. Phys., **51**, 5229 (1969).
11. W. J. Hehre, R. F. Stewart, and J. A. Pople, J. Chem. Phys., **51**, 2657 (1969).

12. F. A. Cotton and G. Wilkinson, Advanced Inorganic Chemistry, Second Edition, Interscience, (New York, 1966) p. 724.

13. C. E. Moore, Atomic Energy Levels, Vol I., National Bureau of Standards Circular 467, U.S. Government Printing Office, (Washington, D.C.), 1949, p. 274 ff.

14. A. P. Mortola and W. A. Goddard, to be published.

Table I. Basis Set

Atom	Angular Function	Exponent
Titanium	1s	21.44
	2s	7.69
	2p	9.03
	3s	3.68
	3p	3.37
	3d	2.71
	4s	1.20
	4p	1.12
Carbon	1s	5.6727
	2s	1.6083
	2p	1.75
Oxygen	1s	7.6579
	2s	2.2458
	2p	2.2266

Note: p functions were split into Φ_σ and p_π functions with the same exponents. The d function was split into a d_σ, d_π, and d_δ functions each with the same exponent.

Table 2. Orbital Energies of TiCO $^3\Phi$ State

Occupation $(11\sigma)^2(4\pi)^1(1\delta)^1$

Orbital	Character	ϵ TiCO (au)	ϵ Ti ^{3}F (au)	ϵ CO (au)
1σ	Ti 1s	-183.599	-183.267	
2σ	Ti 2s	-21.4782	-21.1407	
3σ	O 1s	-20.7884		-20.7388
4σ	Ti 2p	-18.0003	-17.6621	
1π	Ti 2p	-17.9930	-17.6557	
5σ	C 1s	-11.332		-11.3146
6σ	Ti 3s	-3.00912	-2.74888	
7σ	Ti 3p	-1.98117	-1.7272	
2π	Ti 3p	-1.96500	-1.7209	
8σ	O 2s	-1.49885		-1.48638
9σ	C 2s	-.777348		- .716659
10σ	CO bond	-.628875		- .483128
3π	CO bond	-.606536		- .572943
1δ	Ti $3d_{xy}$	-.463807	-.269207	
11σ	Ti 4s	-.230203	-.201376	
4π	$CO\pi^*$-Ti $3d_{xz}$	-.214665	-.268571	

Table 3. Results on TiCO

State	Type	Config*	E (au)	ΔE (au) from HF
$^3\Phi$	HF	$(11\sigma)^2(4\pi)^1(1\delta)^1$	-959.1552383	
$^3\Pi$	HF	$(11\sigma)^2(4\pi)^1(1\delta)^1$	-959.1516207	
$^1\Phi$	HF	$(11\sigma)^2(4\pi)^1(1\delta)^1$	-959.1453861	
$^5\Delta$	HF	$(11\sigma)^1(4\pi)^2(1\delta)^1$	-959.1453057	
$^3\Sigma_A^-$	HF	$(11\sigma)^2(4\pi)^2$	-959.1353014	
$^3\Delta_C$	HF	$(11\sigma)^2(12\sigma)^1(1\delta)^1$	-959.1284372	
$^1\Delta$	HF	$(11\sigma)^2(4\pi)^2$	-959.0911874	
$^3\Gamma$	HF	$(11\sigma)^1(4\pi)^2(1\delta)^1$	-959.0858466	
$^3\Delta_A$	HF	$(11\sigma)^1(4\pi)^2(1\delta)^1$	-959.0691135	
$^3\Sigma_B^-$	HF	$(11\sigma)^2(1\delta)^2$	-959.0557664	
$^1\Sigma_A^-$	HF	$(11\sigma)^2(4\pi)^2$	-959.0550280	
$^3\Pi_B$	HF	$(11\sigma)^1(4\pi)^3$	-959.0306986	
$^1\Sigma_B^+$	HF	$(4\pi)^4$	-958.8902658	
$^3\Phi$		$(4\pi)^3(1\delta)$		
$^5\Sigma^-$		$(4\pi)^2(1\delta)^2$		
$^5\Delta$	GVB 2 conf. 10σ mixed $\overline{\omega}$ 12σ		-959.1538932	.0086
$^3\Sigma^-$	2 conf. (3π mixed $\overline{\omega}$ 4π)		-959.1365075	.0012
	2 conf. (3π mixed $\overline{\omega}$ 5π)		-959.1417191	.0064

* The orbitals through 10σ and 3π are completely filled.

Table 4. Results on $TiCO^+$

State	Type	Config*	E (au)	-ΔE (au) from HF
$^4\Sigma^-$	HF	$(11\sigma)^1(4\pi)^2$	-958.9798494	
$^2\Delta$	HF	$(11\sigma)^2(1\delta)^1$	-958.959778	
$^2\Pi$	HF	$(11\sigma)^2(4\pi)^1$	-958.9499201	
$^4\Phi$	HF	$(11\sigma)^1(4\pi)^1(1\delta)^1$	-958.9374383	
$^2\Pi$	GVB 2 conf (CO lone pair split $\overline{\omega}$ empty π orbital)		-958.9599145	.0100
	GVB 3 conf (11σ mixed $\overline{\omega}$ 5π) (10σ mixed $\overline{\omega}$ 6π) (Ti 4s correlated to Ti $4p_\pi$)		-958.9798494	.0299
	GVB 4 conf 11σ mixed $\overline{\omega}$ 5π 10σ mixed $\overline{\omega}$ 6π 9σ mixed $\overline{\omega}$ 12σ (CO σ bonding pair split)		-958.9843671	.0344
TiC	GVB 5 conf 10σ mixed $\overline{\omega}$ 5π 11σ mixed $\overline{\omega}$ 6π 9σ mixed $\overline{\omega}$ 12σ 3π mixed $\overline{\omega}$ 5π (CO π bonding pair split)		-959.0190692	.0691
$^4\Sigma^-$	GVB 4 conf 9σ mixed $\overline{\omega}$ 5π (CO σ bonding pair) 10σ mixed $\overline{\omega}$ 12σ (CO non-bonding pair $\overline{\omega}$ Ti) 3π mixed $\overline{\omega}$ 5π (CO π bonding pair)		-959.0239232	.0441

Table 4 (Cont'd)

State	Type	Config*	E (au)	$-\Delta E$ (au) from HF
Energy drop for $^2\Pi$ state in adding		$(10\sigma$-$6\pi)$ mix to 2 conf.		.0199
		$(9\sigma$-$12\sigma)$ mix to 3 conf.		.0045
		$(3\pi$ - $5\pi)$ mix to 4 conf.		.0247

* Orbitals up to and including 10σ and 3π are completely filled.

Table 5. Results on Ti and Ti^+

Atom	State	Type	Config*	E (au)	ΔE from HF (au)
Ti	^3F	HF	$(4s)^2(3d)^2$	-846.8403154	
		GVB (4s mixed $\overline{\omega}$ 4p)		-846.8632540	.0229
Ti^+	^4F_A	HF	$(4s)^1(3d)^2$	-846.6436252	
	^2D	HF	$(4s)^2(3d)^1$	-846.5801986	
		GVB (4s mixed $\overline{\omega}$ 4p)		-846.6008134	.0206
	^4F_B	HF	$(3d)^3$	-846.3887346	

* In each case the 18 electron argon core $[(1s)^2(2s)^2(2p)^6(3s)^2(3p)^6]$ is present and solved for self-consistently.

Table 6. CO Results--$^1\Sigma^+$ Ground State

No.	Type of Wavefunction*		E (au)	-ΔE from HF (au)
1	HF	$(4\sigma)(5\sigma)^2(1\pi)^2$	-112.3484192	
2	2 Conf.	(5σ mixed $\overline{\omega}$ 2π)	-112.3637443	.0153
3	2 Conf.	(1π mixed $\overline{\omega}$ 2π)	-112.3786358	.0302
4	3 Conf.	(5σ mixed $\overline{\omega}$ 2π)	-112.3913260	.0429
		(1π mixed $\overline{\omega}$ 2π)		
5	3 Conf.	(5σ mixed $\overline{\omega}$ 2π)	-112.3720157	.0236
		(4σ mixed $\overline{\omega}$ 6σ)		
6	4 Conf.	(5σ mixed $\overline{\omega}$ 2π)	-112.3990638	.0506
		(4σ mixed $\overline{\omega}$ 6σ)		
		(1π mixed $\overline{\omega}$ 2π)		

Energy drop in adding (1π-2π) mix to No. 2(5σ-2π mix) .0276

to No. 5(5σ-2π, 4σ-6π) .0270

(5σ-2π) mix to No. 3(1π-2π) .0127

(4σ-6σ) mix to No. 2(5σ-2π) .0083

(4σ-6σ) mix to No. 4(5σ-2π, 1π-2π) .0077

* GVB wavefunctions are expressed as containing a number of configurations--1 for each set of natural orbitals to be mixed with the HF wavefunction.

Table 7. Correspondence between GVB pairs and natural orbital Names. In Parentheses we Indicate the Symbols by which the Orbitals will be Referred.

		Natural Orbital	
GVB	Pair	First	Second
CO	σ Bond ($CO_{\sigma a}$, $CO_{\sigma b}$)	9σ	12σ
TiC	σ Bond ($TiC_{\sigma a}$, $TiC_{\sigma b}$)	10σ	5π
CO	π Bond ($CO_{\pi a}$, $CO_{\pi b}$)	3π	5π
Ti	4s Pair (Ti $4s_a$, Ti $4s_b$)	11σ	6π
Ti	$3d_\pi$ (Ti $3d_\pi$)	4π	
Ti	$3d_\delta$ (Ti $3d_\delta$)	1δ	

Figure Captions

Figure 1. Sigma Bonding Orbitals from CO Sigma Bonding Pair;

a, b) GVB CO sigma bonding orbitals

c) Ti $3d_{z^2}$ orbital

d, e) GVB CO bonding orbitals in $TiCO^+$ $^4\Sigma^-$ state

f) HF CO bonding orbital in $TiCO^+$ $^4\Sigma^-$ state

g, h) GVB CO bonding orbitals in $TiCO^+$ $^2\Pi$ state

i) HF CO bonding orbital in $TiCO^+$ $^2\Pi$ state

j, k) GVB CO bonding orbitals in TiCO $^5\Delta$ state

l) HF CO bonding orbital in TiCO $^5\Delta$ state

m) HF CO bonding orbital in TiCO $^3\Phi$ state

Figure 2. GVB CO lone pair orbitals as Sigma Bonding Orbitals in $TiCO^+$

a, b) CO lone pair orbitals

c, d) Sigma bonding orbitals in $TiCO^+$ $^4\Sigma^-$ state

e, f) Sigma bonding orbitals in $TiCO^+$ $^2\Pi$ state

Figure 3. Non-bonding Orbitals

a, b) Ti atom GVB 4s orbitals (with 4p character)

c) Ti HF 4s orbital

d) GVB $TiCO^+$ non-bonding orbital $^4\Sigma^-$ state

e) HF $TiCO^+$ non-bonding orbital $^4\Sigma^-$ state

f, g) GVB $TiCO^+$ non-bonding orbitals $^2\Pi$ state

h) HF $TiCO^+$ non-bonding orbital $^2\Pi$ state

i) HF TiCO non-bonding orbital $^3\Phi$ state

j) HF TiCO non-bonding orbital $^5\Phi$ state

Figure 4. CO Pi-Bonding Orbitals

a, b) GVB CO pi bonding orbitals

c, d) GVB CO pi bonding orbitals in $TiCO^+$ $^4\Sigma^-$ state

e, f) GVB CO pi bonding orbitals in $TiCO^+$ $^2\Pi$ state

Figure 5. GVB Pi Back-Bonding Orbitals

a) Ti $3d_{xz}$ orbital

b) GVB back-bonding orbital in $TiCO^+$ $^4\Sigma^-$ state

c) GVB back-bonding orbital in $TiCO^+$ $^2\Pi$ state

Figure 6. Comparison of $TiCO^+$ and TiCO 4π Orbitals

a) 4π orbital ot $TiCO^+$ $^4\Sigma^-$ state

b) 4π orbital of $TiCO^+$ $^3\Sigma_A^-$ state

c) 4π orbital of TiCO $^3\Phi$ state

d) 4π orbital of TiCO $^5\Delta$ state

Figure 7. Diffuse Orbitals in Smaller Scale

a) One of the lone pair GVB orbitals in the $^2\Pi$ state of $TiCO^+$ (figure 3-f)

b) The lone orbital of the $^4\Sigma^-$ state of $TiCO^+$ (figure 3-d)

c) The 4π orbital of the $^3\Phi$ state of TiCO (figure 7-c)

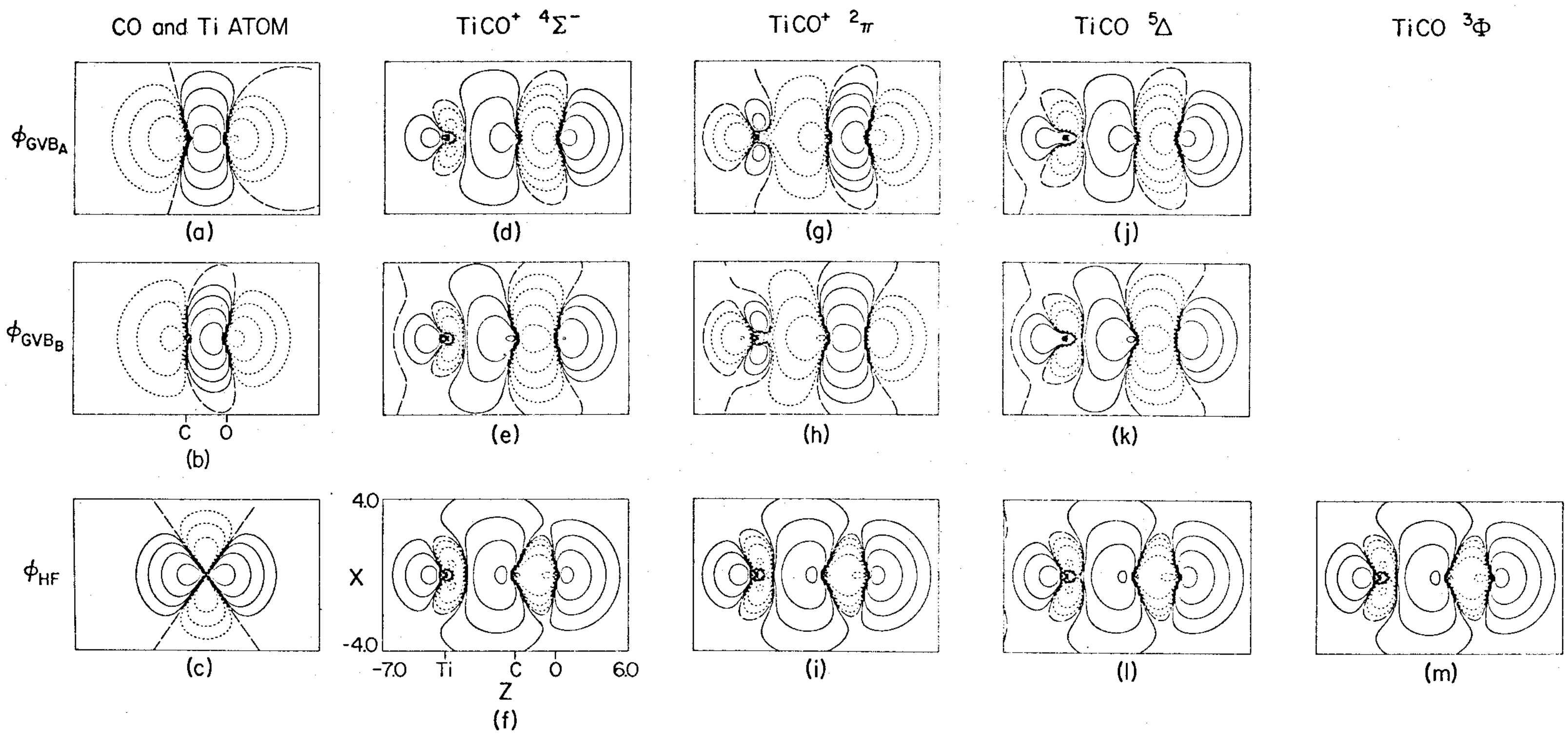

CO and Ti ATOM
TiCO+ 4Σ−
TiCO+ 2π
TiCO 5Δ
TiCO 3Φ
φGVBA
φGVBB
φHF
(a)
(b)
(c)
(d)
(e)
(f)
(g)
(h)
(i)
(j)
(k)
(l)
(m)
C O
4.0
X
-4.0
-7.0 Ti C O 6.0
Z

FIGURE 1

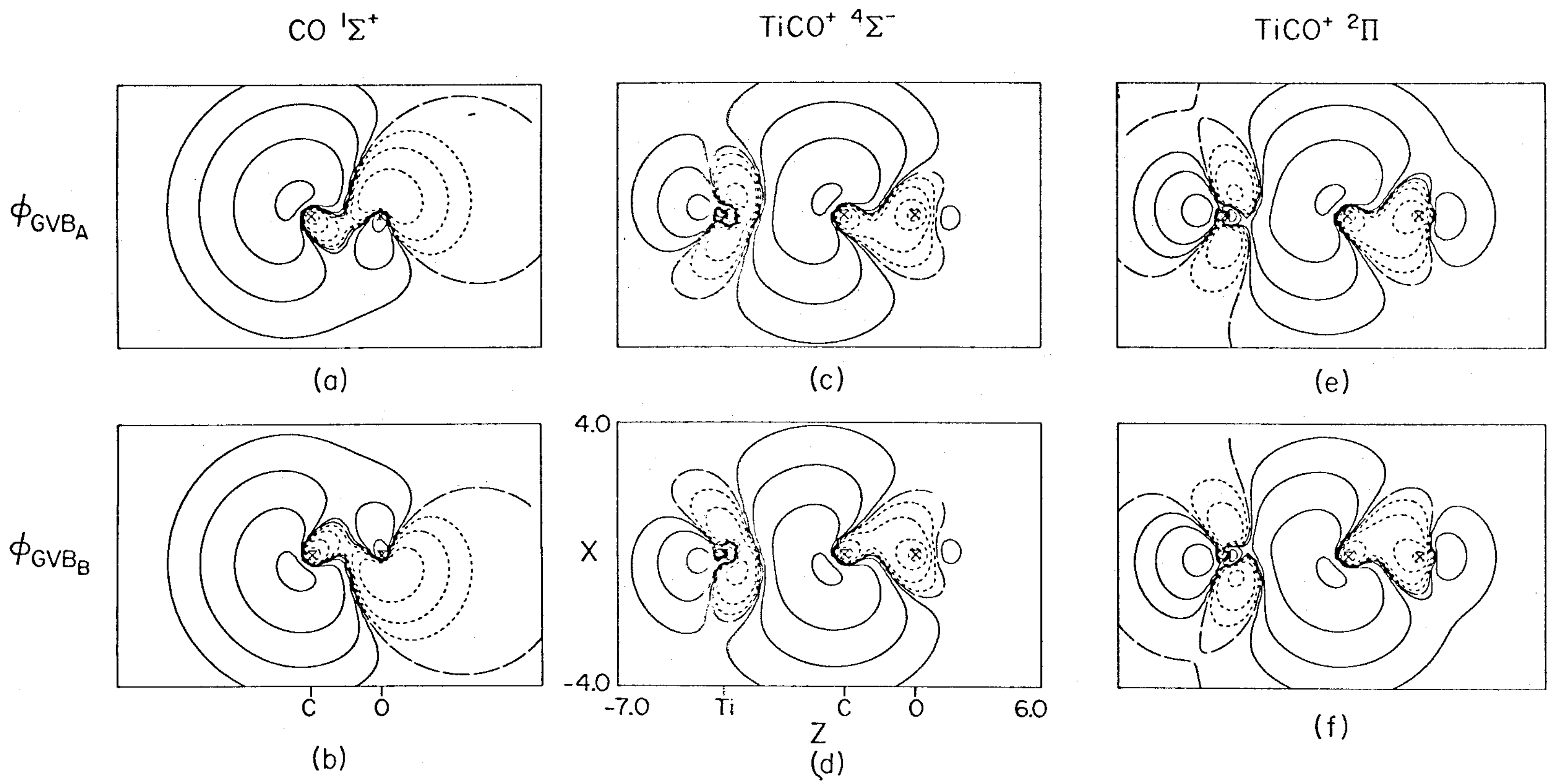

CO $^1\Sigma^+$
TiCO$^+$ $^4\Sigma^-$
TiCO$^+$ $^2\Pi$
ϕ_{GVB_A}
ϕ_{GVB_B}
(a)
(b)
(c)
(d)
(e)
(f)
C
O
Ti
4.0
-4.0
-7.0
6.0
X
Z

FIGURE 2

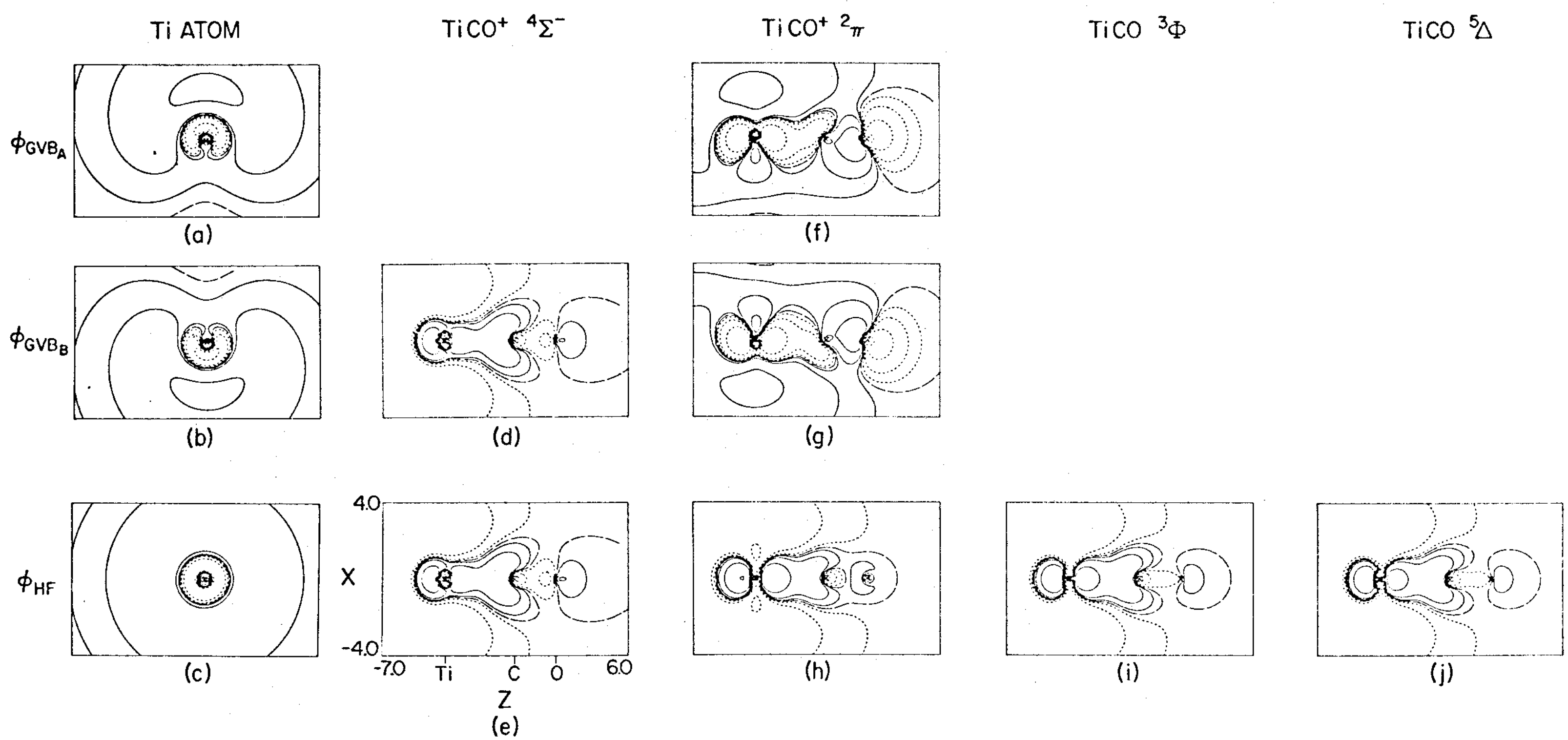
Ti ATOM
TiCO+ 4Σ−
TiCO+ 2π
TiCO 3Φ
TiCO 5Δ
φGVBA
φGVBB
φHF
(a)
(b)
(c)
(d)
(e)
(f)
(g)
(h)
(i)
(j)
4.0
X
-4.0
-7.0
Ti
C
O
6.0
Z

FIGURE 3

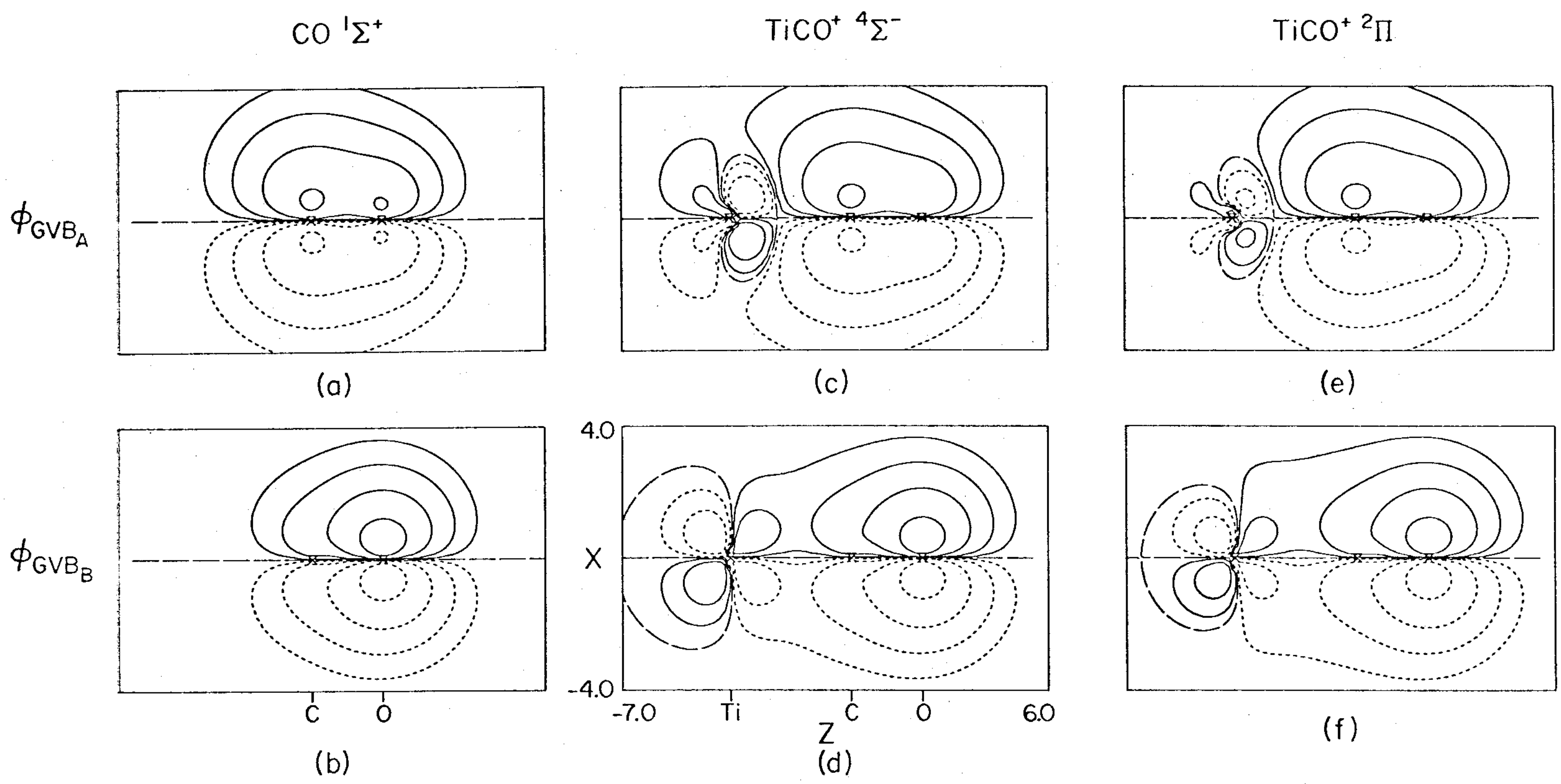
CO $^1\Sigma^+$
TiCO$^+$ $^4\Sigma^-$
TiCO$^+$ $^2\Pi$
ϕ_{GVB_A}
ϕ_{GVB_B}
(a)
(b)
(c)
(d)
(e)
(f)
C
O
Ti
4.0
-4.0
X
-7.0
6.0
Z

FIGURE 4

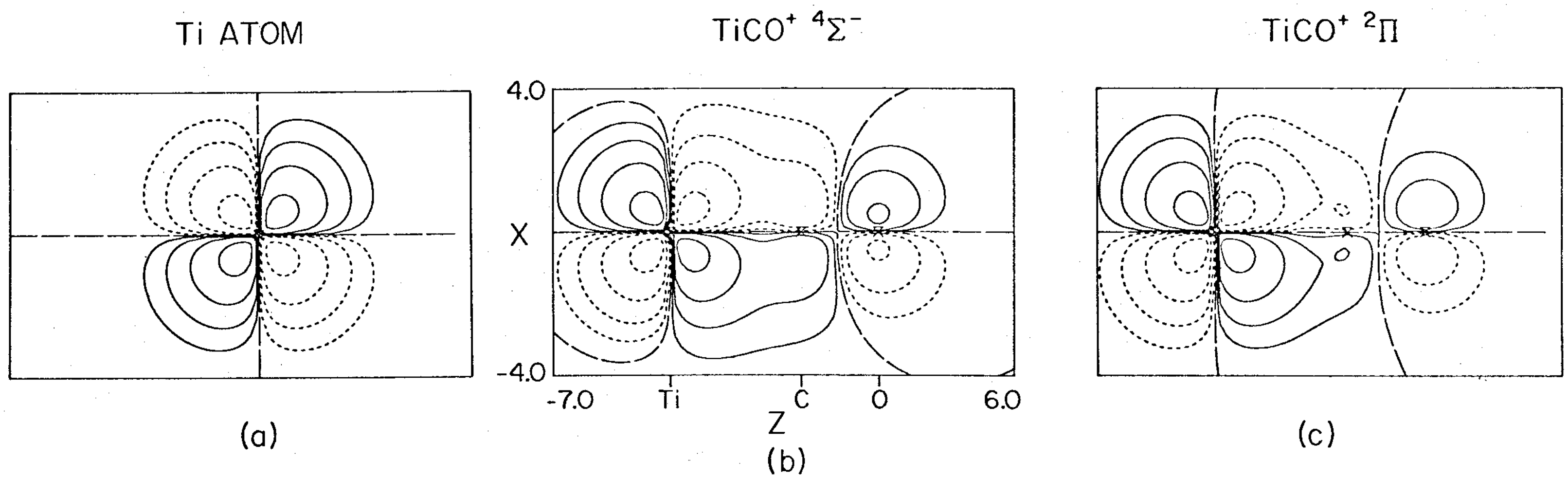

FIGURE 5

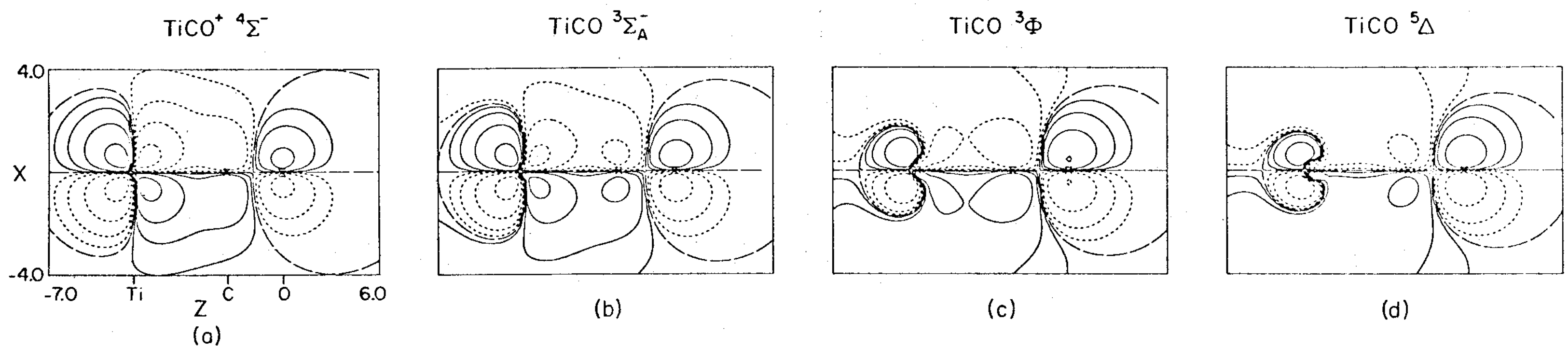

FIGURE 6

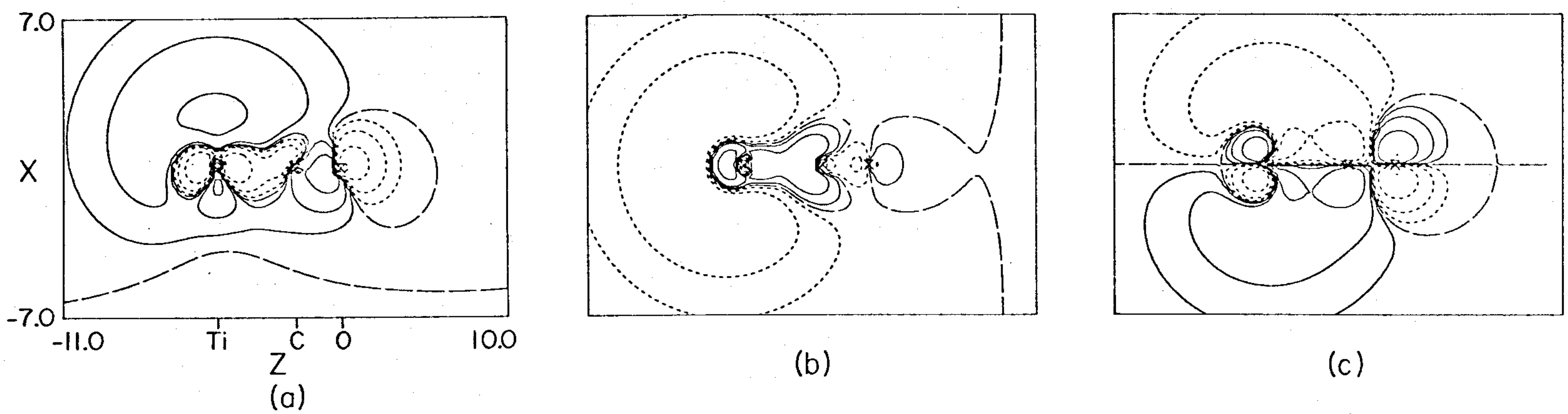

FIGURE 7

VI. CONCLUSION

This study has presented the descriptions of MnO_4^-, TiO, TiCO, and $TiCO^+$ provided by Hartree-Fock Theory and, except for MnO_4^-, by Generalized Valence Bond Theory. There are advantages and disadvantages to the use of either theory. As seen from the study of MnO_4^-, Hartree-Fock Theory gives a good description of the ground state in terms of the energetics of the orbitals. It provides good correlation with experimental data gathered from ESCA and photoionization sources. The energetic ordering of the doubly occupied orbitals of the ground state is the first clue to an interpretation of the spectrum. However, Hartree-FockTheory provides delocalized orbitals which for rather large compounds do not provide one with an intuitive feel for the two atom bonds. The restriction of the orbitals to symmetry orbitals, while simplifying the calculation, can cause bonding and non-bonding electrons to be occupying the same orbital. This is the case in MnO_4^- where the Hartree-Fock description allows only 6 of the 24 valence electrons to be non-bonding and forces two others which one would normally assume to be non-bonding (2 non-bonding electrons per oxygen) to be bonding. Such a restriction results in a poor description of the bonding orbital which now must readjust to account for the presence of the non-bonding electrons. Such a readjustment would make convergence of the calculation very difficult--a problem that was experienced with the calculation. Generalized Valence Bond Theory, on the other hand, provides localized orbitals from which one can understand the nature of the bonding. In TiO, for example, the confusion as to what is the ground state ($^1\Sigma^+$ or $^3\Delta$)

is dealt with very effectively by GVB Theory. The fact that GVB Theory leads to the proper dissociation is quite useful in determining why the $^{1}\Sigma^{+}$ state is the ground state. In TiCO and $TiCO^{+}$, comparison of the HF and GVB wavefunctions shows that the GVB gives a better description of the sigma donating interaction. The almost equal energy of the $^{2}\Pi$ and $^{4}\Sigma^{-}$ states of $TiCO^{+}$ obtained from GVB Theory led to ideas why $TiCO^{+}$ was more stable than TiCO. Such ideas were not obtainable from the HF calculations. As for the calculation of excited states, GVB demonstrated superiority over HF Theory in the spectrum of TiO. This was attributed to the fact that one electron orbitals describe singlets and triplets equally well. In MnO_4^{-}, Virtual Orbital Theory was shown to be useless in predicting the spectrum. However, when the virtual orbitals obtained from the HF calculation are used to obtain energy differences via the velocity and position dipole results, the ordering of the states turns out to be quite reasonable. To obtain quantitative results, one must calculate the energies of both states and perform the subtraction. This has not yet been done for MnO_4^{-} and as such remains a test for HF Theory.

Generalized Valence Bond Theory suffers from the fact that currently, it cannot do systems as large as Hartree-Fock Theory can. Hence, in applying it, one is restricted to model systems such as TiCO. Concepts obtained from these model systems can be directly applied into larger systems, but the quantitative description is lacking even though qualitative understanding is present. The larger systems can be dealt with quantitatively by Hartree-Fock Theory and extrapolation from the differences between GVB and HF theories in the model can be made to give qualitatively the GVB description of the larger system. However, one cannot expect to get the accurate, quantitative GVB description from such a process.

With the facts in, one must conclude that the Generalized Valence Bond Theory provides more insight towards the understanding of bonding in transition metal compounds than does Hartree-Fock Theory. The studies made in TiO and TiCO-$TiCO^+$ show this conclusively. The concepts developed by the application of the GVB Theory to these model compounds have been extended to compounds with similar bonding components and seem to describe these systems well. However, one cannot conclude that Hartree-Fock Theory is useless, since it does provide a quantitative picture for the larger systems to which GVB Theory cannot be applied. Hence, the conclusion is that the future is bright for both types of calculations, though if the choice has to be made, the model systems calculated via GVB Theory seem to be able to provide more information.